

UC Merced

UC Merced Electronic Theses and Dissertations

Title

The heritability of cell fate decisions in *Candida albicans*

Permalink

<https://escholarship.org/uc/item/357814xb>

Author

Quail, Morgan Mitchell

Publication Date

2022

Copyright Information

This work is made available under the terms of a Creative Commons Attribution License, available at <https://creativecommons.org/licenses/by/4.0/>

Peer reviewed|Thesis/dissertation

UNIVERSITY OF CALIFORNIA, MERCED

The heritability of cell fate decisions in *Candida albicans*

A dissertation submitted in partial satisfaction of the requirements for the degree Doctor
of Philosophy

in

Quantitative and Systems Biology

by

Morgan Mitchell Quail

Committee in charge:

Professor Michael D. Cleary, Chair

Professor Aaron D. Hernday

Professor Clarissa J. Nobile

Professor Kirk D.C. Jensen

2022

© Copyright

Chapter 1 © 2020 *Frontiers Cellular and Infection Microbiology*

All other chapters © 2022 Morgan Mitchell Quail

All rights reserved

The dissertation of Morgan Mitchell Quail is approved, and it is acceptable in quality and form for publication on microfilm and electronically:

Aaron D. Hernday

Mike D. Cleary, Chair

Clarissa J. Nobile

Kirk D.C. Jensen

University of California, Merced

2022

DEDICATION

This work, as a pinnacle of my formal education, is dedicated to my family (past and present), both chosen and not, who have always supported me. Special dedication to my aunt:

Ms. Cathy A. Quail

Thank you for instilling me with strength, perseverance, and love. I wouldn't be here without you and, one day, I hope to help you in the same way you have helped me.

TABLE OF CONTENTS

	Page
List of Abbreviations	vi
List of Symbols	vii
List of Tables	viii
List of Figures	ix
Acknowledgements	x
Curriculum Vita	xi
Dissertation Abstract	xvi
Chapter 1	1
References	24
Chapter 2	25
References	39
Figures	44
Chapter 3	57
References	66
Figures	68

LIST OF ABBREVIATIONS

ChIP, Chromatin Immuno Precipitation

CUT&RUN, Cleavage Under Targets & Release Using Nuclease

KO, knockout

OCTF, Opaque Critical Transcription Factor

RT, room temperature

-seq, sequencing

STD, Standard Deviation

TF, Transcription factor

UC, University of California

WCTF, White Critical Transcription Factor

WT, wildtype

LIST OF SYMBOLS

°, degree

+, and or in addition to

LIST OF TABLES

	Page
Table 2-1: Paired switch critical transcription factors	53
Table 2-2: Switch frequency of single deletion mutants	53
Table 2-3: Switch frequency of OCTF knock out paired with sequential deletion of <i>SSN6</i>	54
Table 2-4: Switch frequency of OCTF knock out paired with sequential deletion of <i>RBF1</i>	55
Table 2-5: Switch frequency of single deletion mutants with Wor1-mNeonGreen	56
Table 3-1: CUT&RUN data	71
Table 3-2: TFs shared among the white-opaque, biofilm, and commensal-pathogenic networks	72

LIST OF FIGURES

	Page
Figure 2-1	44
Figure 2-2	45
Figure 2-3	47
Figure 2-4	50
Figure 2-5	52
Figure 3-1	68
Figure 3-2	69
Figure 3-3	70

ACKNOWLEDGEMENTS

I would like to thank everyone that made this possible, by attempting to acknowledge all those who were part of this work. First, I would like to express my gratitude to my advisor and mentor, Dr. Aaron D. Hernday. I appreciate all your guidance, support, and encouragement throughout the entirety of my Ph.D. Thank you for taking me on as your first graduate student. Not only did Aaron teach me the technical and professional skills needed to succeed as an independent scientist, but he also allowed me the space and resources to develop my own leadership skills, public speaking voice, and scientific interests. All of these skills will be invaluable in my scientific endeavors, and I don't think I would have been able to grow as much or as quickly as I have without Aaron's support and guidance. Next, I would like to thank my thesis committee members, Dr. Mike D. Cleary, Dr., Dr. Kirk D.C. Jensen, and Clarissa J. Nobile whose guidance and support has helped me grow into the scientist I am today. Lastly, I would like to thank my graduate school lab mates and friends that supported me graduate school. Whether it was training me on new techniques or letting me practice talks, your help has been graduate school possible.

Chapter 1: Transcriptional Circuits Regulating Developmental Processes in *Candida albicans*.

The text of this thesis/dissertation is a reprint of the material as it appears in the *Frontiers in Cellular and Infection Microbiology*. The co-author listed in this publication directed and supervised research which forms the basis for the thesis/dissertation. Originally published in *Frontiers in Cellular and Infection Microbiology*. Transcriptional Circuits Regulating Developmental Processes in *Candida albicans*. *Front. Cell. Infect. Microbiol.* 10:605711 (2020). Copyright © 2020 10:605711.

This work was supported by the National Institutes of Health (NIH) National Institute of Allergy and Infectious Diseases (NIAID) and National Institute of General Medical Sciences (NIGMS) awards R21AI125801 and R35GM124594, respectively, by a Pew Biomedical Scholar Award from the Pew Charitable Trusts, and by the Kamangar family in the form of an endowed chair to CN. This work was also supported by NIH NIAID award R15AI37975 to AH. DR was supported by the National Science Foundation (NSF) Graduate Research Fellowship Program (GRFP) award 1744620.

CURRICULUM VITA

University of California Merced, 5200 N. Lake Rd, Merced CA 95340 USA
Phone: (408) 782-4507 / Email: mmquail@gmail.com

EDUCATION

- 2022 Ph.D., Quantitative Systems Biology, University of California Merced
(Laboratory of Dr. Aaron Hernday)
- 2020 M.S., Quantitative Systems Biology, University of California Merced
(Laboratory of Dr. Aaron Hernday)
- 2011 B.S., Molecular Cellular Developmental Biology, University of California Santa Cruz
(Laboratory of Dr. Donald Smith)

EXPERIENCE

University of California Merced

- Fall 2020-Spring 2022 Graduate Student Researcher
- Summer 2020 Teaching Assistant (Immunology)
- Fall 2017-Spring 2020 Graduate Student Researcher
- Fall 2015-Spring 2017 Teaching Assistant (Genetics)

Ariosa Diagnostics (now Roche Sequencing)

- 2015 Research Associate 2
- 2013-2015 Research Associate 1
- 2012-2013 Clinical Laboratory Assistant

San Jose Tech Museum of Innovation

- 2011-2015 Wet Lab Tech

University of California Santa Cruz

- 2010-2011 Undergraduate Student Researcher Volunteer, Smith Lab

Google (Adecco Solutions on site)

- 2011-2012 Data Specialist, Mountain View, CA

Northwest YMCA

- 2007-2010 Assistant Director of Science and Specialty Summer Camps, Cupertino, CA

SKILL SETS

- CRISPR/Cas9 tool building
- Illumina & Ion Torrent Next Gen. Seq.
- Sequencing library preparation
- Affymetrix Microarray
- qPCR
- Bioanalyzer
- DNA and RNA extraction and purification
- Protein extractions and purification
- Microbial culture
- Cloning
- Immunohistochemistry

HONORS

2022 *University Friends Circle (UFC) Community Service Organization Award*
Radio Bio, UC Merced

2021 *University Friends Circle (UFC) Community Service Organization Award*
Radio Bio, UC Merced

2020 *University Friends Circle (UFC) Community Service Organization Award*
Radio Bio, UC Merced

2019 *University Friends Circle (UFC) Community Service Organization Award*
Radio Bio, UC Merced

2018 *University Friends Circle (UFC) Community Service Organization Award*
Radio Bio, UC Merced

GRANTS AND FELLOWSHIPS

2022 PhD candidate, *QSB Dean's dissertation Fellowship*
UC Merced, Quantitative and Systems Biology

2017 Graduate Student, *QSB Summer Research Fellowship*
UC Merced, Quantitative and Systems Biology

2016 Graduate Student, *QSB Summer Research Fellowship*
UC Merced, Quantitative and Systems Biology

INVITED TALKS AND LECTURES

2018 *Eukaryotic Transcriptional Regulation and Developmental Genetics*
Genetics Lecture, UC Merced (Merced, CA)

2017 *Molecular Biology and Biotechnology*
Genetics Lecture, UC Merced (Merced, CA)

2016 *Mutation*
Genetics Lecture, UC Merced (Merced, CA)

SERVICE

Advisory Committee

2011-Present Theta Chi Alumni Board Treasurer, Secretary, and Health and Safety Officer
Theta Chi Theta Iota Chapter (Santa Cruz)

Mentorship

2021-2022 Mentor, Undergraduate Researcher of the Hernday Lab, UC Merced (Debbo Elias)

2021-2022 Mentor, Undergraduate Researcher of the Hernday Lab, UC Merced (Elia Vega)

2016-2021 GRAD-EXCEL Peer Mentor, UC Merced

2019-2020 Mentor, Undergraduate Researcher of the Hernday Lab, UC Merced (Edward Sukarto)

2017-2019 Mentor, Undergraduate Researcher of the Hernday Lab, UC Merced (Milana Egrova)

2016-2017 Mentor, Undergraduate Researcher of the Hernday Lab, UC Merced (Brian Wang)

2016-2018 Mentor, Undergraduate Researcher of the Hernday Lab, UC Merced (Leesa Hagerman)

2015-2017 Mentor, Undergraduate Researcher of the Hernday Lab, UC Merced (Isaac Campos)

2015-2017 Mentor, Undergraduate Researcher of the Hernday Lab, UC Merced (Molly Easter)

2015-2016 Mentor, Undergraduate Researcher of the Hernday Lab, UC Merced (Joseph Meyer)

Summer 2014 Internship co-advisor, Ariosa Diagnostics (now Roche), Summer (Kayla Gregory)

Community Service and Outreach

2016-Present Founding member of RadioBio, UC Merced
Merced, CA

2016-2021 Treasurer of RadioBio, UC Merced
Merced, CA

2017 Science and Engineering Fair Judge, San Joaquin County Science Fair,
Wentworth Education Center, Stockton, CA

2008-2011 Beach Cleanup, Santa Cruz Surf Rider Foundation
Santa Cruz, CA

2008-2011 Sexual Violence Awareness and Prevention Teeter-totter-a-thon
Santa Cruz, CA

PUBLICATIONS

First-Author Journal Articles

1. Quail M.M., Rodriguez, D.L., Hernday A.D., Nobile C.J., 2020: Transcriptional Circuits Regulating Developmental Processes in *Candida albicans*. *Front. Cell. Infect. Microbiol.* 10:605711. doi: 10.3389/fcimb.2020.605711

Collaborative Journal Articles

1. Nguyen N., Quail M.M.F., Hernday A.D., 2017: An Efficient, Rapid, and Recyclable System for CRISPR-Mediated Genome Editing in *Candida albicans*. *mSphere*, 2, 2.

Poster Presentations and Acknowledgements

1. Nguyen N., **Quail M.M.F.**, Hernday A.D. An efficient, rapid, and recyclable system for CRISPR-mediated genome editing in *Candida albicans*. Poster presented at: Graduate Student Poster Symposium on Graduate Visitation Day; 2018 Feb 24th, UC Merced, CA

2. Nguyen N., **Quail M.M.F.**, Hernday A.D. An efficient, rapid, and recyclable system for CRISPR-mediated genome editing in *Candida albicans*. Poster presented at: Northern California American Society for Microbiology Poster Session; 2018 March 2-3, Genentech Hall, Pleasanton, CA

3. Juneau K., Bogard P.E., Huang S., Mohseni M., Wang E.T., Ryvkin P., Kingsley C., Struble C.A., Oliphant A., Zahn J.M., 2014: Microarray-Based Cell-Free DNA Analysis Improves Noninvasive Prenatal Testing. *Fetal Diagnosis and Therapy*, **36**, 4.

The heritability of cell fate decisions in *Candida albicans*

by

Morgan Mitchell Quail

Doctor of Philosophy in Quantitative and Systems Biology

University of California, Merced, 2022

Professor Aaron D. Hernday

Biological switches control cell-fate decisions across biological kingdoms. Many of these cell-fate decisions are controlled by complex transcriptional networks, consisting of unique combinations of transcriptional regulators and their respective cis-regulatory targets. An example of such a network is that which controls the white-opaque phenotypic switch in the human fungal pathogen, *Candida albicans*. The white-opaque switch gives rise to two distinct cell types – white and opaque – which differ in their mating competence, adaptation to distinct environmental niches, host immune cell evasion, and morphological characteristics at the single-cell and colony level. Each cell type can be heritably maintained through many generations and stochastic or environmentally induced switching can lead to a transition between these two phenotypic states. Switching between these two heritably maintained transcriptional programs occurs without any changes to the primary sequence of the genome, and thus fits the classic definition of an epigenetic switch. The ability of *C. albicans* to readily switch between the white and opaque phenotypes is controlled by a “core” circuit of eight transcription factors (TFs) that is centered around the opaque-specific master regulator Wor1 (White-Opaque Regulator 1), however, recent work has identified a set of nineteen new regulators that impinge upon the switch. In this work, we characterize these newly identified TFs and their interactions with the previously defined “core” regulators as well as determine how these new regulators affect the establishment and maintenance of the white-opaque switch.

CHAPTER 1

Background and historical context: Transcriptional Circuits Regulating Developmental Processes in *Candida albicans*

CHAPTER 1: BACKGROUND AND HISTORICAL CONTEXT: Transcriptional Circuits Regulating Developmental Processes in *Candida albicans*



Transcriptional Circuits Regulating Developmental Processes in *Candida albicans*

Diana L. Rodriguez^{1,2†}, Morgan M. Quail^{1,2†}, Aaron D. Hernday^{1,3*} and Clarissa J. Nobile^{1,3*}

¹ Department of Molecular and Cell Biology, School of Natural Sciences, University of California—Merced, Merced, CA, United States, ² Quantitative and Systems Biology Graduate Program, University of California—Merced, Merced, CA, United States, ³ Health Sciences Research Institute, University of California - Merced, Merced, CA, United States

Candida albicans is a commensal member of the human microbiota that colonizes multiple niches in the body including the skin, oral cavity, and gastrointestinal and genitourinary tracts of healthy individuals. It is also the most common human fungal pathogen isolated from patients in clinical settings. *C. albicans* can cause a number of superficial and invasive infections, especially in immunocompromised individuals. The ability of *C. albicans* to succeed as both a commensal and a pathogen, and to thrive in a wide range of environmental niches within the host, requires sophisticated transcriptional regulatory programs that can integrate and respond to host specific environmental signals. Identifying and characterizing the transcriptional regulatory networks that control important developmental processes in *C. albicans* will shed new light on the strategies used by *C. albicans* to colonize and infect its host. Here, we discuss the transcriptional regulatory circuits controlling three major developmental processes in *C. albicans*: biofilm formation, the white-opaque phenotypic switch, and the commensal-pathogen transition. Each of these three circuits are tightly knit and, through our analyses, we show that they are integrated together by extensive regulatory crosstalk between the core regulators that comprise each circuit.

Keywords: *Candida albicans*, biofilms, commensal-pathogen transition, transcriptional regulation, transcriptional networks, transcriptional rewiring, white-opaque switching, transcriptional circuits

OPEN ACCESS

Edited by:

Bernard Turcotte,
McGill University, Canada

Reviewed by:

Adnane Sellam,
Université de Montréal, Canada
Rebecca Anne Hall,
University of Kent, United Kingdom

*Correspondence:

Aaron D. Hernday
ahernday@ucmerced.edu
Clarissa J. Nobile
cnobile@ucmerced.edu

[†]These authors have contributed
equally to this work

Specialty section:

This article was submitted to
Fungal Pathogenesis,
a section of the journal
Frontiers in Cellular and
Infection Microbiology

Received: 13 September 2020

Accepted: 04 November 2020

Published: 03 December 2020

Citation:

Rodriguez DL, Quail MM, Hernday AD
and Nobile CJ (2020) Transcriptional
Circuits Regulating Developmental
Processes in *Candida albicans*.
Front. Cell. Infect. Microbiol. 10:605711.
doi: 10.3389/fcimb.2020.605711

INTRODUCTION

C. albicans is a common human commensal that asymptotically colonizes the skin, oral cavity, and gastrointestinal and genitourinary tracts of healthy individuals (Kennedy and Volz, 1985; Kumamoto, 2002; Achkar and Fries, 2010; Spiliopoulou et al., 2010; Kumamoto, 2011; Nobile and Johnson, 2015; Kan et al., 2020). It is also an opportunistic pathogen that is capable of causing superficial mucosal and life-threatening disseminated infections, especially in immunocompromised individuals (Wenzel, 1995; Calderone and Fonzi, 2001; Hube, 2004; Pappas et al., 2004; Mayer et al., 2013), such as in AIDS, chemotherapy and organ transplant patients, as well as in individuals with implanted medical devices (Wenzel, 1995; Nobile and Johnson, 2015). Multiple regulatory pathways controlling important *C. albicans* developmental processes allow this opportunistic fungal pathogen to adapt to and proliferate in distinct

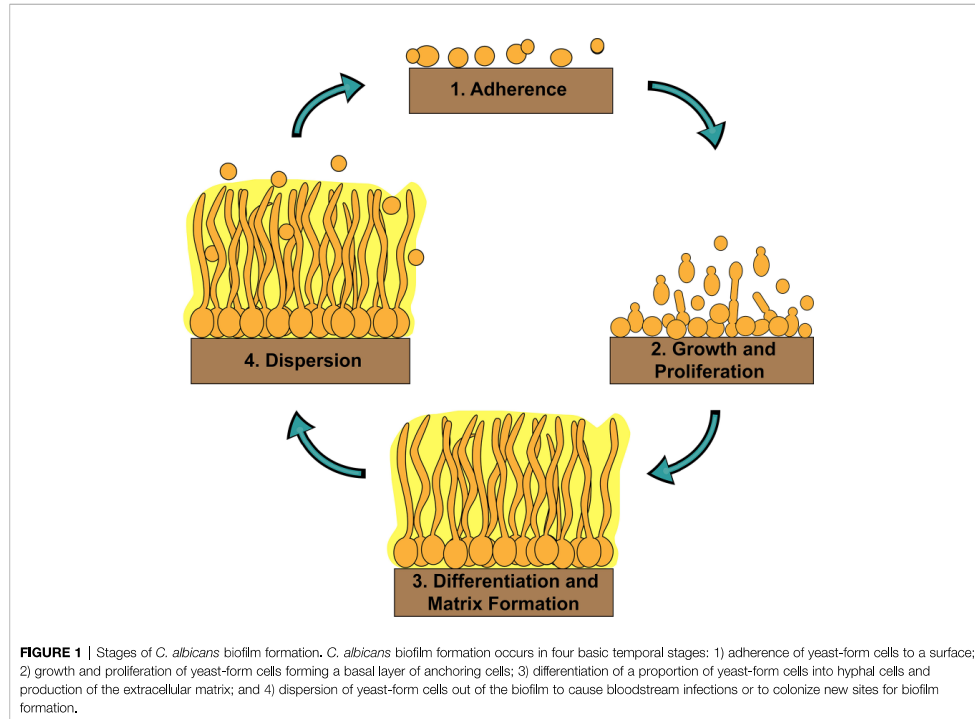
environmental niches in the host. In this review, we discuss the “core” transcriptional circuits controlling three major developmental processes in *C. albicans*: biofilm formation, the white-opaque phenotypic switch, and the commensal-pathogen transition. The core circuitry is defined as the direct physical interactions between transcriptional regulators that control these developmental processes and their respective upstream intergenic regions, where at least one direct binding interaction with other members of the circuit has been experimentally observed. These three circuits were chosen because they regulate persistent phenotypic changes in *C. albicans* that have been characterized using genome-wide transcriptional profiling (RNA-sequencing and/or microarray) and binding (chromatin immunoprecipitation) approaches. In our discussion of these circuits we focus largely on transcription factors (TFs) that bind to DNA in a sequence-specific manner; however, we also include some discussion of important cofactors for which genome-wide transcriptional profiling and binding data are available. In addition, we include information on “auxiliary” transcriptional regulators of these three developmental processes that we define as those that are known to regulate these processes, but that lack direct binding interactions with the core transcriptional regulators or binding data is not available for these transcriptional regulators under the growth condition of interest.

REGULATION OF BIOFILM FORMATION

Biofilms are communities of adherent microbial cells encased in protective extracellular matrices (Kolter and Greenberg, 2006; Nobile and Johnson, 2015; Gulati and Nobile, 2016). Biofilms are ubiquitous in nature and are typically associated with interfaces, such as solid-liquid, liquid-gas, and liquid-liquid interfaces (Davey and O’toole, 2000; Kolter and Greenberg, 2006; Wilking et al., 2011; Desai and Ardekani, 2020). They are problematic when they form in industrial settings, such as in water distribution systems and on food preparation settings, and even more so when they form inside a host on tissues and on implanted medical devices. *C. albicans* biofilms are composed of several cell types, including round budding yeast-form cells, oval pseudohyphal cells, and elongated hyphal cells, encased in a protective extracellular matrix (Chandra et al., 2001; Desai and Mitchell, 2015). *C. albicans* biofilm formation occurs in four basic temporal stages: i) adherence of yeast-form cells to a surface; ii) growth and proliferation of yeast-form cells forming a basal layer of anchoring cells; iii) differentiation of a proportion of yeast-form cells into hyphal cells and production of the extracellular matrix; and iv) dispersion of yeast-form cells out of the biofilm to cause bloodstream infections or to colonize new sites for biofilm formation (Figure 1) (Desai and Mitchell, 2015; Nobile and Johnson, 2015; Gulati and Nobile, 2016). Indeed, *C. albicans* is a common cause of bloodstream infections worldwide, which often originate from biofilms (Edmond et al., 1999; Richards et al., 1999; Pfaller and Diekema, 2007). Given that cells within *C. albicans* biofilms are inherently resistant and

tolerant to most antifungal drug treatments compared to planktonic (free-floating) cells, biofilm infections are particularly challenging to treat in the clinic. Understanding the genetic regulatory mechanisms that control *C. albicans* biofilm formation could lead to the development of novel therapeutic strategies effective in treating biofilm infections.

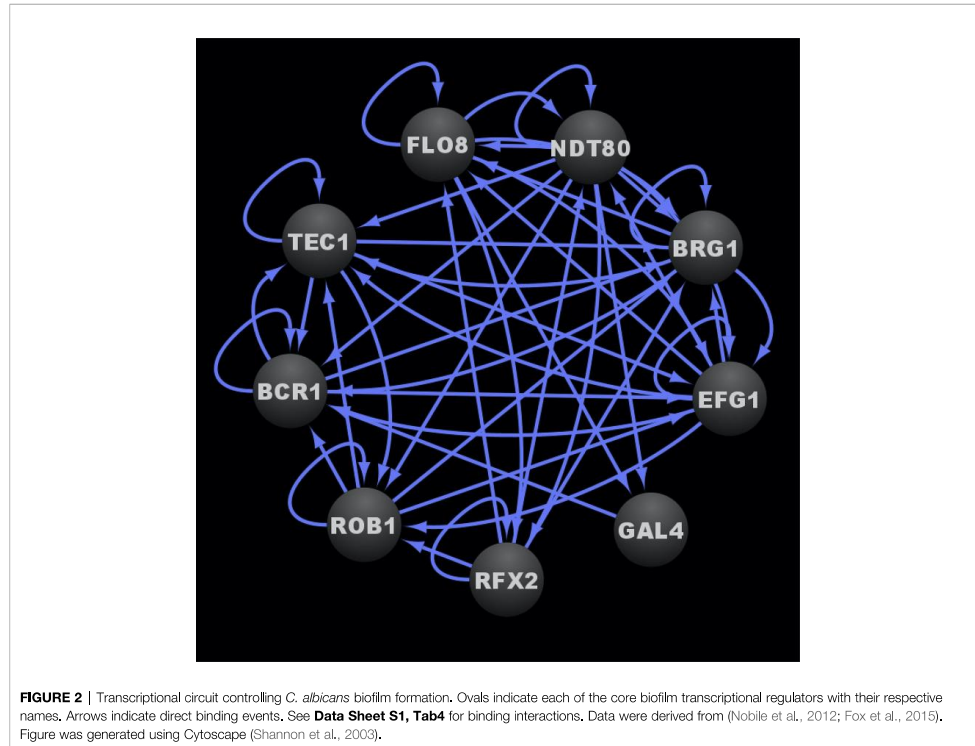
The *C. albicans* transcriptional network controlling biofilm formation was first described eight years ago (Nobile et al., 2012). Six “master” biofilm transcriptional regulators (Bcr1, Tec1, Efg1, Ndt80, Rob1, and Brg1) were identified by screening a library of 165 transcription factor (TF) mutant strains (Homann et al., 2009) for defects in biofilm formation under standard *in vitro* biofilm growth conditions (Nobile et al., 2012). Here, we define a master biofilm transcriptional regulator as one whose deletion impairs biofilm formation throughout a 48-h period of biofilm growth under these standard conditions. All six TF mutant strains identified additionally had clear defects in biofilm formation in at least one of two *in vivo* animal models for biofilm formation (Nobile et al., 2012). Using genome-wide transcriptional profiling and chromatin immunoprecipitation techniques to study mature 48-h biofilms, a complex interconnected transcriptional network was discovered consisting of those six master transcriptional regulators, along with 1,061 downstream “target” genes (Nobile et al., 2012). These six master transcriptional regulators directly bound to the upstream intergenic regions and positively regulated the expression of each other, forming a tightly knit core biofilm circuit (Fox and Nobile, 2012; Nobile et al., 2012). Additionally, with the exception of Tec1, all of the six master biofilm transcriptional regulators acted as both repressors and activators of their directly bound biofilm target genes; Tec1, on the other hand, primarily acted as an activator (Nobile et al., 2012). Each of the six master biofilm transcriptional regulators controlled target genes that were in common with the other core transcriptional regulators in the circuit, as well as target genes that were unique to each transcriptional regulator. These findings suggest that each master biofilm transcriptional regulator in the circuit controls certain elements of biofilm formation independently, but that they also work together to coordinate concerted efforts important for biofilm formation. For example, Ndt80 regulates the expression of drug transporters independent of the other master biofilm transcriptional regulators in the circuit (such as, *CDR4*), and some in common with several of the other master biofilm transcriptional regulators in the circuit (such as, *CDR3*) (Nobile et al., 2012). Additionally, each master biofilm transcriptional regulator likely responds to unique environmental inputs, such as oxygen and nutrient availability, pH, temperature, and waste products. How different environmental inputs influence the biofilm transcriptional circuit is an intriguing area of future research. For example, we know that the six master biofilm transcriptional regulators discovered using *in vitro* biofilm assays are still required for *in vivo* biofilm formation in at least one of two *in vivo* biofilm models (Nobile et al., 2012). The majority (four) of the master biofilm transcriptional regulators discovered in this study were essential for biofilm formation in both *in vivo* biofilm models used; however, two of the master biofilm transcriptional regulators played different roles depending on the *in vivo* biofilm model (Nobile et al., 2012). Specifically, Bcr1 was essential for



biofilm formation in a rat catheter biofilm model but was dispensable in a rat denture biofilm model (Nobile et al., 2012). Similarly, *Brg1* was essential for biofilm formation in a rat denture biofilm model but was dispensable in a rat catheter biofilm model (Nobile et al., 2012). Future work on these master transcriptional regulators will determine their unique influences on biofilm formation dependent on the environmental inputs present.

In a subsequent study, three additional transcriptional regulators, *Gal4*, *Rfx2*, and *Flo8*, were added to the core biofilm transcriptional circuit (Fox et al., 2015). *Gal4*, *Rfx2*, and *Flo8* were found to directly bind to the upstream intergenic regions of one or more of the previously identified six master biofilm transcriptional regulators and vice versa during biofilm development (Nobile et al., 2012; Fox et al., 2015). *Gal4*, *Rfx2*, and *Flo8* were identified (in addition to the six previously identified transcriptional regulators) by screening a TF mutant library containing 192 TF mutant strains (Fox et al., 2015). This TF library contained the same 165 TF mutants (Homann et al., 2009) from the Nobile et al., 2012 study (Nobile et al., 2012) plus 27 additional newly constructed TF mutant strains. The TF mutants in this larger library were screened for their abilities to form biofilms over time at 90 min, 8, 24, and 48 h of biofilm growth (Fox et al., 2015). *Flo8*, like the other six previously identified master biofilm transcriptional regulators, was required for biofilm formation

throughout a 48-h course of biofilm growth, and thus was deemed to be a master biofilm transcriptional regulator; *Gal4* and *Rfx2* were only required for normal biofilm formation at specific intermediate time points (Fox et al., 2015). Given that the initial biofilm circuit consisting of six master transcriptional regulators was discovered by assessing biofilm formation at a single mature time point (48 h) (Nobile et al., 2012), performing the genetic screen as a biofilm develops over time, with the additional TF mutant strains, contributed to the expansion of the core biofilm circuit (Fox et al., 2015). Genome-wide binding data was not performed for *Gal4*, *Rfx2*, and *Flo8* as part of this study; however, directed chromatin immunoprecipitation followed by quantitative PCR was performed to determine that these three new transcriptional regulators are integrated into the core biofilm circuit, which now consists of nine core transcriptional regulators, seven of which are considered to be master biofilm transcriptional regulators (Figure 2) (Nobile et al., 2012; Fox et al., 2015). We note that although genome-wide binding experiments have been performed for *Gal4* and *Flo8* (Askew et al., 2009; Polvi et al., 2019), these experiments were not performed under biofilm conditions and thus the resulting data cannot be integrated into the biofilm transcriptional circuit. Overall, although the logic of the biofilm transcriptional circuit (defined as how each transcriptional regulator contributes to the regulatory dynamics of



the circuit) has yet to be fully elucidated, the high degree of interconnectivity between the core biofilm transcriptional regulators likely contributes to the robustness, yet reversibility, of the biofilm state.

Although the nine core biofilm transcriptional regulators are known to be important for biofilm formation, how each one specifically contributes to biofilm processes (e.g. adhesion, filamentation, antifungal drug resistance, etc.), through detailed analyses of their mutant strains, has not been systematically determined. **Table 1** summarizes the current knowledge of the roles of all known transcriptional regulators in known biofilm-related processes. Eight of the nine core biofilm transcriptional regulators (Bcr1, Brg1, Efg1, Flo8, Ndt80, Rfx2, Rob1, and Tec1) have been implicated in regulating filamentation (Schweizer et al., 2000; Bockmüh and Ernst, 2001; Cao et al., 2006; Elson et al., 2009; Hao et al., 2009; Sellam et al., 2010; Vandeputte et al., 2011; Du et al., 2012b; Nobile et al., 2012), which is a critical process necessary for maintaining the architectural stability of the biofilm structure. Four of the nine core biofilm transcriptional regulators (Bcr1, Efg1, Rfx2, and Tec1) have been implicated in regulating adhesion (Dieterich et al., 2002; Hao et al., 2009; Sahni et al., 2010; Finkel et al., 2012), including

both cell-cell and cell-substrate adhesion, which is an essential process for both the initiation of biofilm formation as well as for the maintenance of a mature biofilm. Three of the nine core biofilm transcriptional regulators (Bcr1, Efg1, and Ndt80) are known to be involved in the regulation of antifungal drug resistance and/or tolerance (Chen et al., 2004; Sellam et al., 2009; Prasad et al., 2010; Desai et al., 2013), an important feature that contributes to the overall recalcitrance of established biofilms to antimicrobial compounds. Of the nine core biofilm transcriptional regulators, we know the least about the biofilm specific roles of Gal4, and only that it contributes to the structure of a biofilm at intermediate stages of biofilm development (Fox et al., 2015). In the future, additional roles of the nine core biofilm transcriptional regulators during biofilm formation will certainly be elucidated. For example, it seems likely that some of the core biofilm transcriptional regulators would be involved in the formation of the extracellular matrix; however, this role has not been examined to date in the mutant strains of the core biofilm transcriptional regulators. In addition, the ability of cells within biofilms to communicate with one another, called quorum sensing, is an important process for coordinating biofilm formation of many microorganisms; however, this role

TABLE 1 | Known transcriptional regulators with roles in *C. albicans* biofilm formation.

Core Biofilm Transcriptional Regulators				
Orf19#	Name	Known biofilm-related process affected in mutant strain	Gene upstream intergenic region bound by one or more of the core biofilm regulators?	References
Orf19.723	Bcr1	Adhesion, Filamentation, Drug Resistance/Tolerance	Yes	(Nobile and Mitchell, 2005; Elson et al., 2009; Homann et al., 2009; Fanning et al., 2012; Finkel et al., 2012; Desai et al., 2013)
Orf19.4056	Brg1	Filamentation	Yes	(Du et al., 2012b; Nobile et al., 2012)
Orf19.610	Efg1	Adhesion, Filamentation, Drug Resistance/Tolerance	Yes	(Bockmüh and Ernst, 2001; Dieterich et al., 2002; Ramage et al., 2002; Li and Palecek, 2003; Prasad et al., 2010; Nobile et al., 2012)
Orf19.1093	Flo8	Filamentation	Yes	(Cao et al., 2006; Fox et al., 2015)
Orf19.5338	Gal4	Unknown	Yes	(Fox et al., 2015)
Orf19.2119	Ndt80	Filamentation, Drug Resistance	Yes	(Chen et al., 2004; Sellam et al., 2009; Sellam et al., 2010; Nobile et al., 2012)
Orf19.4590	Rfx2	Adhesion, Filamentation	Yes	(Hao et al., 2009; Fox et al., 2015)
Orf19.4998	Rob1	Filamentation	Yes	(Vandeputte et al., 2011)
Orf19.5908	Tec1	Adhesion, Filamentation	Yes	(Schweizer et al., 2000; Staib et al., 2004; Nobile and Mitchell, 2005; Sahni et al., 2010)
Auxiliary Biofilm Transcriptional Regulators				
Orf19.6124	Ace2	Adhesion, Filamentation, Drug Resistance/Tolerance	No	(Kelly et al., 2004; Mulhern et al., 2006; Finkel et al., 2012)
Orf19.2331	Ada2	Adhesion, Filamentation, Drug Resistance/Tolerance	No	(Bruno et al., 2006; Pukkila-Worley et al., 2009; Finkel et al., 2012)
Orf19.7381	Ahr1	Adhesion, Filamentation, Drug Resistance/Tolerance	Yes	(Homann et al., 2009; Askew et al., 2011)
Orf19.4766	Arg81	Adhesion, Filamentation, Drug Resistance/Tolerance	No	(Homann et al., 2009; Finkel et al., 2012)
Orf19.6874	Bpr1	Unknown	Yes	(Fox et al., 2015)
Orf19.4670	Cas5	Adhesion, Drug Resistance/Tolerance	Yes	(Finkel et al., 2012; Vasicek et al., 2014)
Orf19.2356	Crz2	Adhesion, Drug Resistance/Tolerance	Yes	(Homann et al., 2009; Finkel et al., 2012)
Orf19.3127	Czf1	Adhesion, Filamentation, Drug Resistance/Tolerance	Yes	(Brown et al., 1999; Finkel et al., 2012; Langford et al., 2013)
Orf19.3252	Dal81	Adhesion	No	(Finkel et al., 2012)
Orf19.3193	Fcr3	Adhesion	Yes	(Finkel et al., 2012)
Orf19.6680	Fgr27	Adhesion, Filamentation	No	(Uhl et al., 2003; Finkel et al., 2012)
Orf19.1358	Gcn4	Filamentation	Yes	(García-Sánchez et al., 2004; Kamthan et al., 2012)
Orf19.4000	Grf10	Adhesion, Filamentation	Yes	(Ghosh et al., 2015)
Orf19.2842	Gzf3	Adhesion, Drug Resistance/Tolerance	Yes	(Homann et al., 2009; Fox et al., 2015)
Orf19.4225	Leu3	Adhesion	No	(Finkel et al., 2012)
Orf19.5312	Met4	Adhesion	No	(Finkel et al., 2012)
Orf19.4318	Mig1	Filamentation, Drug Resistance/Tolerance	Yes	(Homann et al., 2009; Lagree et al., 2020)
Orf19.5326	Mig2	Filamentation	No	(Lagree et al., 2020)
Orf19.6309	Mss11	Adhesion, Filamentation	Yes	(Tsai et al., 2014)
Orf19.2012	No3	Adhesion, Filamentation	No	(Cheng et al., 2003; Finkel et al., 2012)
Orf19.7150	Nrg1	Filamentation, Drug Resistance/Tolerance, Dispersion	Yes	(Wheeler et al., 2008; Uppuluri et al., 2010b)
Orf19.4093	Pes1	Filamentation, Drug Resistance/Tolerance, Dispersion	No	(Xu et al., 2007; Shen et al., 2008; Uppuluri et al., 2010a)
Orf19.2823	Rfg1	Adhesion, Filamentation	Yes	(Kadosh and Johnson, 2001; Fox et al., 2015)
Orf19.1604	Rha1	Filamentation	Yes	(Omran et al., 2020)
Orf19.7247	Rim101	Adhesion, Filamentation, Drug Resistance/Tolerance	Yes	(Cornet et al., 2006; Fox et al., 2015)
Orf19.4662	Rlm1	Drug Resistance/Tolerance, Extracellular Matrix Production	No	(Nett et al., 2011; Delgado-Silva et al., 2014)
Orf19.5953	Slp1	Adhesion	Yes	(Chen and Lan, 2015)
Orf19.5871	Snf5	Adhesion	No	(Finkel et al., 2012)
Orf19.4961	Stp2	Adhesion, Filamentation	Yes	(Böttcher et al., 2020)
Orf19.7319	Suc1	Adhesion	No	(Finkel et al., 2012)
Orf19.798	Taf14	Adhesion, Filamentation	No	(Finkel et al., 2012; Wang et al., 2020)
Orf19.4062	Try2	Adhesion	No	(Finkel et al., 2012)
Orf19.1971	Try3	Adhesion	No	(Finkel et al., 2012)

(Continued)

TABLE 1 | Continued

Core Biofilm Transcriptional Regulators				
Orf19#	Name	Known biofilm-related process affected in mutant strain	Gene upstream intergenic region bound by one or more of the core biofilm regulators?	References
Orf19.5975	Try4	Adhesion	Yes	(Finkel et al., 2012)
Orf19.3434	Try5	Adhesion	Yes	(Finkel et al., 2012)
Orf19.6824	Try6	Adhesion	Yes	(Finkel et al., 2012)
Orf19.4941	Tye7	Filamentation	Yes	(Bonhomme et al., 2011)
Orf19.7317	Uga33	Adhesion	No	(Finkel et al., 2012)
Orf19.1822	Ume6	Filamentation, Dispersion	Yes	(Uppuluri et al., 2010a; Uppuluri et al., 2010b)
Orf19.391	Upc2	Adhesion, Drug Resistance/Tolerance	No	(Silver et al., 2004; Dunkel et al., 2008; Kakade et al., 2019)
Orf19.1035	War1	Adhesion	No	(Finkel et al., 2012)
Orf19.3794	Zap1	Filamentation, Extracellular Matrix Production	Yes	(Kim et al., 2008b; Nobile et al., 2009; Ganguly et al., 2011; Finkel et al., 2012)
Orf19.1718	Zcf8	Adhesion	Yes	(Finkel et al., 2012)
Orf19.4767	Zcf28	Adhesion	No	(Finkel et al., 2012)
Orf19.5924	Zcf31	Adhesion	Yes	(Finkel et al., 2012)
Orf19.5940	Zcf32	Adhesion, Filamentation	No	(Kakade et al., 2016; Kakade et al., 2019)
Orf19.6182	Zcf34	Adhesion, Drug Resistance/Tolerance	No	(Homann et al., 2009; Oh et al., 2010; Finkel et al., 2012)
Orf19.7583	Zcf39	Adhesion	No	(Finkel et al., 2012)
Orf19.6781	Zfu2	Adhesion, Drug Resistance/Tolerance	No	(Finkel et al., 2012; Vandeputte et al., 2012)
Orf19.3187	Znc1	Adhesion	No	(Finkel et al., 2012)

has yet to be examined in the mutant strains of the core biofilm transcriptional regulators. In fact, little is known in general on the regulation of quorum sensing during *C. albicans* biofilm development.

In addition to these nine transcriptional regulators that make up the core biofilm circuit, there are 50 “auxiliary” transcriptional regulators that have been implicated in biofilm formation (Table 1). The majority of these auxiliary biofilm transcriptional regulators are also bound in their upstream intergenic regions by at least one of the initial six master biofilm transcriptional regulators (Bcr1, Tec1, Efg1, Ndt80, Rob1, or Brg1; note that of the nine core biofilm transcriptional regulators, there is not genome-wide chromatin immunoprecipitation data available for Gal4, Rfx2, and Flo8, and thus we do not know whether they bind to the auxiliary biofilm transcriptional regulators) (Table 1) (Nobile et al., 2012). As such, several of the 50 auxiliary transcriptional regulators are integrated into the larger biofilm network that includes the core nine transcriptional regulators and all of their directly bound target genes (Nobile et al., 2012). Based on existing phenotypic analyses of the mutant strains of the auxiliary biofilm transcriptional regulators, the majority (48) are implicated in the regulation of adhesion and/or filamentation (Brown et al., 1999; Kadosh and Johnson, 2001; Cheng et al., 2003; Uhl et al., 2003; García-Sánchez et al., 2004; Kelly et al., 2004; Mulhern et al., 2006; Kim et al., 2008b; Shen et al., 2008; Wheeler et al., 2008; Homann et al., 2009; Nobile et al., 2009; Pukkila-Worley et al., 2009; Uppuluri et al., 2010a; Uppuluri et al., 2010b; Askew et al., 2011; Bonhomme et al., 2011; Ganguly et al., 2011; Finkel et al., 2012; Kamthan et al., 2012; Langford et al., 2013; Delgado-Silva et al., 2014; Tsai et al., 2014; Chen and Lan, 2015; Fox et al., 2015; Ghosh et al., 2015; Kakade et al., 2016; Kakade et al., 2019; Böttcher et al., 2020; Lagree et al., 2020; Omran et al., 2020; Wang et al., 2020); 16 are implicated in

drug resistance and/or tolerance (Bruno et al., 2006; Cornet et al., 2006; Mulhern et al., 2006; Xu et al., 2007; Dunkel et al., 2008; Wheeler et al., 2008; Homann et al., 2009; Prasad et al., 2010; Nett et al., 2011; Vandeputte et al., 2012; Langford et al., 2013; Vasicek et al., 2014); two are implicated in the production of the extracellular matrix (Finkel et al., 2012; Delgado-Silva et al., 2014); and two are implicated in dispersion (Uppuluri et al., 2010b; Uppuluri et al., 2010a). Similar to the core biofilm transcriptional regulators, detailed analyses of the mutant strains of the auxiliary biofilm transcriptional regulators have not been systemically studied for known biofilm processes. Rather, most of their roles in biofilm processes have been determined through large-scale genetic screens. Of the auxiliary biofilm transcriptional regulators, we understand the least about the biofilm specific roles of Bpr1/Orf19.6874, which is only known to contribute to biofilm biomass throughout biofilm development (Fox et al., 2015). Future detailed phenotypic analyses of the auxiliary transcriptional regulator mutant strains in biofilm specific processes will certainly reveal new and additional roles for these transcriptional regulators in biofilm development.

REGULATION OF THE WHITE-OPAQUE PHENOTYPIC SWITCH

The white-opaque switch in *C. albicans* is a form of phenotypic switching that gives rise to two distinct cell types called “white” and “opaque” that display distinct phenotypic characteristics at the single cell and colony levels (Anderson and Soll, 1987; Slutsky et al., 1987; Rikkerink et al., 1988; Bergen et al., 1990; Soll, 1992; Soll et al., 1993). White cells represent the standard budding yeast form of *C. albicans*, forming shiny, white, dome-shaped colonies on solid media plates, while opaque cells are larger and

more elongated than white cells and form dull, off-white, flattened colonies on solid media plates (Slutsky et al., 1987; Soll et al., 1993; Lohse and Johnson, 2009; Noble et al., 2017). White and opaque cells differ in their virulence characteristics, metabolic preferences, mating competencies, interactions with the host innate immune system, and responses to environmental stimuli (Kolotila and Diamond, 1990; Lan et al., 2002; Lockhart et al., 2002; Miller and Johnson, 2002; Bennett et al., 2003; Geiger et al., 2004; Dumitru et al., 2007; Lohse and Johnson, 2008; Ramirez-Zavala et al., 2008; Huang et al., 2009; Huang et al., 2010; Lohse et al., 2013; Xie et al., 2013; Lohse et al., 2016; Du and Huang, 2016; Ene et al., 2016; Dalal et al., 2019). In total, nearly 20% of the transcriptome is differentially expressed, by at least twofold, between the two cell types, highlighting that the white-opaque switch involves major transcriptional rewiring (Tuch et al., 2010; Hernday et al., 2013). Under standard switch permissive growth conditions, switching between the white cell type, considered the “ground” state, and the opaque cell type, considered the “excited” state, occurs stochastically at a frequency of roughly one switch event per 1,000-10,000 cell divisions (Rikkerink et al., 1988; Bergen et al., 1990; Ramirez-Zavala et al., 2008; Alby and Bennett, 2009b). Each cell type is heritably maintained without any change to the primary sequence of the genome, thus fitting the classic definition of an epigenetic switch (Slutsky et al., 1987; Soll et al., 1993; Zordan et al., 2006; Zordan et al., 2007). The switch is responsive to the combined effects of environmental signals, such as carbon source, pH, CO₂ levels, and temperature, which can differentially bias the cell population towards one of the two cell types (Dumitru et al., 2007; Ramirez-Zavala et al., 2008; Alby and Bennett, 2009a; Huang et al., 2009; Huang, 2012; Lohse et al., 2013; Du and Huang, 2016; Ene et al., 2016; Dalal et al., 2019). Mating type can also influence the ability of the cells to undergo white-opaque switching, where *MTL* heterozygous (a/α) cells are typically “locked” in the white state, while *MTL* hemizygous (a/Δ , α/Δ), homozygous (a/a , or α/α), and haploid (a or α) cells are capable of undergoing stochastic white-opaque switching (Hull and Johnson, 1999; Lockhart et al., 2002; Miller and Johnson, 2002). This mating type dependency, however, is not exclusive to all strains; in fact, a significant fraction of *MTL* heterozygous clinical isolates can be induced to form opaque cells under specific growth conditions that promote white to opaque switching in *MTL* hemizygous, homozygous, or haploid cells (Xie et al., 2013).

Through a combination of forward and reverse genetic approaches, a total of 112 transcriptional regulators and one protein binding cofactor (*Ssn6*) have been identified which, when deleted, significantly impact the frequency of white-opaque switching (Table 2) (Huang et al., 2006; Srikantha et al., 2006; Zordan et al., 2006; Zordan et al., 2007; Hernday et al., 2013; Lohse et al., 2013; Du et al., 2015; Hernday et al., 2016; Lohse et al., 2016; Lohse and Johnson, 2016). Of these 113 switch regulating proteins, eight (*Wor1*, *Wor2*, *Wor3*, *Wor4*, *Czfl*, *Efg1*, *Ahr1*, and *Ssn6*) are considered to be core switch regulators, and have been extensively characterized by genome-wide transcriptional profiling and chromatin immunoprecipitation

approaches in white and opaque cell types; the remaining 105 switch regulating proteins are considered to be auxiliary switch regulators (Table 2) (Sonneborn et al., 1999; Srikantha et al., 2000; Huang et al., 2006; Zordan et al., 2006; Zordan et al., 2007; Vinces and Kumamoto, 2007; Lohse and Johnson, 2010; Wang et al., 2011; Hernday et al., 2013; Lohse et al., 2013; Lohse and Johnson, 2016; Hernday et al., 2016). Together, these eight core switch regulators form complex cell type specific networks, with 203 bound target genes in white cells and 756 bound target genes in opaque cells (Hernday et al., 2013; Lohse et al., 2013; Hernday et al., 2016; Lohse and Johnson, 2016). At the center of the white and opaque specific regulatory networks are two distinct transcriptional circuits (see Figure 3A for the white circuit, Figure 3B for the opaque circuit, and Figure 3C for the combined white and opaque overlaid circuits) that consist of interconnected positive and negative feedback loops that govern the cell fate and heritable maintenance of the white and opaque cell types (Vinces et al., 2006; Vinces and Kumamoto, 2007; Zordan et al., 2007; Hernday et al., 2013; Hernday et al., 2016; Lohse and Johnson, 2016). Although several groups have identified kinases, chromatin modifiers, and other proteins that also affect white-opaque switching (Hnisz et al., 2009; Noble et al., 2017; Rai et al., 2018); here, we focus on the eight core switch regulators (TFs: *Wor1*, *Wor2*, *Wor3*, *Wor4*, *Czfl*, *Efg1*, *Ahr1*; and cofactor: *Ssn6*) for which genome-wide transcriptional profiling and chromatin immunoprecipitation data are available.

Wor1 is considered to be the master regulator of the white-opaque switch, as it is the only switch regulator that is known to be required for both the transition to, and heritable maintenance of, the opaque cell type (Huang et al., 2006; Srikantha et al., 2006; Zordan et al., 2006; Zordan et al., 2007; Hernday et al., 2013; Lohse et al., 2013; Hernday et al., 2016; Lohse and Johnson, 2016). Furthermore, ectopic *WOR1* expression can rescue opaque cell formation in all known mutant backgrounds that fail to spontaneously switch to the opaque cell type (Zordan et al., 2007; Du et al., 2012a; Lohse and Johnson, 2016). *WOR1* expression is repressed in white cells, where *Wor1* protein levels have been found to be nearly undetectable (Huang et al., 2006; Srikantha et al., 2006; Zordan et al., 2006; Zordan et al., 2007; Lohse and Johnson, 2010). In opaque cells, *WOR1* is highly transcribed, and *Wor1* protein levels have been found to accumulate to elevated levels (Huang et al., 2006; Srikantha et al., 2006; Zordan et al., 2006; Zordan et al., 2007; Lohse and Johnson, 2010). Stochastic white to opaque switching is thought to be the result of transcriptional noise within the white cell circuit that occasionally allows *Wor1* levels to surpass a critical threshold necessary to induce the transition to the opaque state (Srikantha et al., 2006; Hernday et al., 2010; Lohse and Johnson, 2010; Nobile et al., 2012; Guan and Liu, 2015; Horwitz et al., 2015; Lohse and Johnson, 2016; Lohse et al., 2016a; Tandonnet and Torres, 2017). Once established, the excited opaque cell circuit is stably maintained by a series of nested feedback loops, including a positive autoregulatory feedback loop generated by *Wor1* binding to the upstream intergenic region of *WOR1* (Zordan et al., 2007; Hernday et al., 2013). This *Wor1*-induced positive feedback loop, along with other opaque specific binding

TABLE 2 | Known transcriptional regulators and a protein cofactor with roles in the *C. albicans* white-opaque switch[†].

Core White-Opaque Transcriptional Regulators and a Protein Cofactor				
Orf19#	Name	Known effect on white-opaque switch in mutant strain*		Gene upstream intergenic bound by one or more of the core white-opaque regulators?
		White to Opaque	Opaque to White	
Orf19.7381	Ahr1	2.0	-7.8	Yes
Orf19.3127	Cz11	-21.9	-16.8	Yes
Orf19.610	Efg1	24.0	-62.7	Yes
Orf19.6798	Ssn6	N/A	N/A	Yes
Orf19.4884	Wor1	-20.8	N/A	Yes
Orf19.5992	Wor2	-32.9	N/A	Yes
Orf19.467	Wor3	-2.4	-3.9	Yes
Orf19.6713	Wor4	-13.3	N/A	Yes
Auxiliary White-Opaque Transcriptional Regulators				
Orf19.7436	Aaf1	-1.1	-2.7	Yes
Orf19.2272	Aft2	-2.8	-1.7	Yes
Orf19.4766	Arg81	1.8	-2.3	Yes
Orf19.166	Asg1	-21.6	-22.1	Yes
Orf19.5343	Ash1	-1.2	-26.9	Yes
Orf19.6874	Bas1	-1.5	2.5	Yes
Orf19.723	Bcr1	2.2	N/A	Yes
Orf19.4056	Brg1	1.9	-1.5	Yes
Orf19.1623	Cap1	-1.5	-4.4	Yes
Orf19.4670	Cas5	1.4	-2.3	Yes
Orf19.4433	Cph1	-2.2	-2.6	Yes
Orf19.1187	Cph2	-2.3	-1.4	No
Orf19.7359	Crz1	1.9	-5.6	Yes
Orf19.3794	Csr1	1.0	2.6	Yes
Orf19.7374	Cta4	-1.1	-5.9	Yes
Orf19.4288	Cta7	2.4	-2.1	Yes
Orf19.5001	Cup2	-1.2	-1.6	Yes
Orf19.6514	Cup9	4.7	-15.4	Yes
Orf19.3252	Dal81	-6.1	-1.8	Yes
Orf19.2088	Dpb4	-3.1	-2.4	Yes
Orf19.2623	Ecm22	1.3	-2.2	Yes
Orf19.5498	Efh1	1.7	-1.6	Yes
Orf19.6817	For1	-1.9	-1.6	Yes
Orf19.2054	Fgr15	-17.7	4.8	Yes
Orf19.1093	Flo8	-27.8	N/A	No
Orf19.5338	Gal4	-23.9	-1.3	Yes
Orf19.3182	Gis2	-1.2	-9.4	Yes
Orf19.4000	Grf10	1.4	-6.9	Yes
Orf19.2842	Gzf3	-12.3	1.7	Yes
Orf19.1228	Hap2	-28.6	-1.6	No
Orf19.4647	Hap3	-3.0	1.3	Yes
Orf19.517	Hap31	-22.7	-1.3	Yes
Orf19.740	Hap41	-9.6	1.1	Yes
Orf19.1481	Hap42	-2.0	-1.9	No

(Continued)

TABLE 2 | Continued

Auxiliary White-Opaque Transcriptional Regulators				
Orf19#	Name	Known effect on white-opaque switch in mutant strain*		Gene upstream intergenic bound by one or more of the core white-opaque regulators?
		White to Opaque	Opaque to White	
Orf19.1973	Hap5	-6.7	-3.0	Yes
Orf19.4853	Hcm1	18.3	-3.7	Yes
Orf19.3063	Hfl1	-21.0	2.1	Yes
Orf19.7539	Ino2	-23.5	-3.6	Yes
Orf19.837.1	Ino4	-3.0	-1.2	Yes
Orf19.7401	Isw2	3.4	2.9	Yes
Orf19.3736	Kar4	-2.0	1.2	Yes
Orf19.4776	Lys143	7.3	-1.1	Yes
Orf19.5380	Lys144	1.3	-2.4	Yes
Orf19.7068	Mac1	-19.4	-1.6	Yes
Orf19.4318	Mig1	-29.7	1.4	Yes
Orf19.5326	Mig2	1.6	-1.6	Yes
Orf19.4752	Msn4	1.9	-4.7	Yes
Orf19.2119	Ndt80	-10.1	1.9	Yes
Orf19.5910	Nto1	2.8	-1.5	Yes
Orf19.1543	Opi1	4.0	-2.4	Yes
Orf19.4231	Pth2	3.0	-4.1	Yes
Orf19.1773	Rap1	16.0	-1.6	Yes
Orf19.5558	Rbf1	N/A	-32.4	Yes
Orf19.6102	Rca1	-9.1	-1.9	Yes
Orf19.7521	Rep1	-1.5	2.4	Yes
Orf19.2823	Rtg1	1.1	2.1	Yes
Orf19.3865	Rfx1	1.8	1.7	Yes
Orf19.4590	Rfx2	1.5	-1.7	Yes
Orf19.1604	Rha1	1.0	-2.7	Yes
Orf19.4438	Rme1	2.1	-1.8	Yes
Orf19.513	Ron1	-1.2	-1.7	Yes
Orf19.1069	Rpn4	18.2	-1.5	No
Orf19.4722	Rtg1	-2.1	-2.9	Yes
Orf19.2315	Rtg3	-2.8	-2.2	Yes
Orf19.1926	Sef2	1.1	-3.3	Yes
Orf19.454	Sfl1	-1.1	2.0	Yes
Orf19.971	Skn7	1.1	-1.5	Yes
Orf19.1032	Sko1	-1.8	-2.4	No
Orf19.4961	Stp2	9.2	-6.9	Yes
Orf19.909	Stp4	3.3	-2.2	Yes
Orf19.4545	Swi4	-4.5	1.0	Yes
Orf19.4941	Tye7	2.0	-1.0	Yes
Orf19.7317	Uga33	-1.0	-1.7	Yes
Orf19.1822	Ume6	-1.6	2.0	Yes
Orf19.2745	Ume7	-2.0	1.4	Yes
Orf19.391	Upc2	-1.1	3.1	Yes
Orf19.1035	War1	-3.2	-1.1	No
Orf19.5210	Xbp1	-6.4	-1.2	Yes
Orf19.2808	Zcf16	1.5	1.2	Yes

(Continued)

TABLE 2 | Continued

Auxiliary White-Opaque Transcriptional Regulators				
Orf19#	Name	Known effect on white-opaque switch in mutant strain*		Gene upstream intergenic bound by one or more of the core white-opaque regulators?
		White to Opaque	Opaque to White	
Orf19.3305	Zcf17	1.3	2.2	Yes
Orf19.431	Zcf2	-1.7	-2.8	Yes
Orf19.4145	Zcf20	-1.5	-2.2	Yes
Orf19.4166	Zcf21	-4.1	-40.4	Yes
Orf19.4251	Zcf22	1.8	-1.1	Yes
Orf19.4524	Zcf24	-1.0	-3.2	Yes
Orf19.4568	Zcf25	8.5	-2.9	Yes
Orf19.4649	Zcf27	-1.9	1.5	Yes
Orf19.5251	Zcf30	1.1	-1.7	Yes
Orf19.5924	Zcf31	-2.4	3.2	Yes
Orf19.6182	Zcf34	-2.9	-4.6	Yes
Orf19.1685	Zcf7	4.7	-2.7	Yes
Orf19.1718	Zcf8	-2.1	-2.2	Yes
Orf19.6781	Zfu2	-1.9	2.3	Yes
Orf19.6888	Zfu3	-5.0	-16.2	Yes
Orf19.5026	Zms1	-2.8	-1.2	Yes
Orf19.1150		1.2	-1.3	No
Orf19.1274		-1.4	1.2	No
Orf19.1577		-1.1	-1.5	No
Orf19.1757		1.0	-1.6	Yes
Orf19.217		-1.7	-1.7	Yes
Orf19.2476		1.9	2.5	Yes
Orf19.2612		2.4	1.4	Yes
Orf19.2961		7.0	2.0	Yes
Orf19.3928		5.7	-4.4	Yes
Orf19.7098		7.8	1.1	Yes

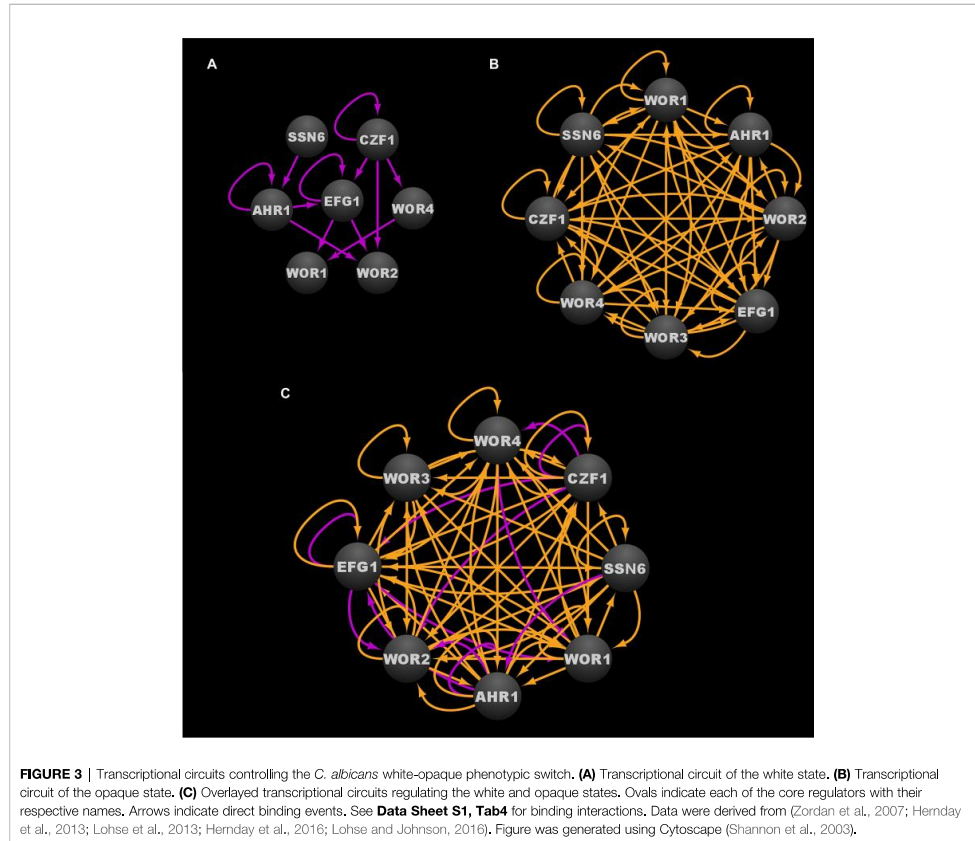
*Data derived from (Zordan et al., 2007; Hernday et al., 2013; Lohse et al., 2013; Hernday et al., 2016; Lohse et al., 2016; Lohse and Johnson, 2016). *Fold change in switch frequency is relative to a wildtype reference strain.

interactions between the white and opaque regulators and their respective upstream intergenic regions, is proposed to be a central mechanism that mediates the epigenetic heritability of the opaque cell type (Huang et al., 2006; Srikantha et al., 2006; Zordan et al., 2006; Zordan et al., 2007; Lohse and Johnson, 2010; Wang et al., 2011; Hernday et al., 2013; Lohse et al., 2013; Lohse and Johnson, 2016; Hernday et al., 2016). Stochastic opaque to white switching is believed to occur when transcriptional noise causes *Wor1* levels to drop below a critical threshold, thus leading to a collapse of the excited opaque cell transcriptional program and a return to the ground white cell transcriptional program (Srikantha et al., 2006; Zordan et al., 2006; Lohse and Johnson, 2010).

The core transcriptional circuit in white cells consists of a series of feed-forward loops that ultimately repress the expression of *WOR1* and *WOR2*, both of which are key players

in the establishment and/or maintenance of the opaque cell type (Zordan et al., 2007). *Efg1*, *Ahr1*, and *Ssn6* all contribute to the stability of the white cell circuit and are believed to directly or indirectly repress the expression of *WOR1* and *WOR2* (Zordan et al., 2007; Tuch et al., 2010; Hernday et al., 2013; Hernday et al., 2016). Deletion of *EFG1*, *AHR1*, or *SSN6* destabilizes the white cell circuit such that most, if not all, of the cells in the population transition to the opaque state (Sonneborn et al., 1999; Srikantha et al., 2000; Vinces et al., 2006; Vinces and Kumamoto, 2007; Zordan et al., 2007; Wang et al., 2011; Hernday et al., 2016). *Czf1*, *Wor3*, and *Wor4* are capable of destabilizing the white cell circuit, and induced expression of *CZF1*, *WOR3*, or *WOR4* in white cells can promote white to opaque switching in a *Wor1* dependent manner (Zordan et al., 2007; Hernday et al., 2013; Lohse et al., 2013; Lohse and Johnson, 2016). Interestingly, neither *Czf1* nor *Wor3* is required for the heritable maintenance of the opaque state once switching has occurred (Zordan et al., 2007; Lohse et al., 2013). Based on these results and the structure of the white cell regulatory circuit (Figure 3A), *Czf1* and *Wor4* are thought to destabilize the white cell type by directly and indirectly antagonizing the white cell stabilizing activities of *Ssn6*, *Ahr1*, and *Efg1*, and by inducing opaque promoting factors such as *WOR3*, thus introducing the transcriptional noise that leads to the stochastic activation of the *WOR1* positive feedback loop and the transition to the opaque state. In addition to repression of *WOR1* and *WOR2*, the white cell transcriptional program results in repression of opaque enriched transcripts (e.g. *WOR3* and *CZF1*) as well as the activation of white enriched transcripts (e.g. *EFG1*), thus creating a series of feed-forward loops that act to stabilize the white cell circuit and prevent activation of the opaque state (Zordan et al., 2007; Hernday et al., 2013; Lohse et al., 2013).

In contrast to the core transcriptional circuit of the white cell type (Figure 3A), the core transcriptional circuit of the opaque cell type is extensively intertwined (Figure 3B). All of the core switch regulators are active in opaque cells, and they are each found to bind to their own upstream intergenic regions, along with the upstream intergenic regions of most, if not all, of the other core switch regulators (Figure 3B) (Huang et al., 2006; Srikantha et al., 2006; Zordan et al., 2006; Zordan et al., 2007; Wang et al., 2011; Hernday et al., 2013; Lohse et al., 2013; Hernday et al., 2016; Lohse and Johnson, 2016). To highlight this point, 58 of the 64 possible binding interactions between the core switch regulators and their respective upstream intergenic regions are observed in opaque cells (Data Sheet S1, Tab1). Although the logic of the opaque transcriptional circuit has yet to be fully elucidated, the high degree of interconnectivity between the core opaque regulators likely contributes to the robustness, yet reversibility, of the opaque cell state. Similar to the white cell circuit, *Wor1* is a critical player in the opaque cell circuit; however, it is the sustained high levels of *WOR1* expression, rather than its repression, that is required for the formation and stable maintenance of the opaque cell type (Huang et al., 2006; Srikantha et al., 2006; Zordan et al., 2006). Although not strictly required for the formation of an opaque cell, *Wor2* and *Wor4* also play important roles in the heritable maintenance of the



opaque transcriptional program (Zordan et al., 2007; Lohse and Johnson, 2016). Strains lacking *WOR2* or *WOR4* are locked in the white cell type and fail to undergo spontaneous white to opaque switching, yet can be induced to form opaque cells by ectopic expression of *WOR1* (Frazer et al., 2020). These induced opaque cells, however, are unstable, and quickly revert to the white cell type when ectopic *WOR1* expression is repressed, indicating that *Wor2* and *Wor4* play essential roles in the heritability of opaque cells (Zordan et al., 2007). Interestingly, with the exception of *Ahr1*, all switch regulators discovered to date have been found to contain prion-like domains that enable liquid-liquid demixing and the formation of phase-separated condensates (Frazer et al., 2020). Several of the switch regulators, including *Wor1* and *Wor4*, have been shown to undergo phase separation *in vitro*, and to form condensates at genomic loci *in vivo*, in a manner similar to the formation of mammalian super-enhancers (Frazer et al., 2020). Combined with the observation that many of the target genes bound by the switch regulators are flanked by unusually large upstream

intergenic regions (Zordan et al., 2007; Hernday et al., 2013), and the discovery that specific residues within the *Wor1* prion-like domain are required for condensate formation and white to opaque switching, it seems likely that these phase-separated condensates formed by the core switch regulators in opaque cells are critical factors that contribute to the formation and heritable maintenance of the opaque cell type.

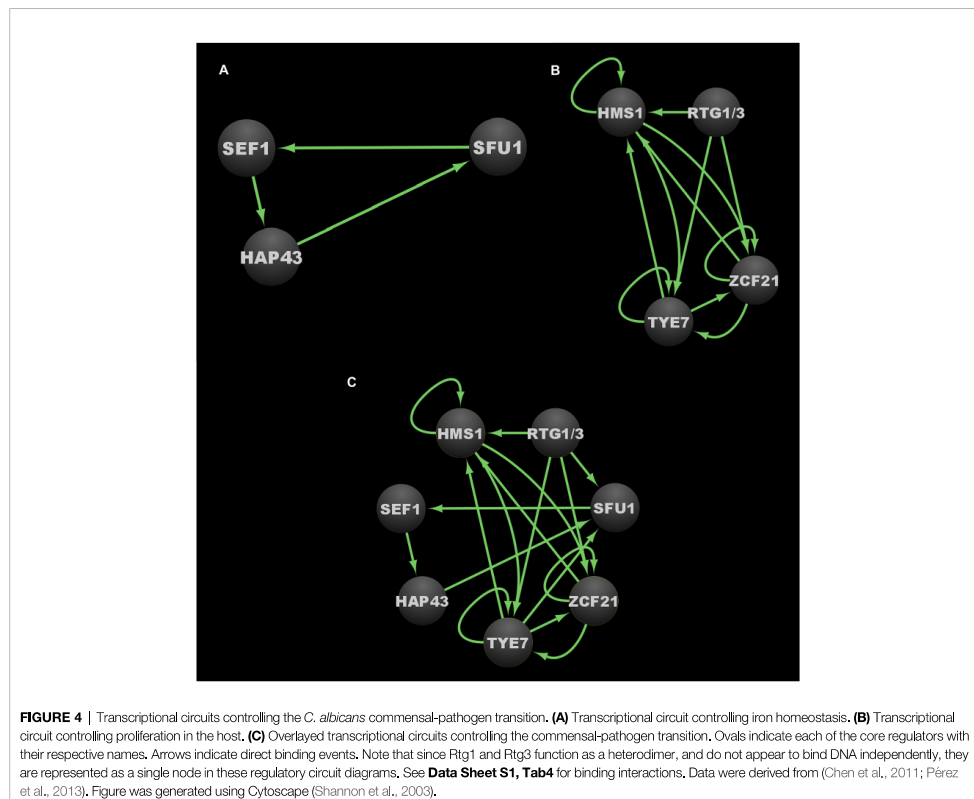
REGULATION OF THE COMMENSAL-PATHOGEN TRANSITION

C. albicans typically exists as a commensal member of the healthy human microbiota. It can also transition into a pathogen in response to specific host environmental cues. In its pathogenic state, *C. albicans* can cause a wide range of infections, from acute to chronic superficial mucosal infections to severe and life-threatening disseminated bloodstream infections (Wenzel, 1995; Hube, 2004;

Pappas et al., 2004). Although immunocompetent individuals with healthy and balanced microbiota are typically not adversely affected by *C. albicans*, immunocompromised individuals can suffer severe infections with significant morbidity and mortality (Wenzel, 1995; Nobile and Johnson, 2015). Understanding the genetic regulatory mechanisms that control the *C. albicans* commensal-pathogen transition has the potential to lead to the development of targeted therapeutic strategies against *C. albicans* in its pathogenic state, without affecting its commensal state and the delicate balance of the microbiota.

Two distinct *C. albicans* transcriptional networks controlling the commensal-pathogen transition were described in 2011 and 2013, one governing iron homeostasis, and the other governing proliferation in the host, respectively (see **Figure 4A** for the iron homeostasis circuit, **Figure 4B** for the proliferation in the host circuit, and **Figure 4C** for the combined commensal-pathogen overlaid circuits) (Chen et al., 2011; Pérez et al., 2013). As a commensal of the gastrointestinal (GI) tract, *C. albicans* is exposed to varying and often abundant levels of iron from food, and thus a tightly regulated transcriptional response is important for *C.*

albicans to control iron assimilation and to avoid iron toxicity in the GI tract (McCance and Widdowson, 1938; Martin et al., 1987; Miret et al., 2003). On the other hand, when *C. albicans* causes a disseminated bloodstream infection, iron is extremely limiting, and to survive, *C. albicans* must conserve and scavenge iron from the bloodstream. Three transcriptional regulators, Sef1, Sfu1, and Hap43, were found to form a tightly knit transcriptional network, encompassing 214 downstream target genes (Chen et al., 2011). These three transcriptional regulators control iron homeostasis and were found to be essential for *C. albicans* to survive as both a commensal and as a pathogen within the mammalian host (Chen et al., 2011). Iron homeostasis in many other fungi (such as in other ascomycetes and the basidiomycete, *Cryptococcus neoformans*) is commonly regulated by a bipartite regulatory circuit composed of orthologs of Sfu1 and Hap43, where Sfu1 orthologs repress iron acquisition genes and *HAP43* orthologs, while Hap43 orthologs repress nonessential iron utilization genes and *SFU1* orthologs. This mutually repressive regulatory interaction between orthologs of Sfu1 and Hap43 in other fungi is significantly altered in *C. albicans* by the intercalation of Sef1 as a third player within this circuit



(Figure 4A) (Chen et al., 2011). In *C. albicans*, Sfu1 directly represses *SEF1* and iron acquisition genes under iron replete conditions (Chen et al., 2011). In response to iron limitation, Sef1 serves to directly activate *HAP43* and iron uptake genes, while Hap43 directly represses *SFU1* and iron utilization genes (Chen et al., 2011). Although the roles for Hap43 in *C. albicans* are similar to those of other fungi, the reciprocal interaction between Sfu1 and *HAP43* is altered in *C. albicans* by the inclusion of Sef1, which serves as an intermediary between Sfu1 and *HAP43*. *C. albicans* *SEF1* and *SFU1* are differentially expressed between growth in the GI tract versus growth in the bloodstream (Chen et al., 2011), thus providing dual inputs into the circuit controlling iron acquisition and utilization. While both Sef1 and Sfu1 serve to promote commensalism in a mouse GI commensal model, only Sef1 is required for virulence in a mouse disseminated infection model (Chen et al., 2011). Interestingly, deletion of *SFU1* conferred a significant competitive advantage over wildtype cells in the disseminated infection model (Chen et al., 2011), indicating that Sfu1 serves not only to promote commensalism in the GI tract, but also to attenuate virulence in the bloodstream. (See Table 3 for information on these three core transcriptional regulators in the commensal-pathogen transition.) Ultimately the *C. albicans* iron homeostasis circuit produces a well conserved transcriptional output consisting of increased iron uptake and reduced iron utilization in iron limited environments, and decreased iron uptake and increased iron utilization in iron replete conditions. Despite being well conserved in its transcriptional output, the iron homeostasis circuit appears to be uniquely evolved in *C. albicans* to control the delicate balance between its commensal and pathogenic growth states.

A subsequent study identified eight transcriptional regulators (Tye7, Orf19.3625, Lys144, Zcf21, Lys14, Hsm1, Rtg1, and Rtg3) that influence *C. albicans* proliferation in the commensal and/or pathogenic growth states (Pérez et al., 2013). These regulators were identified by screening a subset of the commonly used *C. albicans*

TF mutant library (Homann et al., 2009) for defects in a commensal (GI colonization) mouse model and a pathogenic (disseminated infection) mouse model. This subset of the TF mutant library consisted of those mutant strains that revealed no phenotypes in a diverse panel of *in vitro* growth conditions, and was screened to identify transcriptional regulators that were specifically required for normal (wildtype) levels of growth in either of the two mouse models (Homann et al., 2009; Pérez et al., 2013). Of the eight regulators that were identified, six (Rtg1, Rtg3, Tye7, Hms1, Orf19.3625, and Lys144) were required for GI colonization, while five (Rtg1, Rtg3, Hms1, Lys14, and Zcf21) were required for robust growth in the disseminated infection model (Pérez et al., 2013). Overall, Tye7, Orf19.3625, and Lys144 were found to be specific to commensal colonization of the GI tract; Zcf21 and Lys14 were found to be specific to disseminated infections; and Rtg1, Rtg3, and Hms1 were found to be associated generally with growth in the host (Pérez et al., 2013). Based on genome-wide transcriptional profiling and chromatin immunoprecipitation data, seven of these regulators (Tye7, Lys144, Zcf21, Lys14, Hsm1, Rtg1, and Rtg3) were found to form a transcriptional network consisting of 808 directly bound target genes. Significant overlap was observed between the bound target genes of this network and those genes that were upregulated in the mouse GI model compared to growth *in vitro*. Orf19.3625 was excluded from this analysis as it is a predicted subunit of a histone remodeling complex, and thus was not considered to be a specific regulator within the commensal-pathogen network. In contrast to the transcriptional network defined by Sef1, Sfu1, and Hap43, which is primarily responsible for regulating genes involved in iron homeostasis (Chen et al., 2011), the transcriptional network defined by Tye7, Lys144, Zcf21, Lys14, Hsm1, Rtg1, and Rtg3 appears to primarily regulate genes involved in the acquisition and metabolism of carbon and nitrogen, as well as genes that encode transporters and cell surface proteins (Pérez et al., 2013). The binding profiles for Rtg1 and Rtg3 were observed to be identical, and thus they likely function as a heterodimer to bind DNA (Pérez

TABLE 3 | Known transcriptional regulators with roles in the *C. albicans* commensal-pathogen transition.

Core Iron Homeostasis Transcriptional Regulators				
Orf19#	Name	Known commensal-pathogen-related process affected in mutant strain	Gene upstream intergenic region bound by one or more of the core regulators?	References
Orf19.681	Hap43	Iron Utilization	Yes	(Baek et al., 2008; Chen et al., 2011; Hsu et al., 2011)
Orf19.3753	Sef1	Iron Uptake	Yes	(Chen et al., 2011)
Orf19.4869	Sfu1	Iron Acquisition	Yes	(Lan et al., 2004; Chen et al., 2011)
Core Host Proliferation Transcriptional Regulators				
Orf19#	Name	Known commensal-pathogen-related process affected in mutant strain	Gene upstream intergenic region bound by one or more of the core biofilm regulators?	References
Orf19.921	Hms1	GI Colonization, Disseminated Infection	Yes	(Shapiro et al., 2012; Pérez et al., 2013)
Orf19.4722	Rtg1	GI Colonization, Disseminated Infection	Yes	(Jia et al., 1997; Pérez et al., 2013)
Orf19.2315	Rtg3	GI Colonization, Disseminated Infection	Yes	(Jia et al., 1997; Pérez et al., 2013)
Orf19.4941	Tye7	GI Colonization	Yes	(Pérez et al., 2013)
Orf19.4166	Zcf21	Disseminated Infection	Yes	(Pérez et al., 2013)

et al., 2013), which is consistent with their orthologs in *Saccharomyces cerevisiae* (Liu and Butow, 2006). Of the 153 direct target genes in this network that are upregulated during GI colonization and disseminated infection, 108 of them are bound by the Rtg1/3 heterodimer (Pérez et al., 2013), highlighting the central role that Rtg1/3 plays in this network. We note that a subsequent study by the same group identified five transcriptional regulators that influence fitness in an oropharyngeal candidiasis model (Cup9, Zcf8, Zcf21, Zcf27, and Orf19.217), and identified a set of genes that are differentially regulated in response to deletion of *CUP9* (Meir et al., 2018). We did not include these data in our analyses since binding experiments that would be necessary to integrate these additional regulators into the commensal-pathogen transcriptional circuit have not been performed.

At the core of this commensal-pathogen transcriptional network lies a tightly interwoven regulatory circuit defined by the binding interactions between five of these transcriptional regulators (Hms1, Zcf21, Tye7, Rtg1, and Rtg3) and their respective upstream intergenic regions (Figure 4B). While Lys14 and Lys144 are clearly important for pathogenic and commensal growth, respectively, they are not integrated into the core transcriptional circuit and instead appear to function as auxiliary regulators. Interestingly, *RTG1* and *RTG3* are not regulated at the transcriptional level in response to growth in the GI tract and are not direct targets of any of the members of this commensal-pathogen transcriptional circuit (Pérez et al., 2013). Instead, Rtg1/3 seems to function as a major regulatory input into, rather than target of, this commensal-pathogen circuit. In *S. cerevisiae*, the Rtg1/3 heterodimer is known to be post-translationally modified and translocated into the nucleus in response to growth on poor nitrogen sources or mitochondrial dysfunction, suggesting that nitrogen assimilation and metabolic adaptation could be critical factors for the proliferation of *C. albicans* in the host (Liao and Butow, 1993; Jia et al., 1997; Liu and Butow, 2006). Hms1, which is also required for both commensal and pathogenic growth in the host, is known to be activated in response to elevated temperatures (Shapiro et al., 2012), indicating that temperature, along with nitrogen source(s), represent two critical environmental signals that influence the commensal and pathogenic growth programs of *C. albicans*. Zcf21 represses a variety of genes that encode key virulence factors, and plays a major role in pathogenesis by balancing the positive effects of these virulence factors during disseminated infection against the increased susceptibility to host immune system recognition and clearance that is correlated with their expression (Böhm et al., 2016). Finally, Tye7 has been implicated in the metabolism of carbohydrates, such as oligosaccharides and polysaccharides, as well as in the regulation of hyphal growth and biofilm formation (Askew et al., 2009; Bonhomme et al., 2011). (See Table 3 for information on these five core transcriptional regulators in the commensal-pathogen transition.) Although both the iron homeostasis and the host proliferation transcriptional networks are critical to the ability of *C. albicans* to grow as a commensal and as a pathogen, there is limited interconnectivity between these networks at the level of the core regulators of each circuit (Figure 4C). *SFU1* serves as the sole point of integration between the two circuits, being bound by Rtg1/3

and Tye7. There are no binding interactions observed between the iron homeostasis regulators (Sef1, Sfu1, and Hap43) and the genes encoding the host proliferation regulators, suggesting that under certain growth conditions which alter the binding of Rtg1/3 and/or Tye7, the iron homeostasis circuit may function as a sub-circuit of the host proliferation circuit. Together, the transcriptional regulators involved in iron homeostasis and acquisition, and host proliferation, confer *C. albicans* with the ability to proliferate in different niches of the host as well as to transition between commensal and pathogenic states in response to changes in the host environment.

INTEGRATION OF NETWORKS

In total, the three larger regulatory networks, consisting of the core regulators and all of their directly bound target genes involved in biofilm formation, the white-opaque phenotypic switch, and the commensal-pathogen transition in *C. albicans* encompass at least 1657 directly bound individual target genes, making up a little over 25% of genes in the entire genome (note that Flo8, Gal4, and Rfx2 were excluded from this analysis since there is not genome-wide chromatin immunoprecipitation data available for them) (Data Sheet S1, Tab2) (Zordan et al., 2007; Chen et al., 2011; Nobile et al., 2012; Hernday et al., 2013; Lohse et al., 2013; Pérez et al., 2013; Fox et al., 2015; Hernday et al., 2016; Lohse and Johnson, 2016). These three networks are highly intertwined, with 40% (667/1657) of the target genes shared between at least two of the networks, and 11% (188/1657) of the target genes shared between all three networks (Data Sheet S1, Tab2). This high degree of interconnectivity is even more pronounced at the level of the core transcriptional circuits that control these three networks, as is evident by the extensive binding interactions present between the core regulators themselves (Figure 5 and Data Sheet S1, Tab1). Together, the twenty transcriptional regulators for which we have genome-wide chromatin immunoprecipitation data available form a total of 225 binding interactions within and between their core circuits, distributed roughly evenly between intra-circuit (49%) and inter-circuit (51%) interactions (note that the Rtg1/3 heterodimer is counted as a single regulator since neither subunit is known to bind independently) (Data Sheet S1, Tab3). The commensal-pathogen circuit and the biofilm circuit are highly intertwined with the regulators in the other circuits, with 66% and 59% inter-circuit interactions, respectively, while the opaque cell circuit appears to be much more isolated, with the majority (64%) of its interactions being intra-circuit (Data Sheet S1, Tab3). Perhaps the most striking example of integration between the circuits is exemplified by Ndt80 in the biofilm circuit, which binds to the upstream intergenic regions of 22 out of 24 of the core regulators (all but the upstream intergenic regions of *RTG1* and *RTG3*) (Data Sheet S1, Tab1). The percentage of inter-circuit binding events is highest for Tye7 (79%), Zcf21 (75%), Bcr1 (71%), Brg1 (67%), and Rtg1/3 (67%), accounting for at least two out of three binding events for each of these regulators within the three core circuits (Data Sheet S1, Tab3). At the opposite end of the spectrum, Hap43, Hms1, and Sfu1 are exclusive to the commensal-pathogen circuit. In addition, at

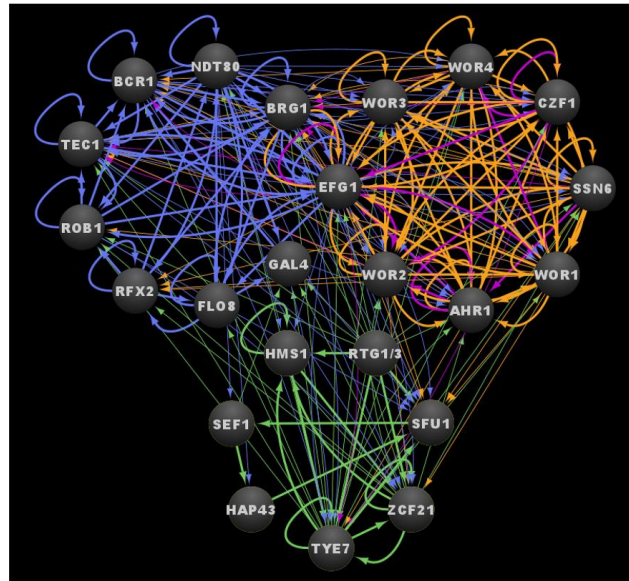


FIGURE 5 | Integrated transcriptional circuits of *C. albicans* biofilm formation, the white-opaque switch and the commensal-pathogen transition. Ovals indicate each of the core regulators with their respective names. Arrows indicate direct binding events. See **Data Sheet S1, Tab4** for binding interactions. Data were derived from (Zordan et al., 2007; Chen et al., 2011; Nobile et al., 2012; Hernday et al., 2013; Lohse et al., 2013; Pérez et al., 2013; Fox et al., 2015; Hernday et al., 2016; Lohse and Johnson, 2016). Figure was generated using Cytoscape (Shannon et al., 2003).

least two thirds of the binding events observed for Wor3 (88%), Czf1 (75%), Rob1 (71%), Ahr1 (70%), and Wor4 (70%) within the three core circuits occur within their respective core circuits (**Data Sheet S1, Tab3**). Interestingly, the degree of Efg1 inter-circuit interaction is unique to the circuit within which it lies, where 61% inter-circuit interactions are observed for Efg1 in the biofilm circuit, while only 42% inter-circuit interactions are observed for Efg1 in the white-opaque circuit (**Data Sheet S1, Tab3**). *BRG1* is the most highly integrated target within the three circuits, where it is bound by seventeen of the twenty core regulators evaluated (leaving out Gal4, Rfx2, and Flo8, and considering Rtg1 and Rtg3 as a single regulator) (**Data Sheet S1, Tab1**). Overall, more than half (thirteen out of twenty-four) of the regulators that make up the three core circuits are bound by at least half (eleven or more) of the twenty core regulators evaluated (**Data Sheet S1, Tab1**). These rather striking numbers highlight the degree to which these circuits are intertwined, and these numbers are only likely to increase as additional core regulators are identified and incorporated into the three transcriptional circuits.

The extensive integration between these core transcriptional circuits appears to have significant functional relevance. For example, 14 of the 24 regulator genes discussed (*AHR1*, *BCR1*, *BRG1*, *CZF1*, *GAL4*, *HAP43*, *HMS1*, *RFX2*, *SEF1*, *SFU1*, *TEC1*,

WOR1, *WOR3*, *ZCF21*) are differentially expressed by at least twofold between planktonic and biofilm growth conditions; of these fourteen genes, all but *GAL4* are upregulated in biofilms (**Data Sheet S1, Tab1**) (Nobile et al., 2012). A similar trend is observed during white-opaque switching, where eleven of the twenty-four regulator genes (*BRG1*, *CZF1*, *EFG1*, *GAL4*, *HMS1*, *RFX2*, *ROB1*, *TYE7*, *WOR1*, *WOR2*, *WOR3*) are differentially expressed by at least twofold between white and opaque cell types (**Data Sheet S1, Tab1**) (Tuch et al., 2010). The interactions between the biofilm circuit and the white-opaque circuit are particularly striking. All eight of the core white-opaque regulator genes are bound by at least four of the six core biofilm regulators, and six of the eight white-opaque regulator genes (all but *EFG1* and *WOR4*) are differentially expressed by twofold or more between planktonic and biofilm conditions (*WOR1*, *AHR1*, *CZF1*, and *WOR3* are upregulated by 3-, 5-, 8-, and 32-fold, respectively, while *WOR2* and *SSN6* are both downregulated by 2-fold) (**Data Sheet S1, Tab1**). Conversely, five of the nine core biofilm regulator genes are bound by at least four of the eight white-opaque regulators in opaque cells (*EFG1*, *BRG1*, *BCR1*, *TEC1*, and *RFX2* are bound by eight, eight, five, five, and four white-opaque regulators, respectively), and five of the nine biofilm regulator genes are differentially expressed by at least

2-fold between white and opaque cells (*BRG1* and *RFX2* are upregulated in opaque cells, while *EFG1*, *GALA*, and *ROB1* are upregulated in white cells) (**Data Sheet S1, Tab1**). The commensal-pathogen circuit regulators are closely intertwined with the biofilm circuit; however, there is relatively little overlap between the overlaid white-opaque circuit and the overlaid commensal-pathogen circuit. Six of the eight commensal-pathogen regulator genes (all but *RTG1* and *RTG3*) are bound by at least one biofilm core regulator, half of which (*SFU1*, *TYE7*, and *ZCF21*) are bound by at least four of the biofilm regulators (**Data Sheet S1, Tab1**). All six of the commensal-pathogen regulator genes that are bound by biofilm regulators are differentially expressed by twofold or more between planktonic and biofilm conditions, with all but *TYE7* being upregulated in biofilms (**Data Sheet S1, Tab1**). In contrast to the high degree of functional interaction between the biofilm circuit and the overlaid commensal-pathogen circuit, only three of the eight commensal-pathogen regulator genes (*SFU1*, *TYE7*, and *ZCF21*) are bound by any of the white-opaque regulators, and of the three target genes, only *TYE7* is differentially expressed between white and opaque cells (upregulated twentyfold in opaque cells). The effect of growth under conditions relevant to the overlaid commensal-pathogen circuit (i.e. low iron or growth in the GI tract) is relatively limited when compared to the effects of biofilm formation and white-opaque switching. Upon growth in low iron, only the three regulator genes involved in iron homeostasis (*HAP43*, *SEF1*, *SFU1*) are differentially expressed (**Data Sheet S1, Tab1**) (Chen et al., 2011). While growth in the GI tract does affect the expression of core regulator genes in the other circuits, the impact of this expression is relatively limited, where *AHRI* and *TEC1* are upregulated and *ROB1* is downregulated in the GI tract versus growth *in vitro* (Rosenbach et al., 2010).

PERSPECTIVES

The *C. albicans* transcriptional regulatory circuits controlling the developmental processes of biofilm formation, the white-opaque phenotypic switch, and the commensal-pathogen transition are individually tightly knit and we show that they are integrated together by extensive regulatory crosstalk between the core regulators that comprise each circuit. If we take into consideration all of the target genes in each of the larger transcriptional networks, each regulator controls individual subsets of target genes regulating distinct functions as well as subsets of target genes with functions in common with the other core regulators in each network. Strikingly, these three major transcriptional networks, together, encompass a little over 25% of genes in the entire genome, indicating that there is a high degree of functional redundancy across the networks. The complexity and functional redundancy of these network structures often make dissecting the logic of each network extremely challenging. The networks we discuss here in this review are overall structurally very similar to networks controlling complex transcriptional developmental processes in higher eukaryotes, such as the mammalian embryonic stem cell state (pluripotency) network (Boyer et al., 2005; Kim et al., 2008a). Given that mammals and

C. albicans diverged from a common ancestor around 1.5 million years ago (Wang et al., 1999), it is notable that the structures of these independently evolved transcriptional networks are so similar. There are a couple hypotheses as to how these transcriptional networks could appear so structurally similar (Sorrells and Johnson, 2015). The first hypothesis is that these complex transcriptional networks represent the optimal solutions for organizing the biological processes they control (François and Hakim, 2004; Prill et al., 2005). The second hypothesis is that these transcriptional networks are not optimal solutions but are rather non-adaptive structures that have been retained over evolutionary time scales by purifying selection and are thus the result of high-probability evolutionary trajectories (Sorrells and Johnson, 2015). As we begin to discover and deconvolute complex transcriptional networks, we will begin to test these hypotheses and shed new light on the logic of these complex network structures.

AUTHOR CONTRIBUTIONS

Conceptualization: DR, MQ, AH, and CN. Formal Analysis: DR, MQ, AH, and CN. Investigation: DR, MQ, AH, and CN. Resources: AH, and CN. Data Curation: DR, MQ, AH, and CN. Writing—Original Draft Preparation: DR, MQ, AH, and CN. Writing—Review and Editing: DR, MQ, AH, and CN. Visualization: DR, AH, and CN. Supervision: AH and CN. Project Administration: AH and CN. Funding Acquisition: AH and CN. All authors contributed to the article and approved the submitted version.

FUNDING

This work was supported by the National Institutes of Health (NIH) National Institute of Allergy and Infectious Diseases (NIAID) and National Institute of General Medical Sciences (NIGMS) awards R21AI125801 and R35GM124594, respectively, by a Pew Biomedical Scholar Award from the Pew Charitable Trusts, and by the Kamangar family in the form of an endowed chair to CN. This work was also supported by NIH NIAID award R15AI37975 to AH. DR was supported by the National Science Foundation (NSF) Graduate Research Fellowship Program (GRFP) award 1744620. The funders had no role in the study design, data collection and interpretation, or the decision to submit the work for publication.

ACKNOWLEDGMENTS

We thank all members of the Nobile and Hernday labs for insightful discussions on the topic of this manuscript.

SUPPLEMENTARY MATERIAL

The Supplementary Material for this article can be found online at: <https://www.frontiersin.org/articles/10.3389/fcimb.2020.605711/full#supplementary-material>

SUPPLEMENTARY DATA SHEET 1 | Compilation and analysis of regulator binding interactions and target gene expression. **Tab1** labeled "Tab1_Combined Core Circuits" contains compiled genome-wide chromatin immunoprecipitation (ChIP-seq or ChIP-chip) and expression profiling (RNA-seq or microarray) data for the core circuit regulators and their respective target genes. ChIP data and RNA-seq data values are in \log_2 format. Biofilm regulators ChIP data and differential gene expression data were derived from (Nobile et al., 2012). White-opaque regulators ChIP data were derived from (Zordan et al., 2007; Hernday et al., 2013; Lohse et al., 2013; Hernday et al., 2016; Lohse and Johnson, 2016). White-opaque differential gene expression data were derived from (Tuch et al., 2010). Iron homeostasis regulators ChIP data and differential gene expression data were derived from (Chen et al., 2011). Host proliferation ChIP data were derived from (Pérez et al., 2013). Host proliferation differential gene expression data were derived from (Rosenbach et al., 2010). **Tab2** labeled "Tab2_Combined Networks" contains compiled genome-wide chromatin immunoprecipitation (ChIP-seq or ChIP-chip) and expression profiling (RNA-seq or microarray) data for the core circuit regulators and all possible target genes in the *C. albicans* genome. ChIP data and RNA-

seq data values are in \log_2 format. Biofilm regulators ChIP data and differential gene expression data were derived from (Nobile et al., 2012). White-opaque regulators ChIP data were derived from (Zordan et al., 2007; Hernday et al., 2013; Lohse et al., 2013; Hernday et al., 2016; Lohse and Johnson, 2016). White-opaque differential gene expression data were derived from (Tuch et al., 2010). Iron homeostasis regulators ChIP data and differential gene expression data were derived from (Chen et al., 2011). Host proliferation ChIP data were derived from (Pérez et al., 2013). Host proliferation differential gene expression data were derived from (Rosenbach et al., 2010). **Tab3** labeled "Tab3_Inter- vs Intra-circuit" contains an analysis of the genome-wide ChIP data from **Tab1**, tabulating the total number of bound targets for each of the regulators for which genome-wide binding data is available, and calculating the percentage of binding events that represent inter- versus intra-circuit binding interactions. **Tab4** labeled "Tab4_Cytoscape Interactions" contains a representation of the genome-wide ChIP data from **Tab1** in an interaction table format for visualization in Cytoscape (Shannon et al., 2003). This dataset was used to generate all of the circuit diagrams shown in **Figures 2–5**.

REFERENCES

- Achkar, J. M., and Fries, B. C. (2010). *Candida* infections of the genitourinary tract. *Clin. Microbiol. Rev.* 23, 253–273. doi: 10.1128/CMR.00076-09
- Alby, K., and Bennett, R. J. (2009a). Stress-induced phenotypic switching in *Candida albicans*. *Mol. Biol. Cell* 20, 3178–3191. doi: 10.1091/mbc.e09-01-0040
- Alby, K., and Bennett, R. J. (2009b). To switch or not to switch?: Phenotypic switching is sensitive to multiple inputs in a pathogenic fungus. *Commun. Integr. Biol.* 2, 509–511. doi: 10.4161/cib.2.6.9487
- Anderson, J. M., and Soll, D. R. (1987). Unique phenotype of opaque cells in the white-opaque transition of *Candida albicans*. *J. Bacteriol.* 169, 5579–5588. doi: 10.1128/JB.169.12.5579-5588.1987
- Askew, C., Sellam, A., Epp, E., Hogues, H., Mullick, A., Nantel, A., et al. (2009). Transcriptional regulation of carbohydrate metabolism in the human pathogen *Candida albicans*. *PLoS Pathog.* 5, e1000612. doi: 10.1371/journal.ppat.1000612
- Askew, C., Sellam, A., Epp, E., Mallick, J., Hogues, H., Mullick, A., et al. (2011). The zinc cluster transcription factor Ahrlp directs Mcm1p regulation of *Candida albicans* adhesion. *Mol. Microbiol.* 79, 940–953. doi: 10.1111/j.1365-2958.2010.07504.x
- Baek, Y. U., Li, M., and Davis, D. A. (2008). *Candida albicans* ferric reductases are differentially regulated in response to distinct forms of iron limitation by the Rim101 and CBF transcription factors. *Eukaryot. Cell* 7, 1168–1179. doi: 10.1128/EC.00108-08
- Bennett, R. J., Uhl, M. A., Miller, M. G., and Johnson, A. D. (2003). Identification and characterization of a *Candida albicans* mating pheromone. *Mol. Cell. Biol.* 23, 8189–8201. doi: 10.1128/MCB.23.22.8189-8201.2003
- Bergen, M. S., Voss, E., and Soll, D. R. (1990). Switching at the cellular level in the white-opaque transition of *Candida albicans*. *J. Gen. Microbiol.* 136, 1925–1936. doi: 10.1099/00221287-136-10-1925
- Bockmüh, D. P., and Ernst, J. F. (2001). A potential phosphorylation site for an A-Type kinase in the Efg1 regulator protein contributes to hyphal morphogenesis of *Candida albicans*. *Genetics* 157, 1523–1530.
- Böhm, L., Muralidhara, P., and Pérez, J. C. (2016). A *Candida albicans* regulator of disseminated infection operates primarily as a repressor and governs cell surface remodeling. *Mol. Microbiol.* 100, 328–344. doi: 10.1111/mmi.13320
- Bonhomme, J., Chauvel, M., Goyard, S., Roux, P., Rossignol, T., and D'Enfert, C. (2011). Contribution of the glycolytic flux and hypoxia adaptation to efficient biofilm formation by *Candida albicans*. *Mol. Microbiol.* 80, 995–1013. doi: 10.1111/j.1365-2958.2011.07626.x
- Böttcher, B., Hoffmann, B., Garbe, E., Weise, T., Cseresnyés, Z., Brandt, P., et al. (2020). The transcription factor Stp2 is important for *Candida albicans* biofilm establishment and sustainability. *Front. Microbiol.* 11, 794. doi: 10.3389/fmicb.2020.00794
- Boyer, L. A., Tong, I. L., Cole, M. F., Johnstone, S. E., Levine, S. S., Zucker, J. P., et al. (2005). Core transcriptional regulatory circuitry in human embryonic stem cells. *Cell* 122, 947–956. doi: 10.1016/j.cell.2005.08.020
- Brown, D. H., Giusani, A. D., Chen, X., and Kumamoto, C. A. (1999). Filamentous growth of *Candida albicans* in response to physical environmental cues and its regulation by the unique *CZF1* gene. *Mol. Microbiol.* 34, 651–662. doi: 10.1046/j.1365-2958.1999.01619.x
- Bruno, V. M., Kalachikov, S., Subaran, R., Nobile, C. J., Kyratsous, C., and Mitchell, A. P. (2006). Control of the *C. albicans* cell wall damage response by transcriptional regulator Cas5. *PLoS Pathog.* 2, e21. doi: 10.1371/journal.ppat.0020021
- Calderone, R. A., and Fonzi, W. A. (2001). Virulence factors of *Candida albicans*. *Trends Microbiol.* 9, 327–335. doi: 10.1016/S0966-842X(01)02094-7
- Cao, F., Lane, S., Raniga, P. P., Lu, Y., Zhou, Z., Ramon, K., et al. (2006). The Flo8 transcription factor is essential for hyphal development and virulence in *Candida albicans*. *Mol. Biol. Cell* 17, 295–307. doi: 10.1091/mbc.e05-06-0502
- Chandra, J., Kuhn, D. M., Mukherjee, P. K., Hoyer, L. L., McCormick, T., and Ghannoum, M. A. (2001). Biofilm formation by the fungal pathogen *Candida albicans*: development, architecture, and drug resistance. *J. Bacteriol.* 183, 5385–5394. doi: 10.1128/JB.183.18.5385-5394.2001
- Chen, C. G., Yang, Y. L., Shih, H. I., Su, C. L., and Lo, H. J. (2004). CaNdt80 is involved in drug resistance in *Candida albicans* by regulating *CDR1*. *Antimicrob. Agents Chemother.* 48, 4505–4512. doi: 10.1128/AAC.48.12.4505-4512.2004
- Chen, C., Pande, K., French, S. D., Tuch, B. B., and Noble, S. M. (2011). An iron homeostasis regulatory circuit with reciprocal roles in *Candida albicans* commensalism and pathogenesis. *Cell Host Microbe* 10, 118–135. doi: 10.1016/j.chom.2011.07.005
- Chen, H. F., and Lan, C. Y. (2015). Role of *SFP1* in the regulation of *Candida albicans* biofilm formation. *PLoS One* 10, e0129903. doi: 10.1371/journal.pone.0129903
- Cheng, S., Nguyen, M. H., Zhang, Z., Jia, H., Handfield, M., and Clancy, C. J. (2003). Evaluation of the roles of four *Candida albicans* genes in virulence by using gene disruption strains that express *URA3* from the native locus. *Infect. Immun.* 71, 6101–6103. doi: 10.1128/IAI.71.10.6101-6103.2003
- Cornet, M., Gaillardin, C., and Richard, M. L. (2006). Deletions of the endocytic components *VPS28* and *VPS32* in *Candida albicans* lead to echinocandin and azole hypersensitivity. *Antimicrob. Agents Chemother.* 50, 3492–3495. doi: 10.1128/AAC.00391-06
- Dalal, C. K., Zuleta, I. A., Lohse, M. B., Zordan, R. E., El-Samad, H., and Johnson, A. D. (2019). A population shift between two heritable cell types of the pathogen *Candida albicans* is based both on switching and selective proliferation. *Proc. Natl. Acad. Sci. U.S.A.* 116, 26918–26924. doi: 10.1073/pnas.1908986116
- Davey, M. E., and O'toole, G. A. (2000). Microbial biofilms: from ecology to molecular genetics. *Microbiol. Mol. Biol. Rev.* 64, 847–867. doi: 10.1128/MMBR.64.4.847-867.2000
- Delgado-Silva, Y., Vaz, C., Carvalho-Pereira, J., Carneiro, C., Nogueira, E., Correia, A., et al. (2014). Participation of *Candida albicans* transcription factor *RLM1* in cell wall biogenesis and virulence. *PLoS One* 9, e86270. doi: 10.1371/journal.pone.0086270
- Desai, J. V., and Mitchell, A. P. (2015). *Candida albicans* biofilm development and its genetic control. *Microbiol. Spectr.* 5, 99–114. doi: 10.1128/microbiolspec.MB-0005-2014
- Desai, J. V., Bruno, V. M., Ganguly, S., Stamper, R. J., Mitchell, K. F., Solis, N., et al. (2013). Regulatory role of glycerol in *Candida albicans* biofilm formation. *mBio* 4, 637–649. doi: 10.1128/mBio.00637-12
- Desai, N., and Ardekani, A. M. (2020). Biofilms at interfaces: microbial distribution in floating films. *Soft Matter* 16, 1731–1750. doi: 10.1039/C9SM20388A

- Dieterich, C., Chandar, M., Noll, M., Johannes, F. J., Brunner, H., Graeve, T., et al. (2002). *In vitro* reconstructed human epithelia reveal contributions of *Candida albicans* EFG1 and CPH1 to adhesion and invasion. *Microbiology* 148, 497–506. doi: 10.1099/00221287-148-2-497
- Du, H., Guan, G., Xie, J., Cottier, F., Sun, Y., Jia, W., et al. (2012a). The transcription factor Flo8 mediates CO₂ sensing in the human fungal pathogen *Candida albicans*. *Mol. Biol. Cell* 23, 2692–2701. doi: 10.1091/mbc.e12-02-0094
- Du, H., Guan, G., Xie, J., Sun, Y., Tong, Y., Zhang, L., et al. (2012b). Roles of *Candida albicans* Gat2, a GATA-Type zinc finger transcription factor in biofilm formation, filamentous growth and virulence. *PLoS One* 7, e29707. doi: 10.1371/journal.pone.0029707
- Du, H., Li, X., Huang, G., Kang, Y., and Zhu, L. (2015). The zinc-finger transcription factor, Ofi1, regulates white-opaque switching and filamentation in the yeast *Candida albicans*. *Acta Biochim. Biophys. Sin.* 47, 335–341. doi: 10.1093/abbs/gmv011
- Du, H., and Huang, G. (2016). Environmental pH adaptation and morphological transitions in *Candida albicans*. *Curr. Genet.* 62, 283–286. doi: 10.1007/s00294-015-0540-8
- Dumitru, R., Navarathna, D. H. M. L. P., Semighini, C. P., Elowsky, C. G., Dumitru, R. V., Dignard, D., et al. (2007). *In vivo* and *in vitro* anaerobic mating in *Candida albicans*. *Eukaryot. Cell* 6, 465–472. doi: 10.1128/EC.00316-06
- Dunkel, N., Liu, T. T., Barker, K. S., Homayouni, R., Morschhäuser, J., and Rogers, P. D. (2008). A gain-of-function mutation in the transcription factor Upc2p causes upregulation of ergosterol biosynthesis genes and increased fluconazole resistance in a clinical *Candida albicans* isolate. *Eukaryot. Cell* 7, 1180–1190. doi: 10.1128/EC.00103-08
- Edmond, M. B., Wallace, S. E., McClish, D. K., Pfäller, M. A., Jones, R. N., and Wenzel, R. P. (1999). Nosocomial bloodstream infections in United States hospitals: a three-year analysis. *Clin. Infect. Dis.* 29, 239–244. doi: 10.1086/520192
- Eison, S. L., Noble, S. M., Solis, N. V., Filler, S. G., and Johnson, A. D. (2009). An RNA transport system in *Candida albicans* regulates hyphal morphology and invasive growth. *PLoS Genet.* 5, e1000664. doi: 10.1371/journal.pgen.1000664
- Ene, I. V., Lohse, M. B., Vladu, A. V., Morschhäuser, J., Johnson, A. D., and Bennett, R. J. (2016). Phenotypic profiling reveals that *Candida albicans* opaque cells represent a metabolically specialized cell state compared to default white cells. *mBio* 7, e01269-16. doi: 10.1128/mBio.01269-16
- Fanning, S., Xu, W., Solis, N., Woolford, C. A., Filler, S. G., and Mitchell, A. P. (2012). Divergent targets of *Candida albicans* biofilm regulator Bcr1 *in vitro* and *in vivo*. *Eukaryot. Cell* 11, 896–904. doi: 10.1128/EC.00103-12
- Finkel, J. S., Xu, W., Huang, D., Hill, E. M., Desai, J. V., Woolford, C. A., et al. (2012). Portrait of *Candida albicans* adherence regulators. *PLoS Pathog.* 8, e1002525. doi: 10.1371/journal.ppat.1002525
- Fox, E. P., Bui, C. K., Nett, J. E., Hartooni, N., Mui, M. C., Andes, D. R., et al. (2015). An expanded regulatory network temporally controls *Candida albicans* biofilm formation. *Mol. Microbiol.* 96, 1226–1239. doi: 10.1111/mmi.13002
- Fox, E. P., and Nobile, C. J. (2012). A sticky situation: untangling the transcriptional network controlling biofilm development in *Candida albicans*. *Transcription* 3, 315–322. doi: 10.4161/trns.22281
- François, P., and Hakim, V. (2004). Design of genetic networks with specified functions by evolution *in silico*. *Proc. Natl. Acad. Sci. U.S.A.* 101, 580–585. doi: 10.1073/pnas.0304532101
- Frazer, C., Staples, M. II, Kim, Y., Hirakawa, M., Dowell, M. A., Johnson, N. V., et al. (2020). Epigenetic cell fate in *Candida albicans* is controlled by transcription factor condensates acting at super-enhancer-like elements. *Nat. Microbiol.* 5, 1374–1389. doi: 10.1038/s41564-020-0760-7
- Ganguly, S., Bishop, A. C., Xu, W., Ghosh, S., Nickerson, K. W., Lanni, F., et al. (2011). Zap1 control of cell-cell signaling in *Candida albicans* biofilms. *Eukaryot. Cell* 10, 1448–1454. doi: 10.1128/EC.05196-11
- García-Sánchez, S., Aubert, S., Ibraqui, I., Janbon, G., Ghigo, J. M., and D'Enfert, C. (2004). *Candida albicans* biofilms: A developmental state associated with specific and stable gene expression patterns. *Eukaryot. Cell* 3, 536–545. doi: 10.1128/EC.3.2.536-545.2004
- Geiger, J., Wessels, D., Lockhart, S. R., and Soll, D. R. (2004). Release of a potent polymorphonuclear leukocyte chemoattractant is regulated by white-opaque switching in *Candida albicans*. *Infect. Immun.* 72, 667–677. doi: 10.1128/IAI.72.2.667-677.2004
- Ghosh, A. K., Wangsanut, T., Fonzi, W. A., and Rolfes, R. J. (2015). The *GRF10* homeobox gene regulates filamentous growth in the human fungal pathogen *Candida albicans*. *FEMS Yeast Res.* 15, fov093. doi: 10.1093/femsyr/fov093
- Guan, Z., and Liu, H. (2015). The *WOR1* 5' untranslated region regulates white-opaque switching in *Candida albicans* by reducing translational efficiency. *Mol. Microbiol.* 97, 125–138. doi: 10.1111/mmi.13014
- Gulati, M., and Nobile, C. J. (2016). *Candida albicans* biofilms: development, regulation, and molecular mechanisms. *Microbes Infect.* 18, 310–321. doi: 10.1016/j.micinf.2016.01.002
- Hao, B., Clancy, C. J., Cheng, S., Raman, S. B., Iczkowski, K. A., and Nguyen, M. H. (2009). *Candida albicans* *RFX2* encodes a DNA binding protein involved in DNA damage responses, morphogenesis, and virulence. *Eukaryot. Cell* 8, 627–639. doi: 10.1128/EC.00246-08
- Herday, A. D., Noble, S. M., Mitrovich, Q. M., and Johnson, A. D. (2010). Genetics and molecular biology in *Candida albicans*. *Methods Enzymol.* 470, 737–758. doi: 10.1016/S0076-6879(10)70031-8
- Herday, A. D., Lohse, M. B., Fordyce, P. M., Nobile, C. J., DeRisi, J. L., and Johnson, A. D. (2013). Structure of the transcriptional network controlling white-opaque switching in *Candida albicans*. *Mol. Microbiol.* 90, 22–35. doi: 10.1111/mmi.12329
- Herday, A. D., Lohse, M. B., Nobile, C. J., Noiman, L., Laksana, C. N., and Johnson, A. D. (2016). *Ssn6* Defines a new level of regulation of white-opaque switching in *Candida albicans* and is required for the stochasticity of the switch. *mBio* 7, e01565-e01515. doi: 10.1128/mBio.01565-15
- Hnisz, D., Sehrawmüller, T., and Kuchler, K. (2009). Transcriptional loops meet chromatin: a dual-layer network controls white-opaque switching in *Candida albicans*. *Mol. Microbiol.* 74, 1–15. doi: 10.1111/j.1365-2958.2009.06772.x
- Homann, O. R., Dea, J., Noble, S. M., and Johnson, A. D. (2009). A phenotypic profile of the *Candida albicans* regulatory network. *PLoS Genet.* 5, e1000783. doi: 10.1371/journal.pgen.1000783
- Horwitz, A. A., Walter, J. M., Schubert, M. G., Kung, S. H., Hawkins, K., Platt, D. M., et al. (2015). Efficient multiplexed integration of synergistic alleles and metabolic pathways in yeasts via CRISPR-Cas. *Cell Syst.* 1, 88–96. doi: 10.1016/j.cels.2015.02.001
- Hsu, P. C., Yang, C. Y., and Lan, C. Y. (2011). *Candida albicans* Hap43 is a repressor induced under low-iron conditions and is essential for iron-responsive transcriptional regulation and virulence. *Eukaryot. Cell* 10, 207–225. doi: 10.1128/EC.00158-10
- Huang, G., Wang, H., Chou, S., Nie, X., Chen, J., and Liu, H. (2006). Bistable expression of *WOR1*, a master regulator of white-opaque switching in *Candida albicans*. *Proc. Natl. Acad. Sci.* 103, 12813–12818. doi: 10.1073/pnas.0605270103
- Huang, G., Srikantha, T., Sahni, N., Yi, S., and Soll, D. R. (2009). CO₂ regulates white-to-opaque switching in *Candida albicans*. *Curr. Biol.* 19, 330–334. doi: 10.1016/j.cub.2009.01.018
- Huang, G., Yi, S., Sahni, N., Daniels, K. J., Srikantha, T., and Soll, D. R. (2010). N-acetylglucosamine induces white to opaque switching, a mating prerequisite in *Candida albicans*. *PLoS Pathog.* 6, e1000806. doi: 10.1371/journal.ppat.1000806
- Huang, G. (2012). Regulation of phenotypic transitions in the fungal pathogen *Candida albicans*. *Virulence* 3, 251–261. doi: 10.4161/viru.20010
- Hube, B. (2004). From commensal to pathogen: stage- and tissue-specific gene expression of *Candida albicans*. *Curr. Opin. Microbiol.* 7, 336–341. doi: 10.1016/j.mib.2004.06.003
- Hull, C. M., and Johnson, A. D. (1999). Identification of a mating type-like locus in the asexual pathogenic yeast *Candida albicans*. *Science* 285, 1271–1275. doi: 10.1126/science.285.5431.1271
- Jia, Y., Rothermel, B., Thornton, J., and Butow, R. A. (1997). A basic helix-loop-helix-leucine zipper transcription complex in yeast functions in a signaling pathway from mitochondria to the nucleus. *Mol. Cell. Biol.* 17, 1110–1117. doi: 10.1128/MCB.17.3.1110
- Kadosh, D., and Johnson, A. D. (2001). Rfg1, a protein related to the *Saccharomyces cerevisiae* hypoxic regulator Rox1, controls filamentous growth and virulence in *Candida albicans*. *Mol. Cell. Biol.* 21, 2496–2505. doi: 10.1128/MCB.21.7.2496-2505.2001
- Kakade, P., Sadhale, P., Sanyal, K., and Nagaraja, V. (2016). ZCF32, a fungus specific Zn(II)2 Cys6 transcription factor, is a repressor of the biofilm development in the human pathogen *Candida albicans*. *Sci. Rep.* 6, 1–15. doi: 10.1038/srep31124

- Kakade, P., Mahadik, K., Balaji, K. N., Sanyal, K., and Nagaraja, V. (2019). Two negative regulators of biofilm development exhibit functional divergence in conferring virulence potential to *Candida albicans*. *FEMS Yeast Res.* 19, foy078. doi: 10.1093/femsyr/foy078
- Kamthan, M., Mukhopadhyay, G., Chakraborty, N., Chakraborty, S., and Datta, A. (2012). Quantitative proteomics and metabolomics approaches to demonstrate N-acetyl-d-glucosamine inducible amino acid deprivation response as morphological switch in *Candida albicans*. *Fungal Genet. Biol.* 49, 369–378. doi: 10.1016/j.fgb.2012.02.006
- Kan, S., Pang, Q., Song, N., Mei, H., Zheng, H., Li, D., et al. (2020). Study on vulvovaginal candidiasis: clinical epidemiology and *in vitro* susceptibility of pathogenic yeasts in China. SSRN. doi: 10.2139/ssrn.3521422
- Kelly, M. T., MacCallum, D. M., Clancy, S. D., Odds, F. C., Brown, A. J. P., and Butler, G. (2004). The *Candida albicans* CaACE2 gene affects morphogenesis, adherence and virulence. *Mol. Microbiol.* 53, 969–983. doi: 10.1111/j.1365-2958.2004.04185.x
- Kennedy, M. J., and Volz, P. A. (1985). Ecology of *Candida albicans* gut colonization: inhibition of *Candida* adhesion, colonization, and dissemination from the gastrointestinal tract by bacterial antagonism. *Infect. Immun.* 49, 654–663. doi: 10.1128/IAI.49.3.654-663.1985
- Kim, J., Chu, J., Shen, X., Wang, J., and Orkin, S. H. (2008a). An extended transcriptional network for pluripotency of embryonic stem cells. *Cell* 132, 1049–1061. doi: 10.1016/j.cell.2008.02.039
- Kim, M. J., Kil, M., Jung, J. H., and Kim, J. (2008b). Roles of zinc-responsive transcription factor Csr1 in filamentous growth of the pathogenic yeast *Candida albicans*. *J. Microbiol. Biotechnol.* 18, 242–247.
- Kolotila, M. P., and Diamond, R. D. (1990). Effects of neutrophils and *in vitro* oxidants on survival and phenotypic switching of *Candida albicans* WO-1. *Infect. Immun.* 58, 1174–1179. doi: 10.1128/IAI.58.5.1174-1179.1990
- Kolter, R., and Greenberg, E. P. (2006). Microbial sciences: the superficial life of microbes. *Nature* 441, 300–302. doi: 10.1038/441300a
- Kumamoto, C. A. (2002). *Candida* biofilms. *Curr. Opin. Microbiol.* 5, 608–611. doi: 10.1016/S1369-5274(02)00371-5
- Kumamoto, C. A. (2011). Inflammation and gastrointestinal *Candida* colonization. *Curr. Opin. Microbiol.* 14, 386–391. doi: 10.1016/j.mib.2011.07.015
- Lagree, K., Woolford, C. A., Huang, M. Y., May, G., McManus, C. J., Solis, N. V., et al. (2020). Roles of *Candida albicans* Mig1 and Mig2 in glucose repression, pathogenicity traits, and SNF1 essentiality. *PLoS Genet.* 16, e1008582. doi: 10.1371/journal.pgen.1008582
- Lan, C. Y., Newport, G., Murillo, L. A., Jones, T., Scherer, S., Davis, R. W., et al. (2002). Metabolic specialization associated with phenotypic switching in *Candida albicans*. *Proc. Natl. Acad. Sci. U.S.A.* 99, 14907–14912. doi: 10.1073/pnas.232566499
- Lan, C. Y., Rodarte, G., Murillo, L. A., Jones, T., Davis, R. W., Dungan, J., et al. (2004). Regulatory networks affected by iron availability in *Candida albicans*. *Mol. Microbiol.* 53, 1451–1469. doi: 10.1111/j.1365-2958.2004.04214.x
- Langford, M. L., Hargarten, J. C., Patefield, K. D., Marta, E., Blankenship, J. R., Fanning, S., et al. (2013). *Candida albicans* Czf1 and Efg1 coordinate the response to farnesol during quorum sensing, white-opaque thermal dimorphism, and cell death. *Eukaryot. Cell* 12, 1281–1292. doi: 10.1128/EC.00311-12
- Li, F., and Palecek, S. P. (2003). *EAP1*, a *Candida albicans* gene involved in binding human epithelial cells. *Eukaryot. Cell* 2, 1266–1273. doi: 10.1128/EC.2.6.1266-1273.2003
- Liao, X., and Butow, R. A. (1993). *RTG1* and *RTG2*: two yeast genes required for a novel path of communication from mitochondria to the nucleus. *Cell* 72, 61–71. doi: 10.1016/0092-8674(93)90050-Z
- Liu, Z., and Butow, R. A. (2006). Mitochondrial retrograde signaling. *Annu. Rev. Genet.* 40, 159–185. doi: 10.1146/annurev.genet.40.110405.090613
- Lockhart, S. R., Pujol, C., Daniels, K. J., Miller, M. G., Johnson, A. D., Pfaller, M. A., et al. (2002). In *Candida albicans*, white-opaque switchers are homozygous for mating type. *Genetics* 162, 737–745.
- Lohse, M. B., Hernday, A. D., Fordyce, P. M., Noiman, L., Sorrells, T. R., Hanson-Smith, V., et al. (2013). Identification and characterization of a previously undescribed family of sequence-specific DNA-binding domains. *Proc. Natl. Acad. Sci. U.S.A.* 110, 7660–7665. doi: 10.1073/pnas.1221734110
- Lohse, M. B., Ene, I. V., Craik, V. B., Hernday, A. D., Mancera, E., Morschhäuser, J., et al. (2016). Systematic genetic screen for transcriptional regulators of the *Candida albicans* white-opaque switch. *Genetics* 203, 1679–1692. doi: 10.1534/genetics.116.190645
- Lohse, M. B., and Johnson, A. D. (2008). Differential phagocytosis of white versus opaque *Candida albicans* by *Drosophila* and mouse phagocytes. *PLoS One* 3, e1473. doi: 10.1371/journal.pone.0001473
- Lohse, M. B., and Johnson, A. D. (2009). White-opaque switching in *Candida albicans*. *Curr. Opin. Microbiol.* 12, 650–654. doi: 10.1016/j.mib.2009.09.010
- Lohse, M. B., and Johnson, A. D. (2010). Temporal anatomy of an epigenetic switch in cell programming: the white-opaque transition of *C. albicans*. *Mol. Microbiol.* 78, 331–343. doi: 10.1111/j.1365-2958.2010.07331.x
- Lohse, M. B., and Johnson, A. D. (2016). Identification and characterization of Wor4, a new transcriptional regulator of white-opaque switching. *G3 (Bethesda Md.)* 6, 721–729. doi: 10.1534/g3.115.024885
- Martin, R. B., Savory, J., Brown, S., Bertholf, R. L., and Wills, M. R. (1987). Transferrin binding of Al³⁺ and Fe³⁺. *Clin. Chem.* 33, 405–407. doi: 10.1093/clinchem/33.3.405
- Mayer, F. L., Wilson, D., and Hube, B. (2013). *Candida albicans* pathogenicity mechanisms. *Virulence* 4, 119–128. doi: 10.4161/viru.22913
- McCance, R. A., and Widdowson, E. M. (1938). The absorption and excretion of iron following oral and intravenous administration. *J. Physiol.* 94, 148–154. doi: 10.1113/jphysiol.1938.sp003669
- Meir, J., Hartmann, E., Eckstein, M. T., Guiducci, E., Kirchner, F., Rosenwald, A., et al. (2018). Identification of *Candida albicans* regulatory genes governing mucosal infection. *Cell. Microbiol.* 20, e12841. doi: 10.1111/cmi.12841
- Miller, M. G., and Johnson, A. D. (2002). White-opaque switching in *Candida albicans* is controlled by mating-type locus homeodomain proteins and allows efficient mating. *Cell* 110, 293–302. doi: 10.1016/S0092-8674(02)00837-1
- Miret, S., Simpson, R. J., and McKie, A. T. (2003). Physiology and molecular biology of dietary iron absorption. *Annu. Rev. Nutr.* 23, 283–301. doi: 10.1146/annurev.nutr.23.011702.073139
- Mulhern, S. M., Logue, M. E., and Butler, G. (2006). *Candida albicans* transcription factor Ace2 regulates metabolism and is required for filamentation in hypoxic conditions. *Eukaryot. Cell* 5, 2001–2013. doi: 10.1128/EC.00155-06
- Nett, J. E., Sanchez, H., Cain, M. T., Ross, K. M., and Andes, D. R. (2011). Interface of *Candida albicans* biofilm matrix-associated drug resistance and cell wall integrity regulation. *Eukaryot. Cell* 10, 1660–1669. doi: 10.1128/EC.05126-11
- Nobile, C. J., Nett, J. E., Hernday, A. D., Homann, O. R., Deneault, J. S., Nantel, A., et al. (2009). Biofilm matrix regulation by *Candida albicans* Zap1. *PLoS Biol.* 7, e1000133. doi: 10.1371/journal.pbio.1000133
- Nobile, C. J., Fox, E. P., Nett, J. E., Sorrells, T. R., Mitrovich, Q. M., Hernday, A. D., et al. (2012). A recently evolved transcriptional network controls biofilm development in *Candida albicans*. *Cell* 148, 126–138. doi: 10.1016/j.cell.2011.10.048
- Nobile, C. J., and Johnson, A. D. (2015). *Candida albicans* biofilms and human disease. *Annu. Rev. Microbiol.* 69, 71–92. doi: 10.1146/annurev-micro-091014-104330
- Nobile, C. J., and Mitchell, A. P. (2005). Regulation of cell-surface genes and biofilm formation by the *C. albicans* transcription factor Bcr1p. *Curr. Biol.* 15, 1150–1155. doi: 10.1016/j.cub.2005.05.047
- Noble, S. M., Gianetti, B. A., and Witchley, J. N. (2017). *Candida albicans* cell-type switching and functional plasticity in the mammalian host. *Nat. Rev. Microbiol.* 15, 96–108. doi: 10.1038/nrmicro.2016.157
- Oh, J., Fung, E., Price, M. N., Dehal, P. S., Davis, R. W., Giaever, G., et al. (2010). A universal TagModule collection for parallel genetic analysis of microorganisms. *Nucleic Acids Res.* 38, e146. doi: 10.1093/nar/gkq419
- Omran, R. P., Law, C., Dumeaux, V., Morschhäuser, J., and Whiteway, M. (2020). The zinc cluster transcription factor Rha1 is a positive filamentation regulator in *Candida albicans*. *bioRxiv* 2020.01.21.901744. doi: 10.1101/2020.01.21.901744
- Pappas, P. G., Rex, J. H., Sobel, J. D., Filler, S. G., Dismukes, W. E., Walsh, T. J., et al. (2004). Guidelines for treatment of candidiasis. *Clin. Infect. Dis.* 38, 161–189. doi: 10.1086/380796
- Pérez, J. C., Kumamoto, C. A., and Johnson, A. D. (2013). *Candida albicans* commensalism and pathogenicity are intertwined traits directed by a tightly knit transcriptional regulatory circuit. *PLoS Biol.* 11, e1001510. doi: 10.1371/journal.pbio.1001510

- Pfaller, M. A., and Diekema, D. J. (2007). Epidemiology of invasive candidiasis: a persistent public health problem. *Clin. Microbiol. Rev.* 20, 133–163. doi: 10.1128/CMR.00029-06
- Polvi, E. J., Veri, A. O., Liu, Z., Hossain, S., Hyde, S., Kim, S. H., et al. (2019). Functional divergence of a global regulatory complex governing fungal filamentation. *PLoS Genet.* 15, e1007901. doi: 10.1371/journal.pgen.1007901
- Prasad, T., Hameed, S., Manoharlal, R., Biswas, S., Mukhopadhyay, C. K., Goswami, S. K., et al. (2010). Morphogenic regulator *EFG1* affects the drug susceptibilities of pathogenic *Candida albicans*. *FEMS Yeast Res.* 10, 587–596. doi: 10.1111/j.1567-1364.2010.00639.x
- Prill, R. J., Iglesias, P. A., and Levchenko, A. (2005). Dynamic properties of network motifs contribute to biological network organization. *PLoS Biol.* 3, e343. doi: 10.1371/journal.pbio.0030343
- Pukkila-Worley, R., Peleg, A. Y., Tampakakis, E., and Mylonakis, E. (2009). *Candida albicans* hyphal formation and virulence assessed using a *Caenorhabditis elegans* infection model. *Eukaryot. Cell* 8, 1750–1758. doi: 10.1128/EC.00163-09
- Rai, L. S., Singha, R., Brahma, P., and Sanyal, K. (2018). Epigenetic determinants of phenotypic plasticity in *Candida albicans*. *Fungal Biol. Rev.* 32, 10–19. doi: 10.1016/j.fbr.2017.07.002
- Ramage, G., VandeWalle, K., López-Ribot, J. L., and Wickes, B. L. (2002). The filamentation pathway controlled by the *Efg1* regulator protein is required for normal biofilm formation and development in *Candida albicans*. *FEMS Microbiol. Lett.* 214, 95–100. doi: 10.1111/j.1574-6968.2002.tb11330.x
- Ramirez-Zavala, B., Reuß, O., Park, Y. N., Ohlsen, K., and Morschhäuser, J. (2008). Environmental induction of white-opaque switching in *Candida albicans*. *PLoS Pathog.* 4, e1000089. doi: 10.1371/journal.ppat.1000089
- Richards, M. J., Edwards, J. R., Culver, D. H., and Gaynes, R. P. (1999). Nosocomial infections in medical intensive care units in the United States. National Nosocomial Infections Surveillance System. *Crit. Care Med.* 27, 887–892. doi: 10.1097/00003246-199905000-00020
- Rikkerink, E. H., Magee, B. B., and Magee, P. T. (1988). Opaque-white phenotype transition: a programmed morphological transition in *Candida albicans*. *J. Bacteriol.* 170, 895–899. doi: 10.1128/JB.170.2.895-899.1988
- Rosenbach, A., Dignard, D., Pierce, J. V., Whiteway, M., and Kumamoto, C. A. (2010). Adaptations of *Candida albicans* for growth in the mammalian intestinal tract. *Eukaryot. Cell* 9, 1075–1086. doi: 10.1128/EC.00034-10
- Sahni, N., Yi, S., Daniels, K. J., Huang, G., Srikantha, T., and Soll, D. R. (2010). *Tec1* mediates the pheromone response of the white phenotype of *Candida albicans*: insights into the evolution of new signal transduction pathways. *PLoS Biol.* 8, e1000363. doi: 10.1371/journal.pbio.1000363
- Schweizer, A., Rupp, S., Taylor, B. N., Rölinghoff, M., and Schröppel, K. (2000). The TEA/ATTS transcription factor *CaTec1p* regulates hyphal development and virulence in *Candida albicans*. *Mol. Microbiol.* 38, 435–445. doi: 10.1046/j.1365-2958.2000.02132.x
- Sellam, A., Tebbji, F., and Nantel, A. (2009). Role of *Ndt80p* in sterol metabolism regulation and azole resistance in *Candida albicans*. *Eukaryot. Cell* 8, 1174–1183. doi: 10.1128/EC.00074-09
- Sellam, A., Askew, C., Epp, E., Tebbji, F., Mullick, A., Whiteway, M., et al. (2010). Role of transcription factor *CaNdt80p* in cell separation, hyphal growth, and virulence in *Candida albicans*. *Eukaryot. Cell* 9, 634–644. doi: 10.1128/EC.00325-09
- Shannon, P., Markiel, A., Ozier, O., Baliga, N. S., Wang, J. T., Ramage, D., et al. (2003). Cytoscape: A software Environment for integrated models of biomolecular interaction networks. *Genome Res.* 13, 2498–2504. doi: 10.1101/gr.1239303
- Shapiro, R. S., Sellam, A., Tebbji, F., Whiteway, M., Nantel, A., and Cowen, L. E. (2012). *Pho85*, *Pel1*, and *Hms1* signaling governs *Candida albicans* morphogenesis induced by high temperature or *Hsp90* compromise. *Curr. Biol.* 22, 461–470. doi: 10.1016/j.cub.2012.01.062
- Shen, J., Cowen, L. E., Griffin, A. M., Chan, L., and Köhler, J. R. (2008). The *Candida albicans* *pescadillo* homolog is required for normal hypha-to-yeast morphogenesis and yeast proliferation. *Proc. Natl. Acad. Sci. U.S.A.* 105, 20918–20923. doi: 10.1073/pnas.0809147105
- Silver, P. M., Oliver, B. G., and White, T. C. (2004). Role of *Candida albicans* transcription factor *Upc2p* in drug resistance and sterol metabolism. *Eukaryot. Cell* 3, 1391–1397. doi: 10.1128/EC.3.6.1391-1397.2004
- Slutsky, B., Staebell, M., Anderson, J., Risen, L., Pfaller, M., and Soll, D. R. (1987). White-opaque transition: a second high-frequency switching system in *Candida albicans*. *J. Bacteriol.* 169, 189–197. doi: 10.1128/JB.169.1.189-197.1987
- Soll, D. R., Morrow, B., and Srikantha, T. (1993). High-frequency phenotypic switching in *Candida albicans*. *Trends Genet.* 9, 61–65. doi: 10.1016/0168-9525(93)90189-Q
- Soll, D. R. (1992). High-frequency switching in *Candida albicans*. *Clin. Microbiol. Rev.* 5, 183–203. doi: 10.1128/CMR.5.2.183
- Sonneborn, A., Tebarth, B., and Ernst, J. F. (1999). Control of white-opaque phenotypic switching in *Candida albicans* by the *Efg1p* morphogenic regulator. *Infect. Immun.* 67, 4655–4660. doi: 10.1128/IAI.67.9.4655-4660.1999
- Sorrells, T. R., and Johnson, A. D. (2015). Making sense of transcription networks. *Cell* 161, 714–723. doi: 10.1016/j.cell.2015.04.014
- Spiliopoulou, A., Vamvakopoulou, S., Bartzavali, C., Dimitracopoulos, G., Anastassiou, E. D., and Christofidou, M. (2010). Eleven-year retrospective survey of candidaemia in a university hospital in southwestern Greece. *Clin. Microbiol. Infect.* 16, 1378–1381. doi: 10.1111/j.1469-0691.2010.03193.x
- Srikantha, T., Tsai, L. K., Daniels, K., and Soll, D. R. (2000). *EFG1* null mutants of *Candida albicans* switch but cannot express the complete phenotype of white-phase budding cells. *J. Bacteriol.* 182, 1580–1591. doi: 10.1128/JB.182.6.1580-1591.2000
- Srikantha, T., Borneman, A. R., Daniels, K. J., Pujol, C., Wu, W., Seringhaus, M. R., et al. (2006). *TOS9* regulates white-opaque switching in *Candida albicans*. *Eukaryot. Cell* 5, 1674–1687. doi: 10.1128/EC.00252-06
- Staub, P., Binder, A., Kretschmar, M., Nichterlein, T., Schröppel, K., and Morschhäuser, J. (2004). *Tec1p*-independent activation of a hypha-associated *Candida albicans* virulence gene during infection. *Infect. Immun.* 72, 2386–2389. doi: 10.1128/IAI.72.4.2386-2389.2004
- Tandonnet, S., and Torres, T. T. (2017). Traditional versus 3' RNA-seq in a non-model species. *Genomics Data* 11, 9–16. doi: 10.1016/j.gdata.2016.11.002
- Tsai, P. W., Chen, Y. T., Yang, C. Y., Chen, H. F., Tan, T. S., Lin, T. W., et al. (2014). The role of *Mss11* in *Candida albicans* biofilm formation. *Mol. Genet. Genomics* 289, 807–819. doi: 10.1007/s00438-014-0846-0
- Tuch, B. B., Mitrovich, Q. M., Homann, O. R., Hernday, A. D., Monighetti, C. K., de La Vega, F. M., et al. (2010). The transcriptomes of two heritable cell types illuminate the circuit governing their differentiation. *PLoS Genet.* 6, e1001070. doi: 10.1371/journal.pgen.1001070
- Uhl, M. A., Biery, M., Craig, N., and Johnson, A. D. (2003). Haploinsufficiency-based large-scale forward genetic analysis of filamentous growth in the diploid human fungal pathogen *C. albicans*. *EMBO J.* 22, 2668–2678. doi: 10.1093/emboj/cdg256
- Uppuluri, P., Chaturvedi, A. K., Srinivasan, A., Banerjee, M., Ramasubramanian, A. K., Köhler, J. R., et al. (2010a). Dispersion as an important step in the *Candida albicans* biofilm developmental cycle. *PLoS Pathog.* 6, e1000828. doi: 10.1371/journal.ppat.1000828
- Uppuluri, P., Pierce, C. G., Thomas, D. P., Bubeck, S. S., Saville, S. P., and Lopez-Ribot, J. L. (2010b). The transcriptional regulator *Nrg1p* controls *Candida albicans* biofilm formation and dispersion. *Eukaryot. Cell* 9, 1531–1537. doi: 10.1128/EC.00111-10
- Vandeputte, P., Ischer, F., Sanglard, D., and Coste, A. T. (2011). *In vivo* systematic analysis of *Candida albicans* *Zn2-Cys6* transcription factors mutants for mice organ colonization. *PLoS One* 6, e26962. doi: 10.1371/journal.pone.0026962
- Vandeputte, P., Pradervand, S., Ischer, F., Coste, A. T., Ferrati, S., Harshman, K., et al. (2012). Identification and functional characterization of *Rca1*, a transcription factor involved in both antifungal susceptibility and host response in *Candida albicans*. *Eukaryot. Cell* 11, 916–931. doi: 10.1128/EC.00134-12
- Vasicek, E. M., Berkow, E. L., Bruno, V. M., Mitchell, A. P., Wiederhold, N. P., Barker, K. S., et al. (2014). Disruption of the transcriptional regulator *Cas5* results in enhanced killing of *Candida albicans* by fluconazole. *Antimicrob. Agents Chemother.* 58, 6807–6818. doi: 10.1128/AAC.00064-14
- Vinces, M. D., Haas, C., and Kumamoto, C. A. (2006). Expression of the *Candida albicans* morphogenesis regulator gene *CZF1* and its regulation by *Efg1p* and *Czf1p*. *Eukaryot. Cell* 5, 825–835. doi: 10.1128/EC.5.5.825-835.2006
- Vinces, M. D., and Kumamoto, C. A. (2007). The morphogenic regulator *Czf1p* is a DNA-binding protein that regulates white-opaque switching in *Candida albicans*. *Microbiology* 153, 2877–2884. doi: 10.1099/mic.0.2007/005983-0

- Wang, D. Y. C., Kumar, S., and Hedges, S. B. (1999). Divergence time estimates for the early history of animal phyla and the origin of plants, animals and fungi. *Proc. R. Soc. B: Biol. Sci.* 266, 163–171. doi: 10.1098/rspb.1999.0617
- Wang, H., Song, W., Huang, G., Zhou, Z., Ding, Y., and Chen, J. (2011). *Candida albicans* Zc37, a zinc finger protein, is required for stabilization of the white state. *FEBS Lett.* 585, 797–802. doi: 10.1016/j.febslet.2011.02.005
- Wang, Q., Verma, J., Vidan, N., Wang, Y., Tucey, T. M., Lo, T. L., et al. (2020). The YEATS domain histone crotonylation readers control virulence-related biology of a major human pathogen. *Cell Rep.* 31, 107528. doi: 10.1016/j.celrep.2020.107528
- Wenzel, R. P. (1995). Nosocomial candidemia: risk factors and attributable mortality. *Clin. Infect. Dis.* 20, 1531–1534. doi: 10.1093/clinids/20.6.1531
- Wheeler, R. T., Kombe, D., Agarwala, S. D., and Fink, G. R. (2008). Dynamic, morphotype-specific *Candida albicans* β -Glucan exposure during infection and drug treatment. *PLoS Pathog.* 4, e1000227. doi: 10.1371/journal.ppat.1000227
- Wilking, J. N., Angelini, T. E., Seminara, A., Brenner, M. P., and Weitz, D. A. (2011). Biofilms as complex fluids. *MRS Bull.* 36, 385–391. doi: 10.1557/mrs.2011.71
- Xie, J., Tao, L., Nobile, C. J., Tong, Y., Guan, G., Sun, Y., et al. (2013). White-opaque switching in natural *MTL α* isolates of *Candida albicans*: evolutionary implications for roles in host adaptation, pathogenesis, and sex. *PLoS Biol.* 11, e1001525. doi: 10.1371/journal.pbio.1001525
- Xu, D., Jiang, B., Ketela, T., Lemieux, S., Veillette, K., Martel, N., et al. (2007). Genome-wide fitness test and mechanism-of-action studies of inhibitory compounds in *Candida albicans*. *PLoS Pathog.* 3, e2. doi: 10.1371/journal.ppat.0030092
- Zordan, R. E., Galgoczy, D. J., and Johnson, A. D. (2006). Epigenetic properties of white-opaque switching in *Candida albicans* are based on a self-sustaining transcriptional feedback loop. *Proc. Natl. Acad. Sci. U.S.A.* 103, 12807–12812. doi: 10.1073/pnas.0605138103
- Zordan, R. E., Miller, M. G., Galgoczy, D. J., Tuch, B. B., and Johnson, A. D. (2007). Interlocking transcriptional feedback loops control white-opaque switching in *Candida albicans*. *PLoS Biol.* 5, 2166–2176. doi: 10.1371/journal.pbio.0050256

Conflict of Interest: CN is a cofounder of BioSynesis, Inc., a company developing inhibitors and diagnostics of biofilms.

The remaining authors declare that the research was conducted in the absence of any commercial or financial relationships that could be construed as a potential conflict of interest.

The reviewer AS declared a past co-authorship with one of the authors AH to the handling editor.

Copyright © 2020 Rodriguez, Quail, Hernday and Nobile. This is an open-access article distributed under the terms of the Creative Commons Attribution License (CC BY). The use, distribution or reproduction in other forums is permitted, provided the original author(s) and the copyright owner(s) are credited and that the original publication in this journal is cited, in accordance with accepted academic practice. No use, distribution or reproduction is permitted which does not comply with these terms.

The TFs that comprise these three circuits have been largely characterized through genome-wide approaches to assess DNA binding patterns under growth conditions that support the distinct developmental programs which are controlled by these circuits and transcriptional profiling of strains that lack one or more of these key regulators. Furthermore, significant work has been performed to understand the genetic and regulatory interactions between the regulators within the biofilm and white-opaque regulatory circuits. However, 34 of the new white-opaque switch regulatory TFs that were recently identified by Lohse et al. have yet to be characterized by genome-wide DNA binding analysis, transcriptional profiling of deletion strains, or genetic interaction analysis¹. In this dissertation, I have focused on developing a more complete understanding of the genetic regulatory interactions and transcriptional regulatory network structures that underlie the white-opaque switch in *Candida albicans*. In particular, I have systematically addressed how all eight of the known “switch critical” regulators, which are required for stochastic switching between the two cell types, interact with each other at the genetic level. I have also determined how four of the newly identified switch critical regulators (Fgr15, Flo8, Hfl1, and Rbf1), which have not previously been characterized via genome-wide DNA binding analyses, integrate into the larger white-opaque switch regulatory network. I have also explored the extent to which these newly uncovered regulatory connections further integrate the white-opaque, biofilm, and commensal-pathogenic networks.

To elucidate the genetic, physical, and transcriptional regulatory interactions that govern switching and heritability within the white-opaque switch circuit, I applied a combination of genetic epistasis experiments (chapter two), cleavage under targets and release using nuclease (CUT&RUN) (chapter three), and genome-wide transcriptional profiling (chapter three). To determine the epistatic relationship between each of the critical switch regulators, we generated all possible pairwise combinations of the white-versus opaque-locked transcription factor knock-out strains (double-deletion mutants). These experiments revealed that the “core” of the white-opaque switch consists largely of a series of mutually antagonistic genetic interactions that compete for the relative stability of the white and opaque cell types. Surprisingly, the majority of these double deletion strains restored stochastic switching, rather than revealing clear epistatic interactions, suggesting that these TFs all compete for control of the switch at a common level, and that the relative stability of the white and opaque cell types is in part determined by integrating the regulatory inputs from each of the switch critical regulators. To determine the direct physical regulatory targets of each critical white-opaque regulatory TF we performed CUT&RUN on each of the four newly identified critical regulators in white and opaque cell types (Fgr15, Hfl1, Flo8, and Rbf1); this data was then integrated with the previously published ChIP data sets to further expand the switch regulatory network.

To comprehensively assess the genes that are regulated, either directly or indirectly, by the most impactful regulatory TFs that control white-opaque switching, we perform genome-wide transcriptional profiling (RNA-seq) on a set of 28 TF deletion

strains (including all 8 known switch critical regulators, and 20 of the most impactful switch modulating regulators) in white and opaque cell types (chapter 3). We also compare relative transcript levels for all of the known switch regulators in each of the 28 TF deletion backgrounds to uncover potential direct and indirect regulatory interactions between each of the switch regulators. By integrating the differential expression analysis with the preexisting ChIP and recently produced CUT&RUN data for each of the 12 characterized TFs, we will be able to identify putative direct regulatory interactions between each of the “core” regulators and the newly identified TF genes. Furthermore, by quantifying the degree of variance for each white and opaque-enriched gene across my mutant datasets, we have started to uncover a core set of genes that are strictly correlated with the white or opaque phenotype; these genes collectively define the “foundational” elements of the white- and opaque-specific transcriptomes. Together, by utilizing my differential expression analysis and the combined sets of genome-wide binding data, we have elucidated novel TF-TF regulatory interactions and foundational white or opaque transcriptomes, providing an excellent platform to identify potential mechanisms of how these TFs control the white-opaque switch.

The completion of this work has furthered our understanding of eukaryotic cell fate decisions through use of the biphasic, reversible, and stochastic white-opaque switch of *C. albicans* as a model system. We have unveiled novel TF-target interactions and provide valuable insight into the regulatory mechanisms that govern the formation and heritable maintenance of each cell type. We have begun to identify those “foundational” cell type-specific genes that are most closely linked to each of the two cell types. By developing a complete transcriptional profile of all known major white-opaque switch regulator deletion strains, we have expanded the scope of the characterized transcriptional network by 3-fold and generated essential data for detailed mathematical modeling of the switch. Epistatic interaction experiments uncovered potential mechanisms, such as recruitment of opposing chromatin modifiers or remodelers, that may contribute to the heritability of the white and opaque cell types. Finally, I have laid the groundwork for future studies that will further elucidate the detailed molecular mechanisms and dynamics of this complex epigenetic switch.

REFERENCES

1. Lohse MB, Ene IV, Craik VB, et al. Systematic Genetic Screen for Transcriptional Regulators of the *Candida albicans* White-Opaque Switch. *Genetics*. 2016;203(4):1679-1692. doi:10.1534/genetics.116.190645

CHAPTER 2

Wor1 is not required to establish opaque cell fate through removal of the potent repressor *RBF1* in *Candida albicans*

CHAPTER 2: *Wor1* is not required to establish opaque cell fate through removal of the potent repressor *RBF1* in *Candida albicans*

Introduction

Understanding how cells establish and maintain cellular identity through successive cell divisions is a fundamental problem in cell biology and has important implications in our understanding of transcriptional regulation, developmental biology, microbiology, and pathogenesis. Heritable transcriptional programs are found throughout the tree of life and are often controlled by complex transcriptional regulatory circuits. At their core, these circuits are comprised of sequence-specific regulatory transcription factors (TFs) and their respective regulatory target genes and can range in complexity from a few TFs and a single multi-cistronic operon in bacteria, to highly interwoven transcriptional circuits comprised of dozens of TFs and tens of thousands of target genes in higher eukaryotes¹. These transcriptional circuits are important not only for induced cellular responses to transient environmental signals, but they are also capable of controlling heritable changes in gene expression patterns that can be stably maintained through hundreds or even thousands of successive cell divisions². The sheer scale and complexity of heritable transcriptional circuits in higher eukaryotes, combined with the high degree of regulatory crosstalk between distinct cells and developmental programs, make these circuits daunting to study at a detailed molecular level. In contrast, unicellular fungi represent attractive model systems for understanding transcriptional regulatory mechanisms in eukaryotes thanks to high genetic tractability, a small number of genes, and relatively few heritable transcriptional programs.

The white-opaque phenotypic switch in *Candida albicans*, an opportunistic fungal pathogen of humans, represents a particularly attractive model system for investigating the transcriptional regulatory mechanisms that control cell fate decisions and epigenetic heritability in a “simple” eukaryotic organism. This switch controls heritable differentiation between two distinct cell types named “white” and “opaque” due to their distinct colony morphologies on semi-solid agar growth medium. These white and opaque cells differ in the expression of one out of every six genes in the organism, leading to distinct metabolic preferences, mating abilities, cellular morphologies, responses to environmental signals, and host interactions; essentially, this phenotypic switch generates two distinct pathogens from a single genome³⁻¹⁷. White cells are more pathogenic in disseminated bloodstream infection models, while opaque cells cause increased tissue damage in a skin model of infection¹⁸⁻²⁰. White cells are preferentially phagocytosed over opaque cells¹⁶, indicating that white to opaque switching may serve as a mechanism for immune evasion. Numerous environmental factors, including temperature, carbon source, and CO₂ concentration, can bias switching towards white or opaque cell types, further indicating that each phenotype is adapted to unique niches in the host environment³⁻¹¹. However, switching remains stochastic under a wide range of growth conditions, indicating that the white-opaque switch may also represent a bet-hedging mechanism for *C. albicans*. Under standard switch permissive laboratory growth

conditions, each cell type is stably maintained for hundreds of generations and switching between the two cell types occurs stochastically in a cell-autonomous manner^{4,5,21,22}. Each cell type is heritably maintained without any change in the primary sequence of the genome, thus fitting the classical definition of an epigenetic switch. Many of the transcriptional regulators that control the switch under these growth conditions are known, and an equivalent program is not found in other yeasts like *Saccharomyces cerevisiae*, thus making *C. albicans* an attractive “simple” eukaryotic organism to study how cellular memory is regulated and inherited from generation to generation.

The white-opaque switch is regulated by a complex transcriptional regulatory network that controls the frequency of switching between the two cell types^{8,23–32}. Eight of these white-opaque switch regulators, all but one of which are known to bind DNA directly, have been characterized extensively through a combination of transcriptional profiling and/or genome-wide chromatin immunoprecipitation approaches to identify their direct and indirect regulatory targets^{8,23–26,28–31,33–37}. Together these data led to the identification of the core switch circuits, defined by the direct binding interactions between each of the eight regulators and their respective 5' intergenic regions, as well as the larger switch networks, which include all the direct targets of these core switch regulators in both white and opaque cell types. The structure and transcriptional output of the core switch regulatory circuitry differs significantly between the two cell types (Figure 2-1). In white cells, this circuit is relatively compact, consisting of a series of nested feed forward loops that ultimately impinge upon the *WOR1* and *WOR2* genes, which are both actively repressed in white cells and are critical to the establishment and heritable maintenance of the opaque cell type. In contrast, the opaque circuit is highly intertwined, with over 90% of the possible binding interactions between each of the regulatory TFs and their respective coding genes being observed. This high-dimensional interwoven architecture of the opaque cell circuit (Figure 2-1, bottom right) bears a striking similarity to the transcriptional circuits that govern biofilm formation in *C. albicans* and stem cell maintenance and differentiation in humans³⁸. For example, the core stem cell regulatory circuit contains a minimum of 20 transcriptional regulators that are connected via at least 156 mutual regulator to promoter interactions, thus supporting the idea that the white-opaque switch may represent an attractive “simple” model system which could yield biological insights into the transcriptional regulation of complex cell fate circuits throughout eukaryotes³⁸. A recent study investigating the role of the intrinsically disordered prion-like domains found on most of the white-opaque regulators revealed that *Wor1*, *Wor4*, *Efg1*, and *Czf1* prion-like domains can form phase separated condensates in solution or associated with DNA in vitro and in vivo, suggesting a potential mechanism for the formation of these apparent multivalent regulatory complexes at the core of the opaque regulatory network.³⁹ These observations again highlight similarities between the opaque regulatory network and the more complex regulatory networks that control cell fate decisions in higher eukaryotes.

Wor1 is the master regulator of the opaque cell type and repression or activation of *WOR1* expression is a key component of establishing the white or opaque cell types, respectively^{8,23-29}. In white cells, *WOR1* expression is repressed in an *EFG1*, *AHRI*, and *SSN6*-dependent manner, and deletion of any one of these three genes will destabilize the white cell type or, in the case of *SSN6* deletion, result in an opaque-locked phenotype. *Czf1* and *Wor4* act to promote white-to-opaque switching and, in the case of *Wor4*, directly promote *WOR1* expression in both white and opaque cell types. In opaque cells, *WOR1* expression is upregulated 32-fold relative to white cells and is maintained in part due to a positive autoregulatory feedback loop of *Wor1* binding upstream of *WOR1*. This positive feedback loop, and thus the opaque transcriptional program, is heritably maintained in a *WOR2*-dependent manner; while the white-to-opaque transition and *WOR1* autoregulatory feedback loop can be stimulated by ectopic expression of *WOR1* in Δ/Δ *wor2* strains, the resulting opaque cells are not heritably maintained in the absence of ectopic *WOR1* expression and rapidly revert en masse to the white cell type²⁴. Similarly, *WOR4* expression is required for stable heritable maintenance of *WOR1* expression and the opaque cell type²⁹. *WOR3*, which is normally expressed only in the opaque cell type, can drive white-to-opaque switching en masse when ectopically expressed in white cells, and appears to destabilize opaque cells in a temperature and carbon source-dependent manner, but is otherwise dispensable for normal white-opaque switching under standard switch permissive growth conditions^{8,25}. Stochastic white-to-opaque switching is believed to occur when transcriptional noise within the white-cell regulatory network allows *Wor1* levels to surpass a minimum threshold necessary to induce the *WOR1* positive feedback loop, while opaque-to-white switching is believed to occur once *Wor1* levels drop below a critical threshold, estimated at approximately 20% of normal opaque levels, that is required to maintain the opaque transcriptional program^{23,27,37}. Although the role of *Wor1* in switching is well established, and prior work has elucidated many of the physical and genetic regulatory interactions between *WOR1*, *WOR2*, *WOR3*, *WOR4*, *CZF1*, *EFG1*, *SSN6*, and *AHRI*, many additional regulators have since been identified and have yet to be incorporated into a more comprehensive understanding of the white-opaque switch regulatory network.

A systematic screen of 196 unique homozygous *C. albicans* TF deletion strains identified 33 additional switch regulators that, when deleted, significantly impact the frequency of switching between the white and opaque cell types under standard switch permissive laboratory growth conditions (synthetic minimal media with dextrose, supplemental amino acids, and incubated at 25°C)³⁰. Nineteen of these TF deletions resulted in at least 10-fold changes in the frequency of switching in either the white to opaque or opaque to white direction, while an additional fourteen regulators had more subtle yet significant impacts on switching when deleted³⁰. In addition to *WOR1*, *WOR2*, *WOR4*, *SSN6* and *FLO8*, which had previously been shown to be “critical” regulators of the white-opaque switch, *FGR15*, *HFL1*, and *RBF1* deletion strains were also found to be locked in, or heavily biased towards, either the white or opaque cell type^{23,24,26,27,28,29,37,40}. *WOR1*, *WOR2*, *WOR4*, *FLO8*, *FGR15* and *HFL1* are required for white to opaque

switching or heritable maintenance of the opaque state, while cells lacking *SSN6* or *RBF1* fail to switch to the white cell type and produce only opaque cells. While *Wor1*, *Wor2*, *Wor4* and *Ssn6* have previously been incorporated into the white-opaque switch regulatory networks through genetic interaction analyses, transcriptional profiling of deletion strains, and genome-wide chromatin immunoprecipitation (ChIP) approaches, and *Flo8* has been shown to bind directly upstream of *WOR1* via locus-specific ChIP, the genetic interactions between *FLO8*, *FGR15*, *HFL1*, and *RBF1* with the other more extensively characterized switch critical regulators (*WOR1*, *WOR2*, *WOR4*, and *SSN6*) remains largely unexplored.

In addition to their roles in controlling the white-opaque switch, all four of the more recently identified switch critical TFs (*Flo8*, *Fgr15*, *Hfl1*, and *Rbf1*) have been previously shown to play important roles in controlling the yeast to hyphal switch in *C. albicans*. *Flo8* promotes hyphal development and expression of hyphal-specific genes in liquid cultures but suppresses hyphal development under imbedded growth conditions. *Flo8* contains a LisH domain that is known to be involved in protein:protein interactions with *Mss11* and *Efg1*, which are also involved in the transcriptional activation of hyphal-specific genes^{41,42}. In *Saccharomyces cerevisiae*, *Flo8* is required for flocculation, diploid filamentous growth, and haploid invasive growth, and has been shown to form a heterodimer with *Mss11* which interacts with the *Swi/Snf* chromatin remodeling complex during transcriptional activation of specific target genes. *Fgr15* lacks a direct ortholog in *S. cerevisiae*, but it is annotated as a putative transcription factor in *C. albicans* based on the presence of a zinc finger DNA-binding domain and was identified as a regulator of filamentous growth in a haploinsufficiency screen⁴³. *Rbf1* also lacks a clear ortholog in *S. cerevisiae* but is known to bind RPG-box DNA sequences and repress the yeast to hyphal transition in *C. albicans*⁴⁴⁻⁴⁶. *HFL1* is annotated as a homologue of *DPB3* in *S. cerevisiae*, which encodes the third-largest subunit of DNA polymerase II, however this homology is relatively weak (32% identity) and is restricted to a stretch of 98 amino acids that lie at the core of the *Dpb3* DNA binding domain. *HFL1* has similar levels of homology to a variety of known and putative transcriptional regulators, found throughout eukaryotes, that contain histone-like DNA binding domains, suggesting that *Hfl1* may in fact be a sequence specific DNA binding protein^{46,47}. While these and several other yeast-hyphal switch regulators are shared with the white-opaque switch, and thus what is learned about these them in the context of one switch may inform their function in the other, it is worth noting that these two switches behave very differently. Hyphal development is regulated in a deterministic manner in response to environmental variables that either promote or suppress hyphal development, however hyphal cells readily revert to yeast form cells in the absence of hyphal-inducing culture conditions. In contrast, while the white-opaque switch can be biased in one direction or another by environmental inputs, the switch ultimately behaves in a stochastic manner and both cell type can be heritably maintained for hundreds of generations in the same growth medium.

In this study, we performed a comprehensive genetic epistasis interaction analysis to determine how those genes which are critical for white to opaque switching (*WOR1*, *WOR2*, *WOR4*, *FLO8*, *FGR15* and *HFL1*), interact with those which are critical for opaque to white switching (*SSN6* and *RBF1*). Surprisingly, while we observed that some of the switch critical regulators are clearly epistatic to each other, as previously reported for the interaction between *WOR1* and *SSN6*, several of the pairwise combinations of white- and opaque-locked mutants restored stochastic switching between the white and opaque cell types²⁸. These results suggest that many of the switch critical regulators are likely impinging upon the switch through overlapping, mutually antagonistic regulatory mechanisms, and that the stochastic nature of the switch may be a function of which regulator(s) wins out in any given cell. These findings significantly increase our understanding of the genetic regulatory interactions that are critical to stochastic switching between, and heritable maintenance of, the differentiated white and opaque cell types of *C. albicans*.

Materials and Methods

Media

Synthetic Defined with amino acids and Uridine (SD+aa+Uri) was used to grow strains and maintain the white and opaque states at 25°C. For ectopic expression experiments using the *MET3* promoter, cells were induced in SD+aa+Uri-Met-Cys or repressed in SD+aa+Uri +Met+Cys, as previously described^{14,24,54}.

Strain construction

All yeast strains in this study were constructed using the previously described CRISPR/Cas9 mediated genome editing protocol and verified by colony PCR.

All plasmids were assembled by *in vivo* gap repair cloning into *Escherichia coli* that were derived from DH5alpha and cultured at 37°C in LB medium supplemented with 100ug/mL carbenicillin. The previously reported plasmid pADH98 was used as the base plasmid used in this research as it is an *E. coli* plasmid that contains a Multiple Cloning Site (MCS) digestible with Hind3 and BamH1 to make a clean entry vector (EV)⁵⁵.

Construction of pADH322 (*NEUT5L* integration plasmid): The insert fragment (IF) was ordered as a GeneArt synthetic fragment from ThermoFisher containing the 5' Linker sequence of pADH98 followed by 220bp of 300bp of the 5' segment of *NEUT5L* followed by a MCS that contains digestion sites for Hind3, Not1, Bgl2, and Pst1 which was then followed by with 147bp of 250 of the *NEUT5L* 3' segment, and lastly followed by the 3' linker sequence of pADH98⁵⁵. This IF was amplified with AHO1096 and AHO1097, purified, and assembled by *in vivo* cloned into pADH98 to generate the plasmid pADH322.

Construction of pADH323 (pMET3 driving *WOR1* orf expression vector integratable at the *NEUT5L* sequence): pADH322 was used to make the EV for pADH323 by digesting the MCS with Hind3 and Pst1. The IF containing the promoter for *MET3* driving expression of the *WOR1* orf was PCR amplified from the previously reported pADH35 using oligos AHO1041 and AHO2495, and then assembled by *in vivo* cloned into pADH322-EV to generate pADH323.

White to opaque and Opaque to white switch assays

The white to opaque and opaque to white switch assays were a variation of the previously reported in Miller and Johnson 2002. Strains were streaked from freezer stocks on plate media (SD+aa+Uri at 25°C) and grown for 7-10 days. A single colony isolate (SCI) was resuspended in 750µL of liquid media (SD+AA+Uri at 25°C), serially diluted, and plated at a density of 100-200 colony-forming units per 100mm plate of media (SD+aa+Uri+Phloxin B at 25°C) across 10 plates. After 7-10 days of growth at 25°C, the colonies were examined and counted for the number of switch events (either as sectors or full colonies). This was performed at least three times per strain and phenotypic state across all mutants.

Microscopy

Cells used for microscopy were taken from solid media cultures (SD+aa+Uri at 25°C) that were grown for 7-10 days and placed in liquid media (SD+aa+Uri at 25°C). Cells were resuspended in liquid media (SD+aa+Uri at 25°C). Multiple images of each strain in either the white or opaque state were taken within 30 minutes of resuspension on the EVOS FL microscope with a 40× objective using BF and/or the GFP filter.

Colonies used for microscopy were examined on solid media (SD+aa+Uri+Phloxin B at 25°C) that had grown for 7-10 days. Multiple images of each strain in either the white or opaque state on the National DC4-456H microscope with 3.0MP camera.

Results

To systematically investigate the genetic interactions between the eight switch critical regulators (*FGR15*, *FLO8*, *HFL1*, *RBF1*, *SSN6*, *WOR1*, *WOR2* and *WOR4*), we generated a series of double homozygous deletion strains where the open reading frames for each of the individual Opaque-Critical TFs (OCTFs) (*FGR15*, *FLO8*, *HFL1*, *WOR1*, *WOR2*, and *WOR4*) were deleted in combination with one of the White-Critical TFs (WCTFs) (*RBF1* or *SSN6*) (Table 2-1). To determine how each pairwise combination of deletions impacted the dynamics of white-opaque switching, each of the double gene deletion strains, along with their wild-type and single gene deletion reference strains, were subjected to switch frequency analysis using standard switch permissive conditions (synthetic minimal media with dextrose, supplemental amino acids and Phloxine B, incubated at 25°C) (See Table 2-2, 2-3, and 2-4). Phloxine B is commonly used to facilitate distinguishing between white and opaque cell types at a colony level, with the white colonies appearing light pink to white in color and the opaque colonies appearing dark pink to magenta in color^{14,17,40,48,49}. To further validate the results of our colony switching assay, we also assessed the cellular morphology and *WOR1* expression patterns of white and/or opaque isolates for each of the double deletion strains. To enable assessment of *WOR1* expression, we introduced a *C. albicans* optimized mNeonGreen coding sequence either in-frame with the C-terminus of the *Wor1* coding sequence (translational fusion), or in place of the deleted *WOR1* open reading frame (transcriptional fusion). As expected, we observed that the majority of cells isolated from apparent white colonies displayed typical yeast-form cellular morphologies and no detectable *WOR1* expression, while the majority of cells isolated from apparent opaque colonies displayed elongated cell morphologies and detectable fluorescence from the *WOR1* reporter, indicating that they are likely bona fide white and opaque cells, respectively. We note that tagging *Wor1* with a C-terminal mNeonGreen fusion increased the frequency of white to opaque switching in our wild-type reference strain as well as in several of our single and double gene deletion strains (Table 2-5). A similar effect has been observed with C-terminal GFP tagged forms of *Wor1*, but introduction of mutations that reduce the propensity of GFP to dimerize reduces this impact on white to opaque switching⁵⁰. This suggests that perhaps our mNeonGreen tag may be helping to increase protein:protein interactions between tagged copies of *Wor1*, possibly promoting the liquid-liquid phase separation of *Wor1* which has been shown to be required for white-to-opaque switching³⁹. Regardless, we still observe cell type specific expression of *Wor1* in our wild-type strain and we believe that this reporter fusion is still a valid indicator of whether *WOR1* transcription is activated or repressed. This increased switch frequency is not only seen in multiple isolates of the wildtype reference strain but was also observed in two other single deletion strains as well, $\Delta/\Delta fgr15$ and $\Delta/\Delta hfl1$. This result was perhaps to be expected in the $\Delta/\Delta fgr15$ background since this deletion has been reported to switch to opaque at a very low but measurable frequency³⁰. However, this impact of *Wor1* tagging was not expected in the $\Delta/\Delta hfl1$ strain background, which is otherwise locked in the white cell type³⁰. We do not believe this is an artifact of using

CRISPR/Cas9 to delete *HFL1*, since white to opaque switching was not observed in our CRISPR-generated Δ/Δ *hfl1* base strains that lack the tagged version of Wor1 (Table 2-2). Furthermore, we note that deleting *HFL1* in the wild-type strain harboring Wor1 tagged with mNeonGreen did result in a substantial decrease in white to opaque switching compared to the wild-type strain harboring the tagged Wor1(34-fold), with no full opaque colonies observed and only a small percentage of colonies displaying opaque sectors (0.5%). Also, the observed opaque sectors were extremely unstable and reverted to the white cell type when restreaked (data not shown). Together these results suggest that the observed switch events were likely due to the tagging of Wor1 which increases the propensity of cells to switch to the opaque state, and not a side effect of deleting *HFL1* with CRISPR/Cas9 (Table 2-2 and Table 2-5).

Genetic interactions between *SSN6* and the opaque-critical regulators

Deletion of *SSN6* (WCTF) from strains lacking *WOR1*, *FLO8*, or *FGR15* (OCTF) resulted in white or opaque-locked phenotypes, indicating clear epistatic interactions between *SSN6* and these three opaque-promoting regulators (Table 2-3). Consistent with previously published results using traditional gene deletion strategies, our CRISPR-generated Δ/Δ *wor1* Δ/Δ *ssn6* strain was locked in the white cell type, indicating that Wor1 expression is essential for activation of the opaque transcriptional program, even in the absence of Ssn6²⁸. In contrast, deletion of *SSN6* in either the Δ/Δ *flo8* or Δ/Δ *fgr15* (OCTF) strain backgrounds resulted in opaque-locked phenotypes, indicating that *SSN6* is epistatic to *FLO8* and *FGR15*, and that neither Flo8 nor Fgr15 is required to establish the opaque cell type in the absence of Ssn6. We note that although phloxine B staining was relatively low in the Δ/Δ *flo8* Δ/Δ *ssn6* colonies, we consider this genotype to be opaque locked based on the characteristic elongated cell morphology and elevated Wor1 levels observed at the single cell level (Figure 2-2). Surprisingly, deletion of *SSN6* in the Δ/Δ *wor2*, Δ/Δ *wor4*, and Δ/Δ *hfl1* strain backgrounds (OCTF) restored reversible phenotypic switching to these otherwise white-locked genotypes, indicating that the loss of stochastic opaque to white switching observed in the Δ/Δ *ssn6* background can be restored by removal of these opaque-promoting regulators. The observation of reversible switching in the Δ/Δ *wor2* Δ/Δ *ssn6* and Δ/Δ *wor4* Δ/Δ *ssn6* strains is particularly remarkable, as both *WOR2* and *WOR4* have previously been shown to be essential for, or contribute substantially to, the heritable maintenance of the opaque cell type, respectively^{24,29}. Deletion of *SSN6* from the Δ/Δ *wor2* background not only enables relatively high frequency white-to-opaque switching in this otherwise white-locked background, but the resulting opaque cells are also highly stable, with a 7-fold reduction in opaque-to-white switching relative to wild-type cells (Table 2-3). This observation suggests that unlike the clear epistatic interaction between *WOR1* and *SSN6*, which is consistent with Wor1 functioning downstream of Ssn6, Wor2 and Ssn6 may instead function as directly opposing factors within the same “level” of the core switch circuitry. Unlike the Δ/Δ *wor2* Δ/Δ *ssn6* opaque cells, Δ/Δ *wor4* Δ/Δ *ssn6* opaque cells are highly unstable and revert to the white cell type at a threefold higher frequency than wild-type

opaque cells (Table 2-3), indicating that Wor4 plays a role in stabilizing the opaque cell type that is at least partially distinct from overcoming the opaque-destabilizing impact of Ssn6. Conversely, the Δ/Δ *hfl1* Δ/Δ *ssn6* strain is highly biased toward the opaque cell type, with more than 90% of cells isolated from white colonies giving rise to opaque colonies, and nearly a sixfold reduction in opaque-to-white switching, relative to wild-type (Table 2-3). This result indicates that while loss of *SSN6* is largely dominant to loss of *HFL1*, Hfl1 still plays an important role in stabilizing the opaque cell type, even in the absence of Ssn6.

Genetic interactions between *RBF1* and the opaque-critical regulators

Rbf1, which is best known as a repressor of filamentous growth in *C. albicans*, also plays a critical role in suppressing the opaque phenotypic state. Homozygous *RBF1* deletion strains appear to be locked in the opaque phenotype at the colony level, and regularly display a filamentous opaque phenotype at the single-cell level (Figure 2-3). When *RBF1* was deleted in conjunction with each of the six opaque-critical regulators, only one combination revealed a clearly epistatic genetic interaction; the Δ/Δ *fgf15* Δ/Δ *rbf1* strain was locked in the opaque cell type (Figure 2-4), indicating that *RBF1* is fully epistatic to *FGR15* with regard to control of the white-opaque switch. Remarkably, each of the other five strains that paired opaque-critical regulator deletions with the deletion of *RBF1* displayed measurable switching between apparent white and opaque colony phenotypes (Table 2-4).

The observation of apparent white-opaque switching in the Δ/Δ *wor1* Δ/Δ *rbf1* strain is particularly striking, as *WOR1* is considered to be the master regulator of the opaque cell type and has previously been shown to be essential for white-to-opaque phenotypic switching under the growth conditions used in our assay. At the colony level, the Δ/Δ *wor1* Δ/Δ *rbf1* “white” and “opaque” colonies can be differentiated based on phloxine B staining, with light vs dark staining respectively (Figure 2-4). At the single-cell level we observe activation of the *pWOR1*-mNeonGreen transcriptional fusion in a substantial subset of the cells isolated from “opaque” colonies (Figure 2-4), indicating that the native *WOR1* promoter is being activated independent of Wor1 expression in the Δ/Δ *wor1* Δ/Δ *rbf1* strain. Although mNeonGreen expression was not observed in all cells obtained from “opaque” Δ/Δ *wor1* Δ/Δ *rbf1* colonies, we note that this is consistent with the relatively high opaque-to-white switching frequency of this genotype (Table 2-4). We also note that the observed fluorescence in these strains is lower than that observed for opaque cells isolated from strains which carry the Wor1-mNeonGreen translational fusion construct (Figure 2-4 and 2-5). While it is possible that transcription from the native *WOR1* promoter is reduced in Δ/Δ *wor1* Δ/Δ *rbf1* opaque cells, relative to their counterparts which express Wor1, we believe this is more likely a function of the *pWOR1*-mNeonGreen transcriptional fusion, as similar expression levels are observed from this same construct even when Wor1 is expressed from an inducible *pMET3*>*WOR1* construct (Figure 2-4 and 2-5). Although we have not yet assessed relative transcript levels for other white/opaque regulators or classic white vs opaque marker genes in the

$\Delta/\Delta wor1 \Delta/\Delta rbf1$ strain background, the differential phloxine B staining between apparent “white” and “opaque” colonies indicates that at least a portion of the opaque transcriptional program is being activated despite the absence of *WOR1*. Furthermore, the corresponding cell type specific *WOR1* promoter expression patterns suggest that at least the core circuitry that controls *WOR1* expression, and thus the establishment and maintenance of the opaque transcriptional program, can undergo stochastic, heritable switching in the absence of *WOR1* when *RBF1* is also removed from the circuit.

Deletion of *RBF1* in the $\Delta/\Delta wor2$, $\Delta/\Delta wor4$, $\Delta/\Delta flo8$, and $\Delta/\Delta hfl1$ strain backgrounds also restored switching to these otherwise white-locked genotypes. Remarkably, each of these double deletion strains display increased white to opaque switch frequencies (2 to 10-fold) and decreased opaque to white switch frequencies (2 to 4-fold) relative to wild-type cells (Table 2-4). These switching frequencies are also similar to the $\Delta/\Delta wor1 \Delta/\Delta rbf1$ strain (Table 2-4), suggesting that Rbf1 may play a foundational role in stabilizing the white cell type and/or destabilizing the opaque cell type, and that Wor1, Wor2, Wor4, Flo8, and Hfl1 all contribute complementary regulatory forces to counteract Rbf1.

We note that a filamentous phenotype was observed for several of the double deletion strains that lack *RBF1* (See Figure 2-4). In particular, both $\Delta/\Delta flo8 \Delta/\Delta rbf1$ and $\Delta/\Delta hfl1 \Delta/\Delta rbf1$ strains exhibit filamentous growth in both the white and opaque cell types which can be observed at both the cellular and colony level. The remaining four TF double deletions in this set ($\Delta/\Delta wor1 \Delta/\Delta rbf1$, $\Delta/\Delta wor2 \Delta/\Delta rbf1$, and $\Delta/\Delta wor4 \Delta/\Delta rbf1$) exhibited filamentous growth in the opaque state, but not in the white state.

Discussion

The gene regulatory network responsible for establishment and maintenance of the white-opaque switch in *C. albicans* is a highly interwoven complex network that gives rise to two distinct cell types that can be heritably maintained for thousands of generations. In this study, we systematically tested the genetic interactions between each of the white and opaque-critical TF coding genes which, when deleted, result in opaque or white locked phenotypes, respectively. Of the twelve genotypic combinations tested, only four resulted in white locked ($\Delta/\Delta wor1 \Delta/\Delta ssn6$) or opaque locked ($\Delta/\Delta flo8 \Delta/\Delta ssn6$, $\Delta/\Delta fgr15 \Delta/\Delta ssn6$, and $\Delta/\Delta fgr15 \Delta/\Delta rbf1$) phenotypes. The complete epistasis of one gene over another suggests a hierarchical regulatory relationship between the two deleted genes, with Ssn6 working upstream of Wor1, Fgr15 working upstream of both *SSN6* and *RBF1*, and Flo8 working upstream of *SSN6*. In contrast, the remaining eight double deletion genotypes ($\Delta/\Delta wor1 \Delta/\Delta rbf1$, $\Delta/\Delta wor2 \Delta/\Delta ssn6$, $\Delta/\Delta wor2 \Delta/\Delta rbf1$, $\Delta/\Delta wor4 \Delta/\Delta ssn6$, $\Delta/\Delta wor4 \Delta/\Delta rbf1$, $\Delta/\Delta flo8 \Delta/\Delta rbf1$, $\Delta/\Delta hfl1 \Delta/\Delta ssn6$, and $\Delta/\Delta hfl1 \Delta/\Delta rbf1$) displayed reversible phenotypic switching between apparent white and opaque cell types. Rather than revealing clear epistatic relationships between these regulators, these results suggest more complicated genetic relationships that are consistent with opposing TFs impinging upon the white-opaque switch at the same level. The

observation that deletion of either *SSN6* or *RBF1* restored reversible switching to white-locked strains lacking *WOR2*, *WOR4*, or *HFL1* suggests that these three opaque-critical regulators may promote the stability of the opaque cell type by directly counteracting the opaque-destabilizing forces of both Ssn6 and Rbf1. This also raises the question of whether strains that lack both *SSN6* and *RBF1* might be completely independent of *WOR2*, *WOR4*, or *HFL1* and thus would be locked in the opaque state even in the absence of any one of these three opaque-promoting TFs.

Of the twelve genotypic combinations tested, only the Δ/Δ *wor1* Δ/Δ *ssn6* genotype was locked in the white cell type. This indicates that while Wor1 is essential to promote the opaque transcriptional program even in the absence of Ssn6, none of the other opaque-promoting TFs are strictly necessary to form opaque cells under the conditions and genotypic combinations tested. Perhaps most surprisingly, we observed that *WOR1* itself is dispensable for phenotypic switching between white-like and opaque-like phenotypic states when *RBF1* is also deleted. We observed two distinct heritably maintained phenotypic states in the Δ/Δ *wor1* Δ/Δ *rbf1* genotype, with the phloxine B-stained colonies containing a significant number of cells which expressed a *pWOR1*>mNeonGreen transcriptional reporter, indicating Wor1-independent activation of transcription at the native *WOR1* promoter. Although Park et al. previously found that strains lacking both *EFG1* and *WOR1* can be induced to switch en masse to an opaque-like phenotype by growth in the presence of GlcNAc and 5% CO₂ at 37°C, and Alkafeef et al found that cells lacking *WOR1* can activate expression of several opaque-activated promoters, including *WOR1*, in response to transient depletion of Tup1, to our knowledge this is the first report of bistable switching between apparent white and opaque cell types under standard switch permissive conditions in the absence of *WOR1*^{51,52}. Park et al. propose that removal of the opaque-repressing regulator Efg1, along with growth under specific opaque-promoting conditions, triggers Wor1-independent activation of an alternative opaque pathway. Since Rbf1 is known to suppress activation of the filamentous growth program in an environmentally-regulated manner^{44,46}, and deletion of *RBF1* restored apparent white to opaque switching to our Δ/Δ *wor1* strain, it is tempting to consider the possibility that the switch-inducing conditions used by Park et al. may have resulted in Wor1-independent switching by alleviating Rbf1-mediated repression of the opaque transcriptional program. These results suggest that different environmental cues may promote white to opaque switching through the “traditional” opaque program by impacting the function of opaque-promoting regulators, or through an “alternate” opaque program through inactivation of opaque-destabilizing regulators such as Rbf1. This may explain the ability of *C. albicans* to flourish in a wide range of environmental niches in and on the host. White cells have been shown to more readily colonize organs such as the kidney and gut, while opaque cells tend to colonize the skin, heart, and spleen^{20,53}. These differential colonization preferences is likely due to the fact that opaque cells are less susceptible to phagocytosis by macrophages¹⁶ as well as why the opaque program has been conserved. The next challenge will be to determine how Rbf1 represses the “traditional” opaque transcriptional program, how various environmental cues may

alleviate Rbf1-mediated repression to enable the “alternate” opaque program, and what differentiates the mechanisms by which Ssn6 and Rbf1 suppress the formation and/or stability of the opaque transcriptional program. Further studies will also be needed to determine the mechanisms by which opaque promoting factors directly or indirectly overcome the competing forces of Rbf1 and Ssn6, and how these opposing forces contribute to the stochastic nature of the white-opaque switch.

References

1. Kucinski I, Wilson NK, Hannah R, et al. Interactions between lineage-associated transcription factors govern haematopoietic progenitor states. *EMBO J.* 2020;39(24). doi:10.15252/embj.2020104983
2. Johnston RJ, Desplan C. Stochastic Mechanisms of Cell Fate Specification that Yield Random or Robust Outcomes. *Annu Rev Cell Dev Biol.* 2010;26(1):689-719. doi:10.1146/annurev-cellbio-100109-104113
3. Dumitru R, Navarathna DHMLP, Semighini CP, et al. In Vivo and In Vitro Anaerobic Mating in *Candida albicans*. *Eukaryotic Cell.* 2007;6(3):465-472. doi:10.1128/EC.00316-06
4. Ramírez-Zavala B, Reuß O, Park YN, Ohlsen K, Morschhäuser J. Environmental Induction of White–Opaque Switching in *Candida albicans*. Cormack BP, ed. *PLoS Pathog.* 2008;4(6):e1000089. doi:10.1371/journal.ppat.1000089
5. Alby K, Bennett RJ. Stress-Induced Phenotypic Switching in *Candida albicans*. Chang F, ed. *MBoC.* 2009;20(14):3178-3191. doi:10.1091/mbc.e09-01-0040
6. Huang G, Srikantha T, Sahni N, Yi S, Soll DR. CO₂ Regulates White-to-Opaque Switching in *Candida albicans*. *Current Biology.* 2009;19(4):330-334. doi:10.1016/j.cub.2009.01.018
7. Huang G. Regulation of phenotypic transitions in the fungal pathogen *Candida albicans*. *Virulence.* 2012;3(3):251-261. doi:10.4161/viru.20010
8. Lohse MB, Hernday AD, Fordyce PM, et al. Identification and characterization of a previously undescribed family of sequence-specific DNA-binding domains. *Proceedings of the National Academy of Sciences.* 2013;110(19):7660-7665. doi:10.1073/pnas.1221734110
9. Du H, Huang G. Environmental pH adaption and morphological transitions in *Candida albicans*. *Curr Genet.* 2016;62(2):283-286. doi:10.1007/s00294-015-0540-8
10. Ene IV, Lohse MB, Vladu AV, Morschhäuser J, Johnson AD, Bennett RJ. Phenotypic Profiling Reveals that *Candida albicans* Opaque Cells Represent a Metabolically Specialized Cell State Compared to Default White Cells. *mBio.* 2016;7(6):e01269-16, /mbio/7/6/e01269-16.atom. doi:10.1128/mBio.01269-16
11. Dalal CK, Zuleta IA, Lohse MB, Zordan RE, El-Samad H, Johnson AD. A population shift between two heritable cell types of the pathogen *Candida albicans* is based both on switching and selective proliferation. *Proc Natl Acad Sci USA.* 2019;116(52):26918-26924. doi:10.1073/pnas.1908986116
12. Lan CY, Newport G, Murillo LA, et al. Metabolic specialization associated with phenotypic switching in *Candida albicans*. *Proceedings of the National Academy of Sciences.* 2002;99(23):14907-14912. doi:10.1073/pnas.232566499
13. Kolotila MP, Diamond RD. Effects of neutrophils and in vitro oxidants on survival and phenotypic switching of *Candida albicans* WO-1. *Infection and Immunity.* 1990;58(5):1174-1179. doi:10.1128/IAI.58.5.1174-1179.1990

14. Miller MG, Johnson AD. White-Opaque Switching in *Candida albicans* Is Controlled by Mating-Type Locus Homeodomain Proteins and Allows Efficient Mating. *Cell*. 2002;110(3):293-302. doi:10.1016/S0092-8674(02)00837-1
15. Bennett RJ, Uhl MA, Miller MG, Johnson AD. Identification and Characterization of a *Candida albicans* Mating Pheromone. *MCB*. 2003;23(22):8189-8201. doi:10.1128/MCB.23.22.8189-8201.2003
16. Lohse MB, Johnson AD. Differential Phagocytosis of White versus Opaque *Candida albicans* by Drosophila and Mouse Phagocytes. Beier D, ed. *PLoS ONE*. 2008;3(1):e1473. doi:10.1371/journal.pone.0001473
17. Sasse C, Hasenberg M, Weyler M, Gunzer M, Morschhäuser J. White-Opaque Switching of *Candida albicans* Allows Immune Evasion in an Environment-Dependent Fashion. *Eukaryotic Cell*. 2013;12(1):50-58. doi:10.1128/EC.00266-12
18. Kvaal CA, Srikantha T, Soll DR. Misexpression of the white-phase-specific gene WH11 in the opaque phase of *Candida albicans* affects switching and virulence. *Infect Immun*. 1997;65(11):4468-4475. doi:10.1128/iai.65.11.4468-4475.1997
19. Kvaal C, Lachke SA, Srikantha T, Daniels K, McCoy J, Soll DR. Misexpression of the Opaque-Phase-Specific Gene *PEP1* (*SAP1*) in the White Phase of *Candida albicans* Confers Increased Virulence in a Mouse Model of Cutaneous Infection. Kozel TR, ed. *Infect Immun*. 1999;67(12):6652-6662. doi:10.1128/IAI.67.12.6652-6662.1999
20. Lachke SA, Lockhart SR, Daniels KJ, Soll DR. Skin Facilitates *Candida albicans* Mating. *Infect Immun*. 2003;71(9):4970-4976. doi:10.1128/IAI.71.9.4970-4976.2003
21. Rikkerink EHA. Opaque-White Phenotype Transition: a Programmed Morphological Transition in *Candida albicans*. *J BACTERIOL*. 1988;170:5.
22. Marshall S, Bergen, Edward Voss, David R. Soll. Switching at the cellular level in the white-opaque transition of *Candida albicans*. *Journal of General Microbiology*. 1990;136(10):1925-1936. doi:10.1099/00221287-136-10-1925
23. Zordan RE, Galgoczy DJ, Johnson AD. Epigenetic properties of white-opaque switching in *Candida albicans* are based on a self-sustaining transcriptional feedback loop. *Proceedings of the National Academy of Sciences*. 2006;103(34):12807-12812. doi:10.1073/pnas.0605138103
24. Zordan RE, Miller MG, Galgoczy DJ, Tuch BB, Johnson AD. Interlocking Transcriptional Feedback Loops Control White-Opaque Switching in *Candida albicans*. Heitman J, ed. *PLoS Biol*. 2007;5(10):e256. doi:10.1371/journal.pbio.0050256
25. Hernday AD, Lohse MB, Fordyce PM, Nobile CJ, DeRisi JL, Johnson AD. Structure of the transcriptional network controlling white-opaque switching in *Candida albicans*: White-opaque switching network in *C. albicans*. *Molecular Microbiology*. Published online September 2013:n/a-n/a. doi:10.1111/mmi.12329
26. Huang G, Wang H, Chou S, Nie X, Chen J, Liu H. Bistable expression of *WOR1*, a master regulator of white-opaque switching in *Candida albicans*. *Proceedings of the*

- National Academy of Sciences*. 2006;103(34):12813-12818.
doi:10.1073/pnas.0605270103
27. Srikantha T, Borneman AR, Daniels KJ, et al. TOS9 Regulates White-Opaque Switching in *Candida albicans*. *Eukaryotic Cell*. 2006;5(10):1674-1687.
doi:10.1128/EC.00252-06
 28. Hernday AD, Lohse MB, Nobile CJ, Noiman L, Laksana CN, Johnson AD. Ssn6 Defines a New Level of Regulation of White-Opaque Switching in *Candida albicans* and Is Required For the Stochasticity of the Switch. *mBio*. 2016;7(1):e01565-15,
/mbio/7/1/e01565-15.atom. doi:10.1128/mBio.01565-1
 29. Lohse MB, Johnson AD. Identification and Characterization of Wor4, a New Transcriptional Regulator of White-Opaque Switching. *G3*. 2016;6(3):721-729.
doi:10.1534/g3.115.024885
 30. Lohse MB, Ene IV, Craik VB, et al. Systematic Genetic Screen for Transcriptional Regulators of the *Candida albicans* White-Opaque Switch. *Genetics*. 2016;203(4):1679-1692. doi:10.1534/genetics.116.190645
 31. Wang H, Song W, Huang G, Zhou Z, Ding Y, Chen J. *Candida albicans* Zcf37, a zinc finger protein, is required for stabilization of the white state. *FEBS Letters*. 2011;585(5):797-802. doi:10.1016/j.febslet.2011.02.005
 32. Du H, Li X, Huang G, Kang Y, Zhu L. The zinc-finger transcription factor, Ofi1, regulates white–opaque switching and filamentation in the yeast *Candida albicans*. *Acta Biochimica et Biophysica Sinica*. 2015;47(5):335-341.
doi:10.1093/abbs/gmv011
 33. Tuch BB, Mitrovich QM, Homann OR, et al. The Transcriptomes of Two Heritable Cell Types Illuminate the Circuit Governing Their Differentiation. Copenhaver GP, ed. *PLoS Genet*. 2010;6(8):e1001070. doi:10.1371/journal.pgen.1001070
 34. Sonneborn A, Tebarth B, Ernst JF. Control of White-Opaque Phenotypic Switching in *Candida albicans* by the Efg1p Morphogenetic Regulator. Kozel TR, ed. *Infect Immun*. 1999;67(9):4655-4660. doi:10.1128/IAI.67.9.4655-4660.1999
 35. Srikantha T, Tsai LK, Daniels K, Soll DR. EFG1 Null Mutants of *Candida albicans* Switch but Cannot Express the Complete Phenotype of White-Phase Budding Cells. *J Bacteriol*. 2000;182(6):1580-1591. doi:10.1128/JB.182.6.1580-1591.2000
 36. Vences MD, Kumamoto CA. The morphogenetic regulator Czf1p is a DNA-binding protein that regulates white–opaque switching in *Candida albicans*. *Microbiology*. 2007;153(9):2877-2884. doi:10.1099/mic.0.2007/005983-0
 37. Lohse MB, Johnson AD. Temporal anatomy of an epigenetic switch in cell programming: the white-opaque transition of *C. albicans*: Temporal anatomy of an epigenetic switch in *C. albicans*. *Molecular Microbiology*. 2010;78(2):331-343.
doi:10.1111/j.1365-2958.2010.07331.x
 38. Sorrells TR, Johnson AD. Making Sense of Transcription Networks. *Cell*. 2015;161(4):714-723. doi:10.1016/j.cell.2015.04.014

39. Frazer C, Staples MI, Kim Y, et al. Epigenetic cell fate in *Candida albicans* is controlled by transcription factor condensates acting at super-enhancer-like elements. *Nat Microbiol.* 2020;5(11):1374-1389. doi:10.1038/s41564-020-0760-7
40. Du H, Guan G, Xie J, et al. The transcription factor Flo8 mediates CO₂ sensing in the human fungal pathogen *Candida albicans*. Lew DJ, ed. *MBoC.* 2012;23(14):2692-2701. doi:10.1091/mbc.e12-02-0094
41. Cao F, Lane S, Raniga PP, et al. The Flo8 Transcription Factor Is Essential for Hyphal Development and Virulence in *Candida albicans*. *Molecular Biology of the Cell.* 2006;17:13.
42. Su C, Li Y, Lu Y, Chen J. Mss11, a Transcriptional Activator, Is Required for Hyphal Development in *Candida albicans*. *Eukaryot Cell.* 2009;8(11):1780-1791. doi:10.1128/EC.00190-09
43. Uhl MA, Biery M, Craig N, Johnson AD. Haploinsufficiency-based large-scale forward genetic analysis of filamentous growth in the diploid human fungal pathogen *C. albicans*. :11.
44. Aoki Y, Ishii N, Watanabe M, Yoshihara F, Arisawa M. Rbf1 (RPG-box binding factor), a Transcription Factor Involved in Yeast-hyphal Transition of *Candida albicans*. *Jpn J Med Mycol.* 1998;39(2):67-71. doi:10.3314/jjmm.39.67
45. Ishii N, Yamamoto M, Yoshihara F, Nakayama H, Arisawa M, Aoki Y. A DNA-binding protein from *Candida albicans* that binds to the RPG box of *Saccharomyces cerevisiae* and the telomeric repeat sequence of *C. albicans*. *Jpn J Med Mycol.* 1997;Vol. 39:67-71.
46. Khamooshi K, Sikorski P, Sun N, Calderone R, Li D. The Rbf1, Hfl1 and Dbp4 of *Candida albicans* regulate common as well as transcription factor-specific mitochondrial and other cell activities. *BMC Genomics.* 2014;15(1):56. doi:10.1186/1471-2164-15-56
47. Singh RP, Prasad HK, Sinha I, Agarwal N, Natarajan K. Cap2-HAP Complex Is a Critical Transcriptional Regulator That Has Dual but Contrasting Roles in Regulation of Iron Homeostasis in *Candida albicans*. *Journal of Biological Chemistry.* 2011;286(28):25154-25170. doi:10.1074/jbc.M111.233569
48. Soll DR, Morrow B, Srikantha T. High-frequency phenotypic switching in *Candida albicans*. *Trends in Genetics.* 1993;9(2):61-65. doi:10.1016/0168-9525(93)90189-O
49. Xie J, Tao L, Nobile CJ, et al. White-Opaque Switching in Natural MTL α Isolates of *Candida albicans*: Evolutionary Implications for Roles in Host Adaptation, Pathogenesis, and Sex. Heitman J, ed. *PLoS Biol.* 2013;11(3):e1001525. doi:10.1371/journal.pbio.1001525
50. Ziv N, Brenes LR, Johnson A. Multiple molecular events underlie stochastic switching between 2 heritable cell states in fungi. Heitman J, ed. *PLoS Biol.* 2022;20(5):e3001657. doi:10.1371/journal.pbio.3001657
51. Park YN, Pujol C, Wessels DJ, Soll DR. *Candida albicans* Double Mutants Lacking both *EFG1* and *WOR1* Can Still Switch to Opaque. Mitchell AP, ed. *mSphere.* 2020;5(5):e00918-20. doi:10.1128/mSphere.00918-20

52. Alkafeef SS, Yu C, Huang L, Liu H. Wor1 establishes opaque cell fate through inhibition of the general co-repressor Tup1 in *Candida albicans*. Dudley AM, ed. *PLoS Genet*. 2018;14(1):e1007176. doi:10.1371/journal.pgen.1007176
53. Takagi J, Singh-Babak SD, Lohse MB, Dalal CK, Johnson AD. *Candida albicans* white and opaque cells exhibit distinct spectra of organ colonization in mouse models of infection. Coste AT, ed. *PLoS ONE*. 2019;14(6):e0218037. doi:10.1371/journal.pone.0218037
54. Care RS, Trevethick J, Binley KM, Sudbery PE. The MET3 promoter: a new tool for *Candida albicans* molecular genetics. *Mol Microbiol*. 1999;34(4):792-798. doi:10.1046/j.1365-2958.1999.01641.x
55. Nguyen N, Quail MMF, Hernday AD. An Efficient, Rapid, and Recyclable System for CRISPR-Mediated Genome Editing in *Candida albicans*. Mitchell AP, ed. *mSphere*. 2017;2(2):e00149-17, /msphere/2/2/mSphere149-17.atom. doi:10.1128/mSphereDirect.00149-17

FIGURES AND FIGURE LEGENDS

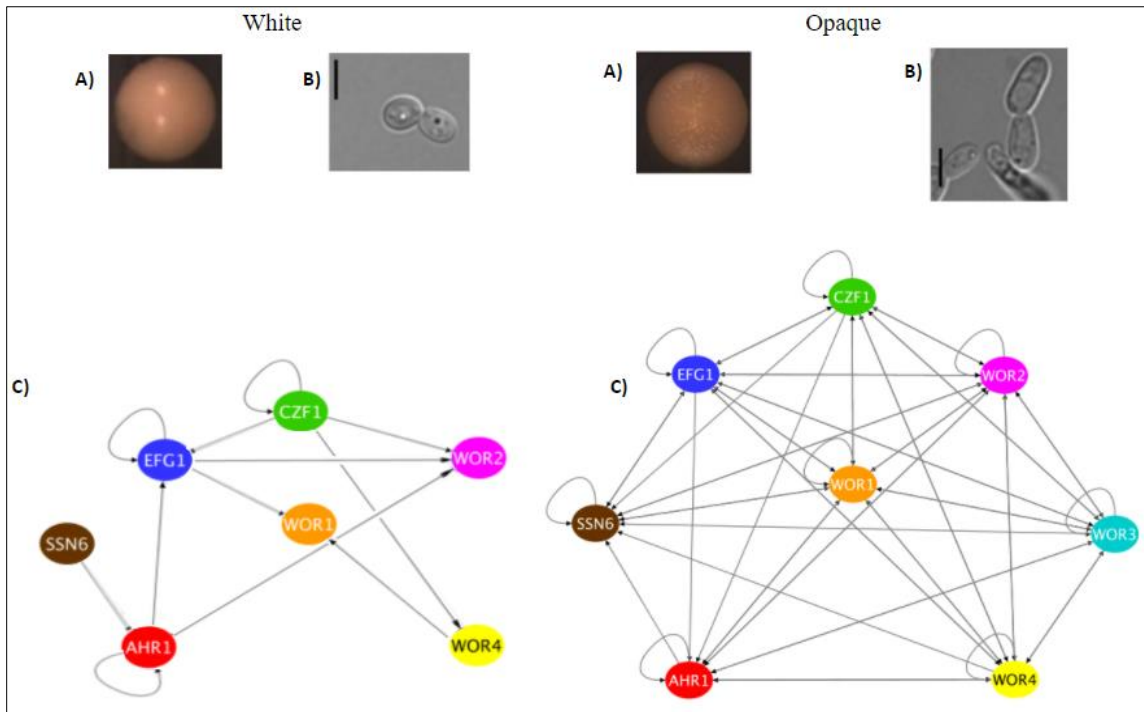
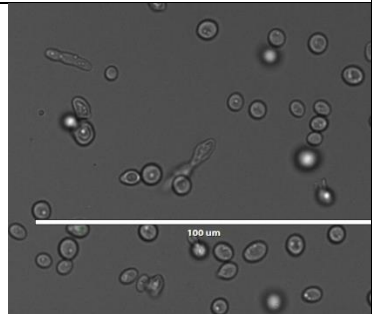

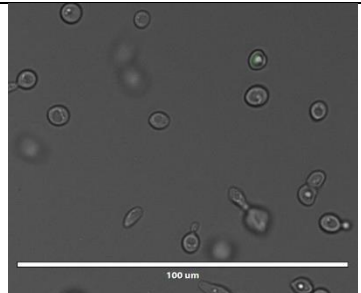

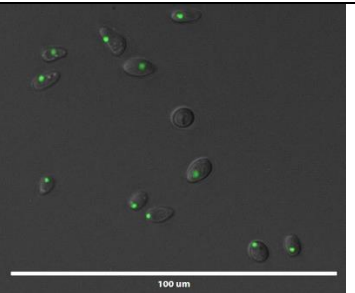
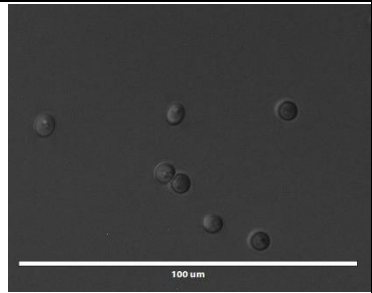

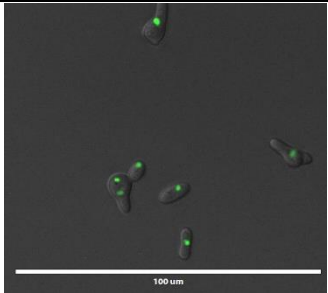

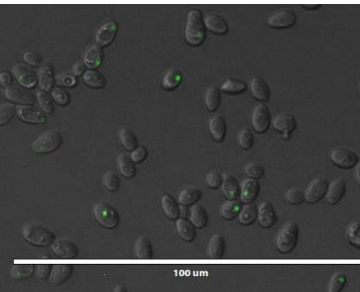


Figure 2-1: White and opaque cells, colonies, and transcriptional circuits are distinct. Visual representation of the (A) colony, (B) cell, and (C) transcriptional circuit of the white (**left**) and the opaque (**right**) cell types of *Candida albicans*²⁸. Each node of the transcriptional circuit represent a given transcription factor and the edges are given directionality to represent each binding event of a given TF in the 5' intergenic region of another TF (i.e. Ahr1 binds in the 5' intergenic region of both *EFG1* and *WOR2* in the white state).

White	AHY1465 ($\Delta/\Delta wor1 \Delta/\Delta ssn6$)	Opaque
		N/A
White	AHY1469 ($\Delta/\Delta wor2 \Delta/\Delta ssn6$)	Opaque
		
White	AHY1473 ($\Delta/\Delta wor4 \Delta/\Delta ssn6$)	Opaque
		
White	AHY1477 ($\Delta/\Delta flo8 \Delta/\Delta ssn6$)	Opaque
N/A		


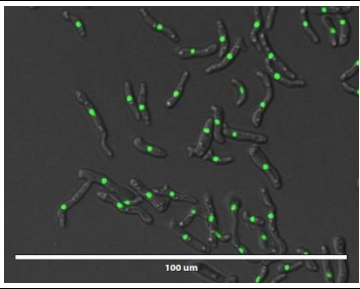
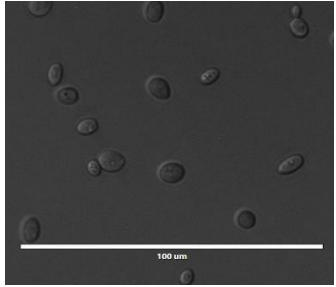

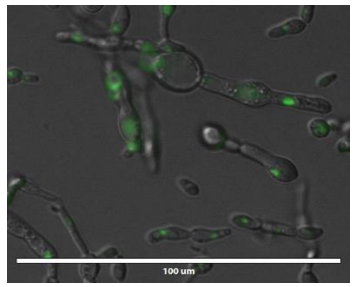
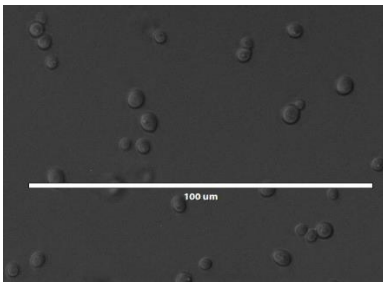

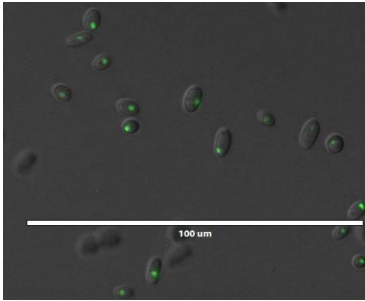
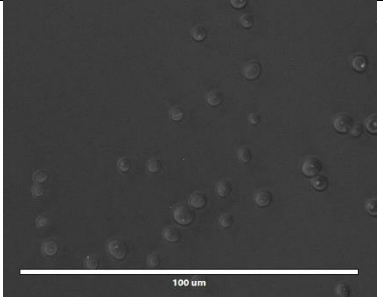

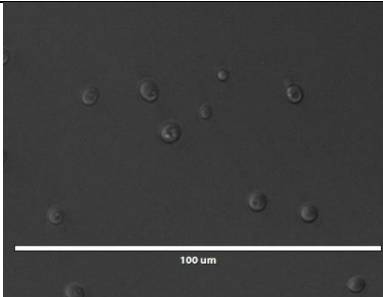

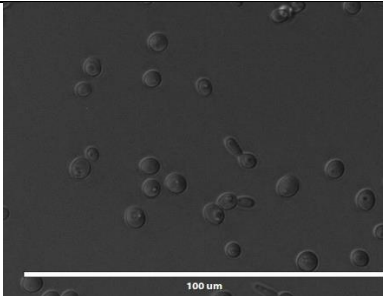
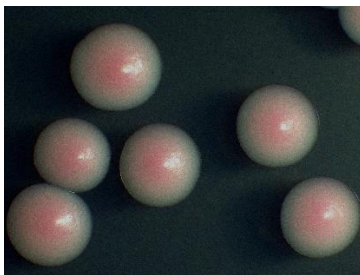
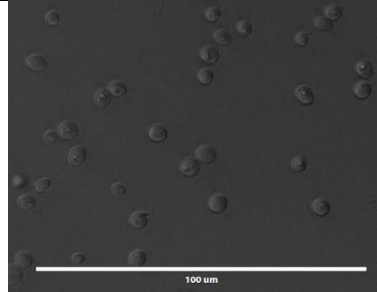
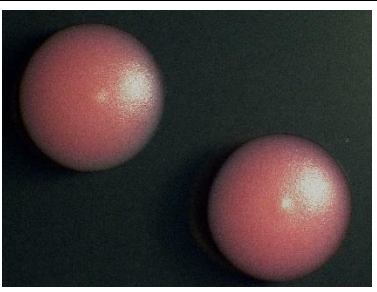
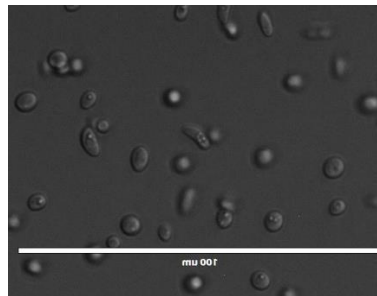

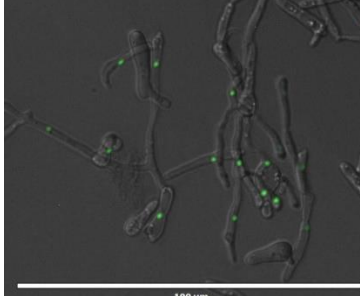
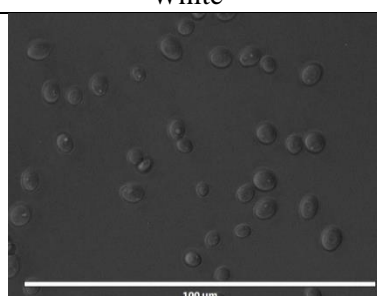
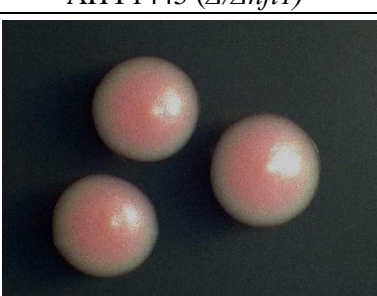
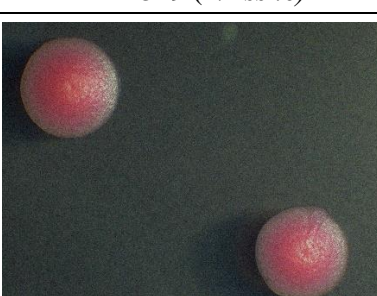
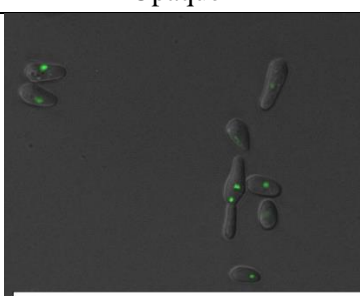
White	AHY1481 (Δ/Δ <i>fgr15</i> Δ/Δ <i>ssn6</i>)	Opaque
N/A		
White	AHY1485 (Δ/Δ <i>hfl1</i> Δ/Δ <i>ssn6</i>)	Opaque
		

Figure 2-2: Visual representation of deletion of each OCTF paired with sequential deletion of *SSN6*. Representation of the white (**left**) and opaque (**right**) cellular phenotype as well as a colony morphology (**middle**) for deletion of each of the OCTFs paired with the deletion of Δ/Δ *ssn6*. N/A indicates ‘not assayed’ as the strain produced no observable white or opaque colonies. Green fluorescence observed in opaque cells indicates expression of Wor1-GFP fusion protein.

White	AHY1433 WT (Wor1-mNeonGreen)	Opaque
		
White	AHY1435 (Δ/Δ <i>wor1</i>)	Opaque
		N/A
White	AHY1437 (Δ/Δ <i>wor2</i>)	Opaque
		N/A
White	AHY1439 (Δ/Δ <i>wor4</i>)	Opaque
		N/A

White  100 um	AHY1441 ($\Delta/\Delta flo8$) 	Opaque N/A
White  mu 001	AHY1443 ($\Delta/\Delta fgr15$) 	Opaque  100 um
White  100 um	AHY1445 ($\Delta/\Delta hf11$) 	Opaque N/A
White N/A	AHY1529 ($\Delta/\Delta ssn6$) 	Opaque  100 um

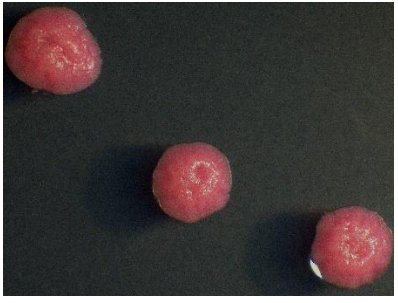
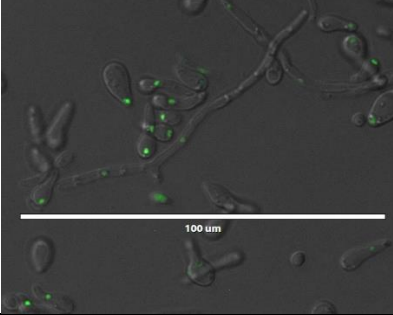
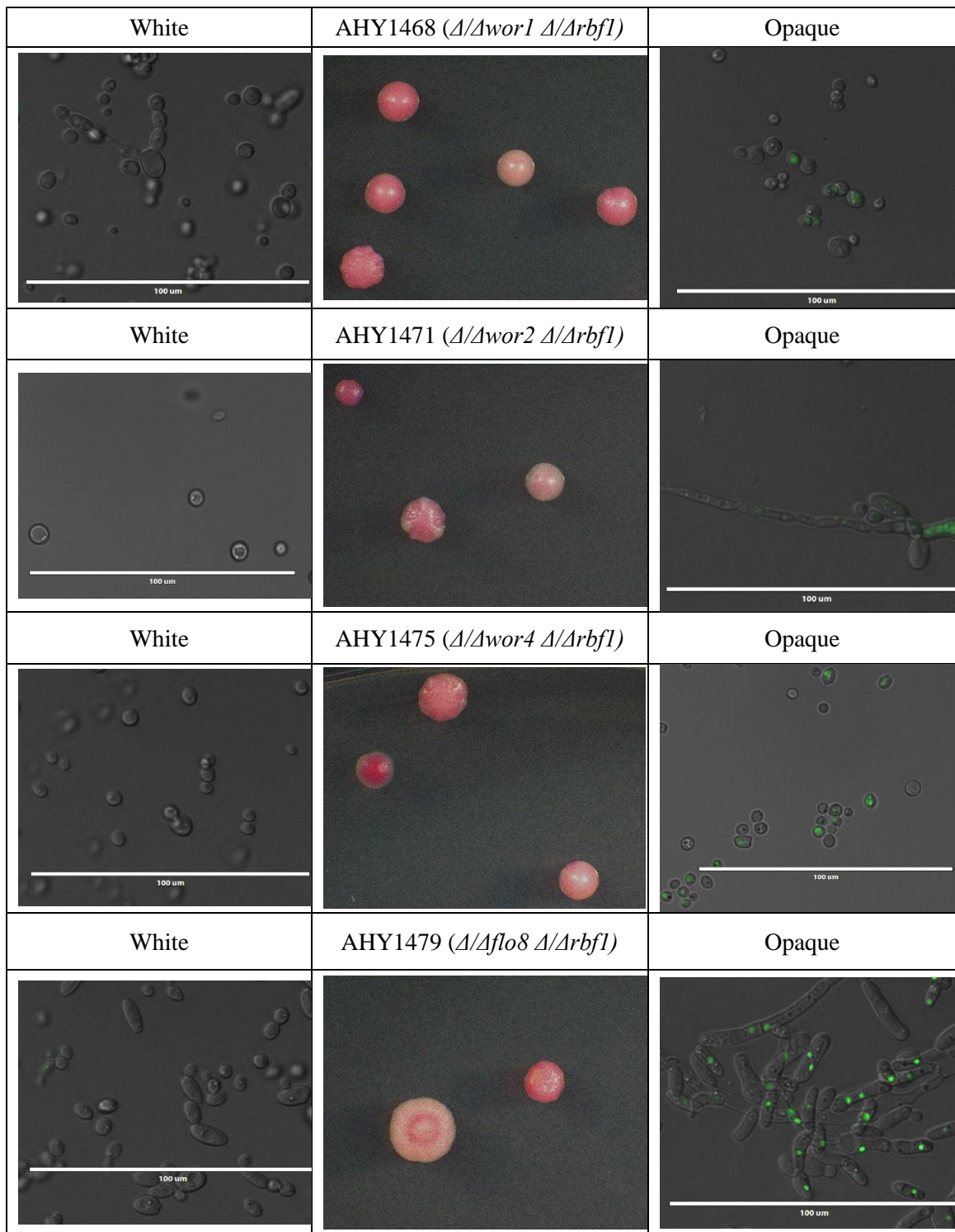
White	AHY1532 (Δ/Δ <i>rbf1</i>)	Opaque
N/A		

Figure 2-3: Visual representation of all switch critical knockouts. Representation of the white (**left**) and opaque (**right**) cellular phenotype as well as a colony morphology (**middle**) for each of the single switch critical TF knockouts. N/A indicates ‘not assayed’ as the strain produced no observable white or opaque colonies for that given state. Green fluorescence observed in opaque cells indicates expression of Wor1-GFP fusion protein.



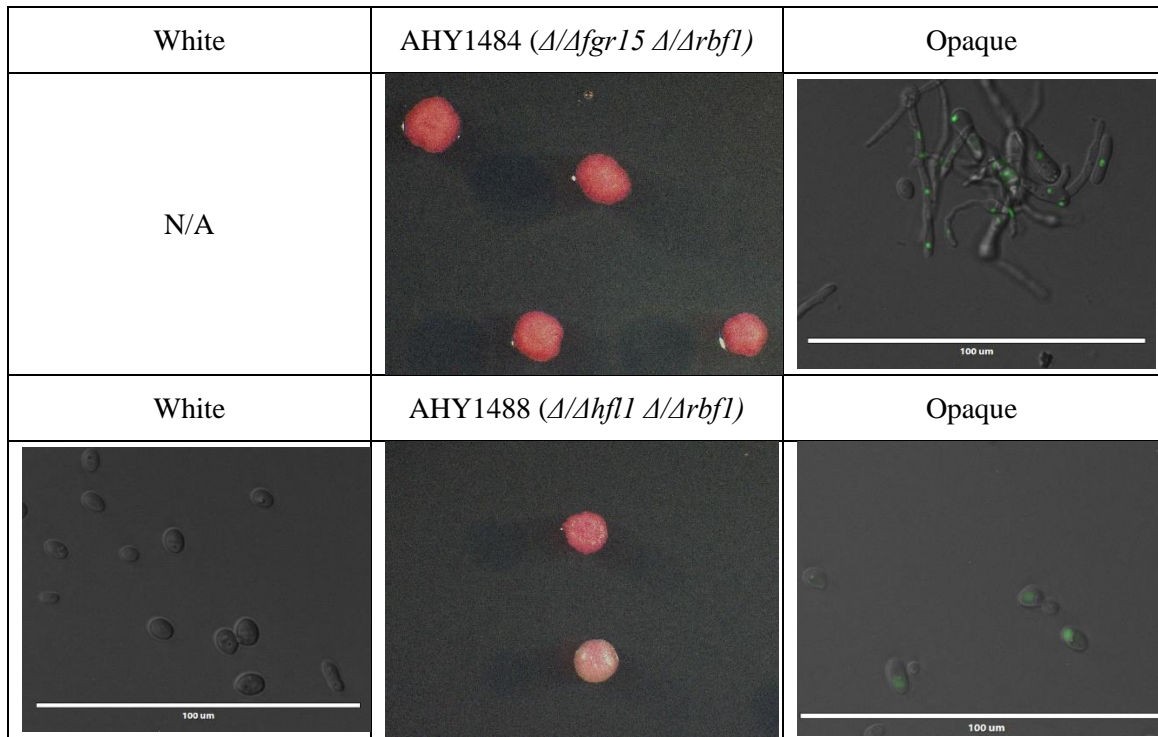


Figure 2-4: Visual representation of deletion of each OCTF paired with sequential deletion of *RBFI*. Representation of the white (**left**) and opaque (**right**) cellular phenotype as well as a colony morphology (**middle**) for deletion of each of the OCTFs paired with the deletion of $\Delta/\Delta rbf1$. N/A indicates ‘not assayed’ as the strain produced no observable white or opaque colonies for that given state. Green fluorescence observed in opaque cells indicates expression of Wor1-GFP fusion protein in strains that contain an intact copy of WOR1 gene or expression of cytosolic GFP in $\Delta/\Delta wor1$ strains that contain a WOR1 transcriptional fusion.

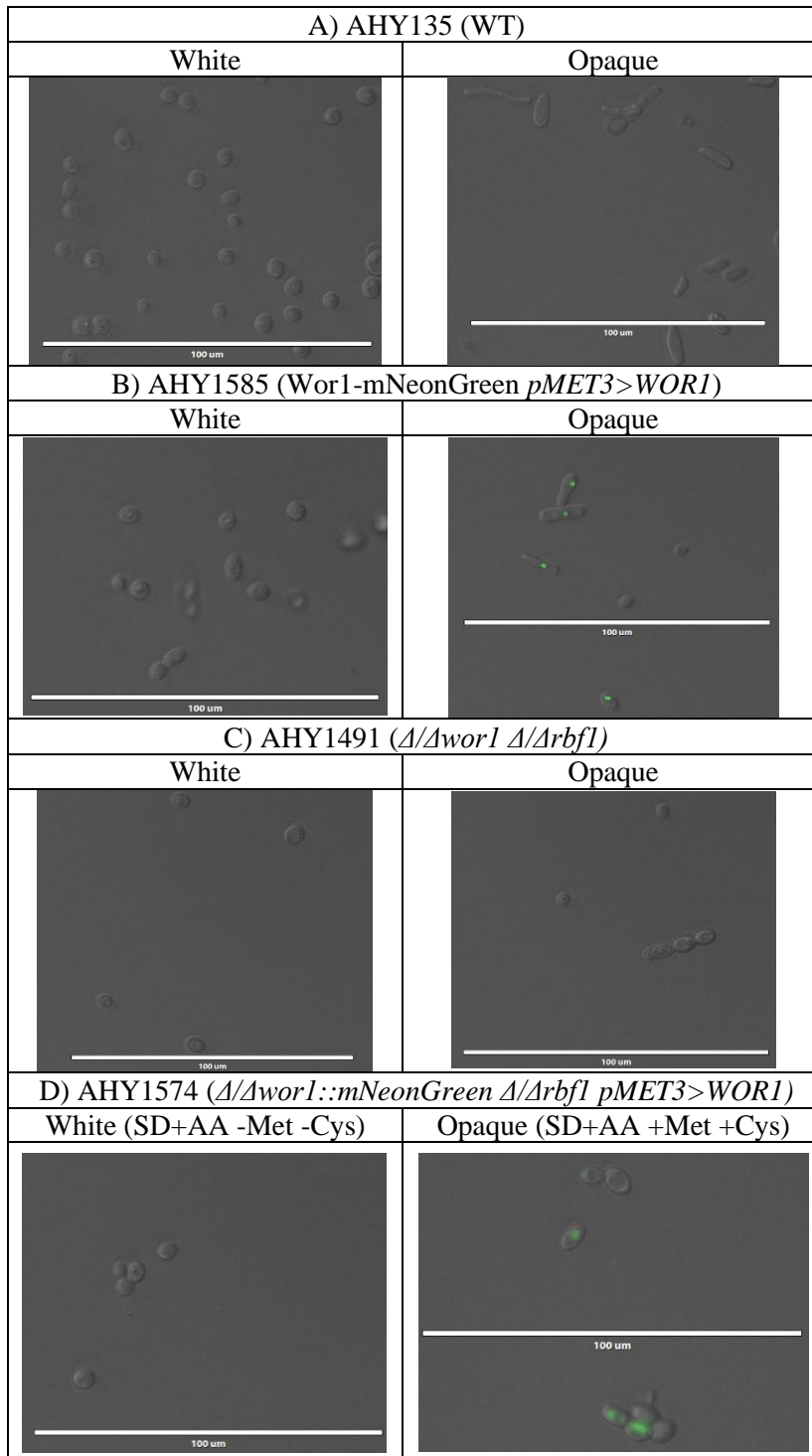


Figure 2-5: Visual representation controls. Representation of the white (**left**) and opaque (**right**) cellular phenotype for each control. (**A**) AHY135 untagged control (base strain) (**B**) *Wor1* c-terminally tagged with mNeonGreen with *pMET3* driving *WOR1* expression in *NEUT5L* locus. (**C**) Δ/Δ *wor1* Δ/Δ *rbf1* untagged control (**D**) *WOR1*-mNeonGreen transcriptional fusion with *pMET3* driving *WOR1* expression in *NEUT5L* locus.

TABLES

Table 2-1: Paired switch critical transcription factors. A list of the pairs of transcription factors that were deleted in this study.

<i>wor1 & ssn6</i>
<i>wor1 & rbf1</i>
<i>wor2 & ssn6</i>
<i>wor2 & rbf1</i>
<i>wor4 & ssn6</i>
<i>wor4 & rbf1</i>
<i>flo8 & ssn6</i>
<i>flo8 & rbf1</i>
<i>fgr15 & ssn6</i>
<i>fgr15 & rbf1</i>
<i>hfl1 & ssn6</i>
<i>hfl1 & rbf1</i>

Table 2-2: Switch frequencies of single deletion mutants. Switch frequency results for all single deletion mutants. % Wh and % Op represent the percentage of total colonies assayed that were in the white or opaque state, respectively. % Sect indicates the percentage of total colonies assayed that contained one or more sector of the opposite phenotype from the starting colony phenotype. % Switch indicates the total percentage of colonies assayed which switched to the opposite phenotype from the starting phenotype or contained sectors of the opposite phenotype. Standard deviation is not reported as a single biological replicate was used to confirm that the switching behavior of each genotype is representative of previously published results.

AHY	TF	Starting Phenotype	Total colonies	% Wh	% Op	% Sect	% Switch
1513	$\Delta\Delta$ <i>wor1</i>	Wh	1,184	100	0	0	0
1515	Δ/Δ <i>wor2</i>	Wh	1,069	100	0	0	0
1517	$\Delta\Delta$ <i>wor4</i>	Wh	1,083	100	0	0	0
1519	Δ/Δ <i>flo8</i>	Wh	1,081	100	0	0	0
1521	Δ/Δ <i>fgr15</i>	Wh	1,101	99.8	0	0.2	0.2
1523	Δ/Δ <i>hfl1</i>	Wh	1,017	100	0	0	0
1526	Δ/Δ <i>ssn6</i>	Op	1,100	0	100	0	0
1527	Δ/Δ <i>rbf1</i>	Op	1,005	0	100	0	0
135	WT	Wh	1,028	99.1	0	0.9	0.9
135	WT	Op	871	21.2	78	0.8	21.2
1433	WT Wor1-mNG	Wh	971	83.0	0.5	16.5	17
1558	WT Wor1-mNG	Op	192	0.0	100	0.0	0

Table 2-3: Switch frequencies of deletion of each OCTF paired with sequential deletion of *SSN6*. Switch frequencies for all OCTFs deletion strains paired with the deletion of Δ/Δ *ssn6*. % Wh and % Op represent the percentage of total colonies assayed that were in the white or opaque state, respectively. % Sect indicates the percentage of total colonies assayed that contained one or more sector of the opposite phenotype from the starting colony phenotype. % Switch indicates the total percentage of colonies assayed which switched to the opposite phenotype from the starting phenotype or contained sectors of the opposite phenotype. STD indicates the standard deviation in reported % Switch data across three or more biological replicates.

AHY	TF	Starting Phenotype	Total colonies	% Wh	% Op	% Sect	% Switch	STD
1489	Δ/Δ <i>wor1</i> Δ/Δ <i>ssn6</i>	Wh	4,160	100	0	0	0	0
1493	Δ/Δ <i>wor2</i> Δ/Δ <i>ssn6</i>	Wh	3,640	86.7	9.9	3.4	13.3	3.2
		Op	3,121	0.1	96.5	3.4	3.5	0.51
1497	Δ/Δ <i>wor4</i> Δ/Δ <i>ssn6</i>	Wh	3,220	95.9	0.5	3.6	4.1	0.6
		Op	3,215	46.6	12.4	38.0	87.6	2.6
1501	Δ/Δ <i>flo8</i> Δ/Δ <i>ssn6</i>	Op	3,961	0	100	0	0	0
1505	Δ/Δ <i>fgr15</i> Δ/Δ <i>ssn6</i>	Op	3,208	0	100	0	0	0
1509	Δ/Δ <i>hfl1</i> Δ/Δ <i>ssn6</i>	Wh	9,868	3.7	92.1	4.1	96.3	3.3
		Op	7,492	2.8	95.6	1.5	4.4	1.5
135	WT	Wh	4,861	99.7	0.1	0.3	0.3	0.1
136	WT	Op	6,327	24.3	73.9	1.8	26.1	3.3

Table 2-4: Switch frequencies of deletion of each OCTF paired with sequential deletion of *RBF1*. Switch frequencies for all OCTFs deletion strains paired with the deletion of Δ/Δ *rbf1*. % Wh and % Op represent the percentage of total colonies assayed that were in the white or opaque state, respectively. % Sect indicates the percentage of total colonies assayed that contained one or more sector of the opposite phenotype from the starting colony phenotype. % Switch indicates the total percentage of colonies assayed which switched to the opposite phenotype from the starting phenotype or contained sectors of the opposite phenotype. STD indicates the standard deviation in reported % Switch data across three or more biological replicates.

AHY	TF	Starting Phenotype	Total colonies	% Wh	% Op	% Sect	% Switch	STD
1491	Δ/Δ <i>wor1</i> Δ/Δ <i>rbf1</i>	Wh	3,215	92.0	3.5	4.5	8.0	6.7
		Op	5,832	3.3	94.9	1.8	5.1	1.2
1495	Δ/Δ <i>wor2</i> Δ/Δ <i>rbf1</i>	Wh	4,792	92.0	4.9	3.1	8.0	6.8
		Op	4,878	1.9	94.9	3.3	5.1	1.3
1499	Δ/Δ <i>wor4</i> Δ/Δ <i>rbf1</i>	Wh	3,648	91.8	3.9	4.3	8.2	1.6
		Op	3,698	1.2	94.9	3.9	5.1	1.8
1503	Δ/Δ <i>flo8</i> Δ/Δ <i>rbf1</i>	Wh	3,161	96.0	2.0	2.0	4.0	2.4
		Op	3,541	4.7	93.3	2.0	6.7	3.7
1507	Δ/Δ <i>fgr15</i> Δ/Δ <i>rbf1</i>	Op	3,321	0	100	0	0	0
1511	Δ/Δ <i>hfl1</i> Δ/Δ <i>rbf1</i>	Wh	3,297	80.7	12.7	6.6	19.3	1.4
		Op	5,047	1.6	90.8	7.6	9.2	2.1
135	WT	Wh	2,787	97.7	0.3	2.0	2.3	4.4
136	WT	Op	1,884	20.4	77.8	1.9	22.2	0.9

Table 2-5: Switch frequencies of each single deletion mutants with Wor1-mNeonGreen. Representation of switch frequency among all single deletion mutants with either a transcriptional or translation Wor1-mNeonGreen reporter. % Wh and % Op represent the percentage of total colonies assayed that were in the white or opaque state, respectively. % Sect indicates the percentage of total colonies assayed that contained one or more sector of the opposite phenotype from the starting colony phenotype. % Switch indicates the total percentage of colonies assayed which switched to the opposite phenotype from the starting phenotype or contained sectors of the opposite phenotype. Standard deviation is not reported as a single biological replicate was used to confirm that the switching behavior of each mNeonGreen reporter strain is comparable to the corresponding untagged genotypes in Table 2-2.

AHY	TF	Starting Phenotype	Total colonies	% Wh	% Op	% Sect	% Switch
1435	<i>Δwor1</i>	Wh	1,318	100	0	0	0
1437	<i>Δwor2</i>	Wh	1,279	100	0	0	0
1439	<i>Δwor4</i>	Wh	1,161	100	0	0	0
1441	<i>Δflo8</i>	Wh	1,262	100	0	0	0
1443	<i>Δfgr15</i>	Wh	1,117	78.6	10.1	11.3	21.4
1445	<i>Δhfl1</i>	Wh	1,041	99.5	0	0.5	0.5
1529	<i>Δssn6</i>	Op	175	0	100	0	0
1531	<i>Δrbf1</i>	Op	102	0	100	0	0
1433	WT Wor1-mNG	Wh	971	83.0	0.5	16.5	17
1558	WT Wor1-mNG	Op	192	0.0	100	0.0	0
135	WT	Wh	1,028	99.1	0	0.9	0.9
135	WT	Op	871	21.2	78	0.8	21.2

CHAPTER 3

Conclusions and Future Directions

CHAPTER 3: Conclusions and Future Directions

The white-opaque phenotypic switch is controlled by multiple transcriptional regulators which form a complex network of interconnected positive and negative feedback loops (Figure 3-1)¹. A combination of genome-wide transcriptional profiling and ChIP experiments identified the direct and indirect transcriptional regulatory interactions involved in cell-type specification and maintenance of the white and opaque cell types and revealed that the structures of these cell-type-specific regulatory networks are quite distinct. In white cells, the network is relatively compact, with a moderate level of overlapping regulatory targets. In contrast, the opaque network encompasses over 2-fold more regulatory target genes, with extensive overlap between direct regulatory targets². At the center of the opaque-specific regulatory network lies a set of regulatory targets that are bound by most, if not all, of the currently characterized switch regulators. This “core” switch circuit, as defined by the interactions between each of the individual switch regulators and their respective promoters, mirrors the unique attributes of each cell-type-specific network (Figure 3-1). This “core” circuit has also been probed by genetic epistasis and ectopic expression experiments that have begun to reveal the regulatory dynamics and logic of this circuit¹⁻⁷. The most essential component of the white and opaque-specific regulatory circuits is a gene named White Opaque Regulator 1 (*WOR1*), which is the master regulator of the opaque cell type^{1-4,6-9}. Transcription of *WOR1* is actively repressed in white cells, while expression of *WOR1* is essential for the formation and heritable maintenance of opaque cells. *WOR1* expression is positively regulated by Wor1 protein binding to the *WOR1* promoter, thus creating a positive transcriptional feedback loop that is hypothesized to contribute to heritable maintenance of the opaque cell type^{3,4,8-10}. The transition from white-to-opaque can be prevented by deletion of *WOR1* or stimulated by induced expression of *WOR1*; for this reason, the white cell type is considered to be the “ground state” of the switch regulatory network, while the opaque cell type is considered to be the “excited state” of the network. Stochastic white-to-opaque switching is believed to occur when transcriptional noise within the ground-state white-cell regulatory network allows Wor1 levels to surpass a critical threshold required to induce transition to the opaque state. Once established, the excited opaque-cell transcriptional network is stably maintained by a series of nested feedback loops, including the positive auto regulatory feedback loop generated by Wor1^{2-4,9,10}. Although the role of Wor1 in switching is well established, many outstanding questions remain regarding the logic and dynamics of the interactions between Wor1 and the other known switch regulators.

In addition to Wor1, several additional regulatory TFs play critical roles in the establishment and heritable maintenance of the opaque cell type. For example, cells that lack *WOR2* fail to undergo white to opaque switching unless *WOR1* is induced via ectopic Wor1 expression, and also fail to sustain *WOR1* expression at the native locus when ectopic Wor1 expression is terminated⁴. These results indicate that Wor2 contributes to the heritable maintenance of the opaque state by stabilizing the Wor1-

dependent positive feedback loop that is central to the opaque transcriptional network. *Wor4*, *Flo8*, *Fgr15*, and *Hfl1* have also been shown to play important roles in white to opaque switching and, when deleted, result in phenotypically white-locked strains^{7,11,12}. Cells lacking *WOR4* fail to switch to the opaque state, while induced expression of *WOR4* in wild-type white cells results in mass conversion of the population to the opaque state. Since induced expression of *WOR1* in a Δ/Δ *wor4* mutant rescues opaque cell formation, it is proposed that *WOR4* functions upstream of *WOR1*. In fact, *Wor4* is bound to the *WOR1* promoter in both white and opaque cells, suggesting that *Wor4* destabilizes the white cell type and stabilizes the opaque cell type through direct positive regulation of *WOR1*⁷. Though *Wor2* and *Wor4* have been integrated into the white-opaque transcriptional circuit through genome-wide chromatin immunoprecipitation studies and their role in regulating the switch has been explored through targeted genetic interaction analyses, the other three opaque-critical TFs (*Flo8*, *Fgr15*, and *Hfl1*) remain relatively unexplored.

In white cells, the core switch circuit consists of several feed-forward loops that contribute to the stabilization or maintenance of the white cell type. *Efg1*, *Ahr1* and *Ssn6* each contribute to the stability of the white cell type, and deletion of any one of these regulatory genes destabilizes the white cell circuit such that most, if not all, of the cells in the population will transition to the opaque cell state^{1,4,5,13-16}. Cells lacking either *EFG1* or *AHR1* switch from white to opaque at a much higher frequency than wild-type cells yet retain the ability to form white colonies. In contrast, cells lacking *SSN6* do not form white colonies and are locked in the opaque state^{1,12}. The importance of *Ssn6* is defined by its interactions with other TFs and how it helps maintain the current state of the cell. In white cells, *Ssn6* prevents the opaque phenotype by inhibiting excitation of the transcriptional network that leads to increased *Wor1* in the cell¹. Recently, *RBF1* was also identified as being critical for heritable maintenance of the white cell type, with Δ/Δ *rbf1* strains exhibiting a similar opaque-locked phenotype as Δ/Δ *ssn6* strains, however prior to the work presented in this dissertation, the mechanism by which *Rbf1* impacts white-opaque switching was entirely uncharacterized¹².

To determine the genetic interactions between the eight switch critical regulators, we performed a systematic genetic epistasis analysis as presented in Chapter 2. All possible pairwise combinations of white- vs opaque-locked switch critical regulator deletions were generated as seen in Table 2-1 of Chapter 2, and the resulting twelve strains were subjected to switch frequency analysis to determine the regulatory hierarchy of these TFs in the genetic circuits that control white-opaque switching. Much to our surprise, only four of the twelve strains from this set revealed complete epistatic interactions, where one TF deletion dominated the observed phenotype and blocked the phenotypic expression of the other TF deletion. The remaining eight strains exhibited bistable switching at both the cellular and colony level. This provides evidence that many of these TFs oppose each other at the same level within the switch regulatory hierarchy and that there is a tug-of-war between them to establish either the white or the opaque state. Most remarkably, we observed white-opaque switching in the strain lacking both *RBF1* and *WOR1*. To our

knowledge, this is the first example of reversible, stochastic switching between heritable white and opaque cell types under standard “switch permissive” growth conditions in the absence of *Wor1* and highlights a critical regulatory competition between *Wor1* (opaque-promoting) and *Rbf1* (white-promoting or opaque-repressing) at the heart of the white-opaque switch.

Work in Progress

To further investigate the regulatory connections between these “switch critical” regulators, we performed genome-wide protein-DNA binding analysis (CUT&RUN) to uncover the direct regulatory targets of these switch critical regulators¹⁷. We identified bound target genes for each of the recently identified switch-critical TFs by performing CUT&RUN on *Fgr15*, *Hfl1*, *Flo8*, and *Rbf1* in white and opaque cell types (Table 3-1 and Figure 3-2, yellow) and combined it with previously published ChIP data (Figure 3-2, gray) for the remaining switch critical regulators (*Wor1*, *Wor2*, *Wor4*, and *Ssn6*) and previously characterized switch modulating regulators (*Ahr1*, *Czf1*, *Efg1*, and *Wor3*). The CUT&RUN data revealed that most of the new switch critical TFs appear to function in a “top-down” manner by binding to many of the other regulatory TF coding genes without reciprocal binding interactions. This suggests that rather than being integrated into the circuit and thus under direct regulatory control of the white-opaque switch, these new switch critical regulators represent foundational components which support, or impinge upon, the formation and regulatory function of the white- and/or opaque-specific transcriptional regulatory complexes that are ultimately responsible for establishing and maintaining these two distinct heritable cell types. *Rbf1* and *Hfl1* appear to have more of a cell type-specific binding pattern within this core circuit, with most of the *Rbf1*-bound targets observed in white cells and the majority of *Hfl1*-bound targets observed in the opaque cell type. *Rbf1* binds to the 5’ intergenic region of most switch regulatory TF genes in the white state, with the exception of itself and *HFL1*, yet is only observed to bind upstream of *WOR1* and *CZF1* in the opaque state. In contrast, *Hfl1* is bound upstream of *RBF1* but none of the other switch regulators in white cells and is found upstream of four key switch regulatory TF coding genes in the opaque circuit (*WOR1*, *WOR3*, *EFG1*, and *CZF1*). Although *Rbf1* and *Hfl1* seem to be largely cell type specific, *Flo8* and *Fgr15* seem to be integral components of both the white and opaque circuits, binding in the upstream 5’ intergenic regions of most of the key regulatory genes in both cell types. *Flo8* and *Fgr15* bind to all the same TFs in the white state (*FLO8*, *WOR1*, *WOR2*, *CZF1*, *SSN6*, *AHR1*, and *EFG1*) and nearly all the same TFs in the opaque state; only the absence of *Fgr15* binding upstream of *FLO8* in the opaque state differentiates the binding patterns of these two regulators. This data suggests *Fgr15*, *Hfl1*, *Flo8*, and *Rbf1* are tightly integrated components of the white – opaque switch and further analysis of each TF transcription profile will be critical to understanding what each of these connections means in terms of regulation within the circuit and greater network.

In addition to identifying the four new switch-critical regulators discussed above, the genetic screen performed by Lohse et al also led to the identification of an

additional 20 new “switch modulating” TFs that, when deleted, alter the frequency of white-opaque switching by at least 10-fold, but do not result in white- or opaque-locked phenotypes¹². While these regulators are shown to have significant effects on the switch, the mechanisms by which they affect switching are unknown. To begin exploring this question, we first examined the regulons for each of the 28 known switch-modulating TFs, including those that had been previously characterized by microarray analysis, by using 3’ RNA-sequencing and differential gene expression analysis. Total RNA was isolated from both white and opaque cell populations of wild-type and TF deletion strains grown under standard switch permissive liquid culture conditions (25 °C, synthetic dextrose + amino acids + uridine), and RNA sequencing libraries were prepared using Lexogen 3’ Quant Seq kits. Sequencing was performed using Lexogen’s QuantSeq 3’ mRNA-Seq Library Prep Kit to generate Illumina-ready sequencing libraries. The Quant Seq kit generates a single cDNA molecule from the 3’ end of each mRNA, thus producing a library of 3’ cDNAs that represent a 1:1 relationship to the number of mRNA molecules for each transcribed gene¹⁸. Each library was uniquely barcoded and combined with 95 other libraries on a single lane of an Illumina HiSeq4000 instrument. The RNA-seq reads were then processed using our lab’s own bioinformatics pipeline that utilizes the most up to date R packages for differential expression analysis. Our pipeline is modeled after a web-based platform that was created in collaboration by Lexogen and the bioinformatics company Bluebee and utilizes Spliced Transcripts Alignment to a Reference (STAR) to align the sequencing results to *C. albicans* SC5314 assembly 21 version 2.7.4a reference genome and DEseq2 for pairwise differential expression analysis. The fold changes in gene expression resulting from deletion of each individual switch critical or switch modulating regulator, relative to a wild-type reference strain, is presented in Figure 3-3. Genes that are upregulated in each TF deletion strain, relative to a wild-type reference of the same cell type, are indicated in blue, while downregulated genes are indicated in yellow. Dysregulated genes in the null background are either directly or indirectly regulated by the TF that has been removed, thus providing insight into the potential regulatory interactions between each of the TFs being examined.

Taking a broad look at the transcriptional profiles depicted in Figure 3-3, we expected to observe patterns of dysregulation upon deletion of specific switch regulatory TF genes which might indicate regulatory cascades that ultimately explain the resulting alterations in switch frequency. In other words, clues as to how each of the TFs ultimately impact the relative stability of the white and opaque cell types could be gleaned from observing patterns of dysregulation in the data. More specifically, elevated levels of *WOR1* and *WOR2* expression are associated with the opaque cell type, while elevated *EFG1* expression is associated with the white cell type. This tracks with our wild type reference (column one of Figure 3-3) where we see *WOR1* and *WOR2* are highly upregulated in the opaque state and *EFG1* is highly downregulated in opaque cells, relative to white cells. Surprisingly, we found that many of the null mutants have irregular impacts on these three genes and other regulatory TFs within the network that are normally differentially expressed between the white and opaque cell types. For example, we observe that *WOR2*

is downregulated in nearly every opaque TF null mutant, even those that have increased opaque stability relative to wild type. This is surprising, given that deletion of *WOR2* in an otherwise wild-type background results in loss of opaque heritability. Although many of the TF knockouts have a surprising level of dysregulation amongst many of the cell type specific genes, the Δ/Δ *flo8* deletion strain perhaps displays the most unexpected expression profile; the Δ/Δ *flo8* white-locked mutant has increased expression of *WOR1* and decreased expression of *EFG1* when compared to wild-type white cells. These types of transcriptional responses indicate that the functional regulatory interactions between these TFs and their respective coding genes are highly complex and often counterintuitive (Figure 3). Previously, many of the switch regulatory TFs were identified through differential expression data when comparing the transcriptional profiles of white and opaque cells. This data shows that not all TFs follow these trends. This indicates that the white-opaque regulatory circuit is highly intertwined at a functional level, well beyond the original eight core TFs that were characterized, and that control of switching involves the combined regulatory inputs from several dozen TFs acting across a wide array of mutually interconnected regulatory pathways.

Discussion

The work completed in this thesis has increased our understanding of the transcriptional regulatory network controlling white-opaque switching in *Candida albicans*. We comprehensively identified the regulatory targets for all of the known regulatory TFs that control white-opaque switching through genome-wide transcriptional profiling (RNA-seq) on the 28 most impactful TF deletion strains (including the “core” eight) in white and opaque cell types (Figure 3-3). Beyond the RNA differential expression analysis, we examined the relationship between each of the critical components of this regulatory network through the identification of the epistatic relationships between all of the switch-critical TFs (Chapter 2 Table 2-3, 2-4), as well as identified genome-wide DNA binding sites for those switch critical regulators that had not been previously assayed via ChIP-chip or ChIP-seq (Flo8, Fgr15, Hfl1, and Rbf1; See Figure 3-2.) This work is foundational in the overall understanding of how these TFs regulate the establishment and heritable maintenance of the white and opaque cell types.

Based on the CUT&RUN data, we suggested that Flo8, Fgr15, Hfl1, and Rbf1 work in a top-down manner and seem to be foundational components that support the formation and regulatory functions of the switch. Both Flo8 and Fgr15 seem to be integral members of both the white and opaque circuits, binding upstream of most of the key regulatory genes in both cell types, whereas Rbf1 and, to a lesser extent Hfl1, appear to have more of a cell type-specific binding pattern within this newly defined core circuit. One possibility is that Flo8 and Fgr15 may potentiate the white-to-opaque transition by marking specific regulatory targets in white cells for subsequent assembly of Wor1-dependent transcriptional regulatory complexes in opaque cells. This idea is supported by the recent observation (Richard Bennett, personal communication) that Flo8 has an extremely high propensity to undergo liquid-liquid phase separation, a process that has

been shown to be essential for Wor1-mediated white-to-opaque switching²⁰. In contrast, Rbf1 may act in opposition to this transition in white cells but appears to be largely excluded from binding at these same target genes in opaque cells. We provided supporting evidence of this through epistasis experiments (Chapter 2) where *RBF1* is deleted in white-locked single deletion strains and all of the newly created double deletion mutants formed bonified opaque cells, or apparent opaque-like cells with corresponding activation of the *WOR1* promoter, even in a Δ/Δ *wor1* Δ/Δ *rbf1* strain. This suggests that eviction of Rbf1 from key regulatory target loci may be a crucial element of the white to opaque switch, requiring the coordinated impacts of Wor1 and other opaque-promoting switch critical regulators. This hypothesis could explain why strains that lack *RBF1* are locked in the opaque cell type and no longer require the function of Wor1, Wor2, Wor4, Flo8, or Hfl1 to activate part or all of the opaque-specific transcriptional program.

The RNA differential expression data (Figure 3), genome wide binding data (Figure 2), and epistatic interaction analysis (Chapter 2) presented in this dissertation together provide a comprehensive foundation upon which to develop a detailed genetic model of the transcriptional regulatory interactions that control the frequency of switching between, and heritable maintenance of, the white and opaque cell types in *Candida albicans*. Essentially, the RNA-seq data will be utilized to identify 1) the complete set of genes that are controlled, either directly or indirectly, by each of the known switch regulators in each cell type, 2) putative direct or indirect regulatory interactions between each of the known switch regulatory TFs, and 3) the “foundational” white- and opaque-specific transcriptomes that are robustly expressed in each cell type, independent of the different switch regulatory mutant backgrounds. Beyond differential expression analysis of each TF, this work is also being applied to mathematical modeling of the white-opaque transcriptional network to infer the detailed regulatory logic of the core switch circuit. Briefly, in collaboration with Ruihao Li (a graduate student in the Hernday lab) a computational model that utilizes machine learning has been created to determine the structure and logic of gene regulatory networks using transcriptional profiles of null mutants, such as the RNA-seq data presented in this thesis, as input data. Understanding the logic of the white-opaque switch regulatory circuit based on RNA-seq data can complement our experimental process by providing possible TF circuit architecture, thus simplifying the process by providing a small set of predicted mutants to investigate instead of creating a large unwieldy set of mutants and screening them. By combining the expression, CUT&RUN, and epistatic interaction data produced in this dissertation along with data from previous studies, it should be possible to create a comprehensive, detailed mathematical model of the white-opaque switch.

Future directions

While this work has identified the direct and indirect regulatory targets of the remaining “switch critical” regulators, there are many switch modulating TFs for which we do not yet know their direct regulatory targets. Complete characterization of all the switch modulating TFs would further define the structure of the white-opaque regulatory

network as well as further strengthen our labs work on computationally modeling the switch. With the recent developments in experimental infrastructure in *C. albicans* as well as the advancements in Next-Gen sequencing, it would be reasonable to expand on the current genome wide binding data through performing CUT&RUN on each of the remaining 20 TFs that affect white-opaque switching by 10-fold or more in both the white and opaque state. Adding this new data set to our existing genome wide binding data and the RNA-seq differential expression data presented in this dissertation would provide a more complete dataset from which to develop a comprehensive model of this complex transcriptional circuit. Furthermore, given the amount of information from these combined data sets, this work would more accurately represent the entirety of the switch network and its dynamics.

It is worth noting that many of the white-opaque regulatory TFs are also integral of other transcriptional networks that control distinct “developmental” programs in *C. albicans*. More than 54% of the TFs known to regulate biofilm-related processes have also been shown to affect white-opaque switching by at least 3-fold when deleted and, of these, 28% of them affect white-opaque switching by 10-fold or more (Table 3-2). Similarly, 50% of the TFs identified in the commensal-pathogenic network have been shown to affect switching, when deleted, by at least 3-fold or higher and 25% of them are known to affect switching by 10-fold or more (Table 3-2). This high level of interconnectedness between these networks suggests there is likely significant crosstalk between these networks, and that the decision to undergo white to opaque switching is highly influenced by a balance between myriad intrinsic and extrinsic regulatory inputs that impinge upon multiple distinct developmental programs in *C. albicans*. While currently outside of the scope and capacity of our computational modeling endeavors, it would be fascinating to model how the constellation of regulatory TFs that are shared between, and unique to, each of these three developmental programs ultimately produce these distinct stable, yet reversible, transcriptional outputs.

Our analysis of the genetic interactions between the white- and opaque-critical switch regulatory TFs suggests that the stochastic nature of white-opaque switching may be governed through competition at the epigenetic level of chromatin modification or remodeling. Perhaps the most compelling indication of this is provided by the genetic interaction between *WOR2* and *SSN6*. Strains that lack *WOR2* are locked in the white cell type unless *WOR1* is ectopically expressed, which then forces expression of the native *WOR1* gene and activation of the opaque transcriptional profile. However, these “induced” opaque cells are unstable and collapse to the white cell type when ectopic *WOR1* expression is removed, indicating that while the phenotypic switch from white to opaque can be activated in the absence of *WOR2*, the epigenetic switch to a heritable opaque cell type requires the presence of *Wor2* within the *Wor1*-induced regulatory complexes found upstream of *WOR1* and many other target genes in opaque cells. This suggests a functional link between *Wor2* and the epigenetic switch to a heritable opaque transcriptional program. Conversely, deletion of *SSN6* results in a *Wor1*-dependent

opaque-locked phenotype, indicating that *Ssn6* is essential for destabilizing the *Wor1*-dependent maintenance of the opaque transcriptional program. Our epistatic interaction studies revealed that removal of *SSN6* from strains that lack *WOR2* restores reversible stochastic switching between heritable white and opaque cell types, thus suggesting that these two opposing players may directly or indirectly impinge upon a common epigenetic regulatory mechanism that lies within the heart of the white-opaque switch. Since the ortholog of *Ssn6* in *S. cerevisiae* (also known as *Cyc8*) controls target genes through recruitment of chromatin modifiers and remodelers, including the SWI/SNF and SAGA complexes, it is tempting to consider the possibility that *Ssn6* may destabilize the epigenetic maintenance of the opaque state through recruitment of one or more such factors. This hypothesis is further supported by recent work in the Hernday lab revealing that strains lacking *SNF2*, the catalytic subunit of SWI/SNF, are also locked in the opaque state and thus phenocopy deletion of *SSN6*. While it remains to be determined whether a *WOR2/SNF2* deletion strain would also restore stochastic switching, our *WOR2/SSN6* epistasis result does suggest that *Wor2* may be actively recruiting competing factors that act to support heritable maintenance of the opaque state. Exploring how the epigenetic landscape is altered between white and opaque cell states, and how *Wor2*, *Ssn6*, and other switch-critical regulators impinge upon this epigenetic layer of the switch, provides an intriguing avenue for future research. Such work could provide valuable insights into the epigenetic mechanisms that maintain each of these distinct transcriptional programs from one generation to the next, and further the establishment of the white-opaque switch as a valuable model system for understanding heritable transcriptional programs in a relatively “simple” eukaryotic organism.

References

1. Hernday AD, Lohse MB, Nobile CJ, Noiman L, Laksana CN, Johnson AD. Ssn6 Defines a New Level of Regulation of White-Opaque Switching in *Candida albicans* and Is Required For the Stochasticity of the Switch. *mBio*. 2016;7(1):e01565-15, /mbio/7/1/e01565-15.atom. doi:10.1128/mBio.01565-15
2. Hernday AD, Lohse MB, Fordyce PM, Nobile CJ, DeRisi JL, Johnson AD. Structure of the transcriptional network controlling white-opaque switching in *Candida albicans*: White-opaque switching network in *C. albicans*. *Molecular Microbiology*. Published online September 2013:n/a-n/a. doi:10.1111/mmi.12329
3. Zordan RE, Galgoczy DJ, Johnson AD. Epigenetic properties of white-opaque switching in *Candida albicans* are based on a self-sustaining transcriptional feedback loop. *Proceedings of the National Academy of Sciences*. 2006;103(34):12807-12812. doi:10.1073/pnas.0605138103
4. Zordan RE, Miller MG, Galgoczy DJ, Tuch BB, Johnson AD. Interlocking Transcriptional Feedback Loops Control White-Opaque Switching in *Candida albicans*. Heitman J, ed. *PLoS Biol*. 2007;5(10):e256. doi:10.1371/journal.pbio.0050256
5. Wang H, Song W, Huang G, Zhou Z, Ding Y, Chen J. *Candida albicans* Zcf37, a zinc finger protein, is required for stabilization of the white state. *FEBS Letters*. 2011;585(5):797-802. doi:10.1016/j.febslet.2011.02.005
6. Lohse MB, Hernday AD, Fordyce PM, et al. Identification and characterization of a previously undescribed family of sequence-specific DNA-binding domains. *Proceedings of the National Academy of Sciences*. 2013;110(19):7660-7665. doi:10.1073/pnas.1221734110
7. Lohse MB, Johnson AD. Identification and Characterization of Wor4, a New Transcriptional Regulator of White-Opaque Switching. *G3*. 2016;6(3):721-729. doi:10.1534/g3.115.024885
8. Huang G, Wang H, Chou S, Nie X, Chen J, Liu H. Bistable expression of *WOR1*, a master regulator of white-opaque switching in *Candida albicans*. *Proceedings of the National Academy of Sciences*. 2006;103(34):12813-12818. doi:10.1073/pnas.0605270103
9. Srikantha T, Borneman AR, Daniels KJ, et al. TOS9 Regulates White-Opaque Switching in *Candida albicans*. *Eukaryotic Cell*. 2006;5(10):1674-1687. doi:10.1128/EC.00252-06
10. Lohse MB, Johnson AD. Temporal anatomy of an epigenetic switch in cell programming: the white-opaque transition of *C. albicans*: Temporal anatomy of an epigenetic switch in *C. albicans*. *Molecular Microbiology*. 2010;78(2):331-343. doi:10.1111/j.1365-2958.2010.07331.x
11. Du H, Guan G, Xie J, et al. The transcription factor Flo8 mediates CO₂ sensing in the human fungal pathogen *Candida albicans*. Lew DJ, ed. *MBoC*. 2012;23(14):2692-2701. doi:10.1091/mbc.e12-02-0094
12. Lohse MB, Ene IV, Craik VB, et al. Systematic Genetic Screen for Transcriptional Regulators of the *Candida albicans* White-Opaque Switch. *Genetics*. 2016;203(4):1679-1692. doi:10.1534/genetics.116.190645

13. Sonneborn A, Tebarth B, Ernst JF. Control of White-Opaque Phenotypic Switching in *Candida albicans* by the Efg1p Morphogenetic Regulator. Kozel TR, ed. *Infect Immun*. 1999;67(9):4655-4660. doi:10.1128/IAI.67.9.4655-4660.1999
14. Srikantha T, Tsai LK, Daniels K, Soll DR. EFG1 Null Mutants of *Candida albicans* Switch but Cannot Express the Complete Phenotype of White-Phase Budding Cells. *J Bacteriol*. 2000;182(6):1580-1591. doi:10.1128/JB.182.6.1580-1591.2000
15. Vinces MD, Haas C, Kumamoto CA. Expression of the *Candida albicans* Morphogenesis Regulator Gene CZF1 and Its Regulation by Efg1p and Czf1p. *Eukaryot Cell*. 2006;5(5):825-835. doi:10.1128/EC.5.5.825-835.2006
16. Vinces MD, Kumamoto CA. The morphogenetic regulator Czf1p is a DNA-binding protein that regulates white–opaque switching in *Candida albicans*. *Microbiology*. 2007;153(9):2877-2884. doi:10.1099/mic.0.2007/005983-0
17. Qasim MN, Valle Arevalo A, Paropkari AD, et al. Genome-wide Profiling of Transcription Factor-DNA Binding Interactions in *Candida albicans*: A Comprehensive CUT&RUN Method and Data Analysis Workflow. *JoVE*. 2022;(182):63655. doi:10.3791/63655
18. Tandonnet S, Torres TT. Traditional versus 3' RNA-seq in a non-model species. *Genomics Data*. 2017;11:9-16. doi:10.1016/j.gdata.2016.11.002
19. Frazer C, Staples MI, Kim Y, et al. Epigenetic cell fate in *Candida albicans* is controlled by transcription factor condensates acting at super-enhancer-like elements. *Nat Microbiol*. 2020;5(11):1374-1389. doi:10.1038/s41564-020-0760-7

FIGURES AND FIGURE LEGENDS

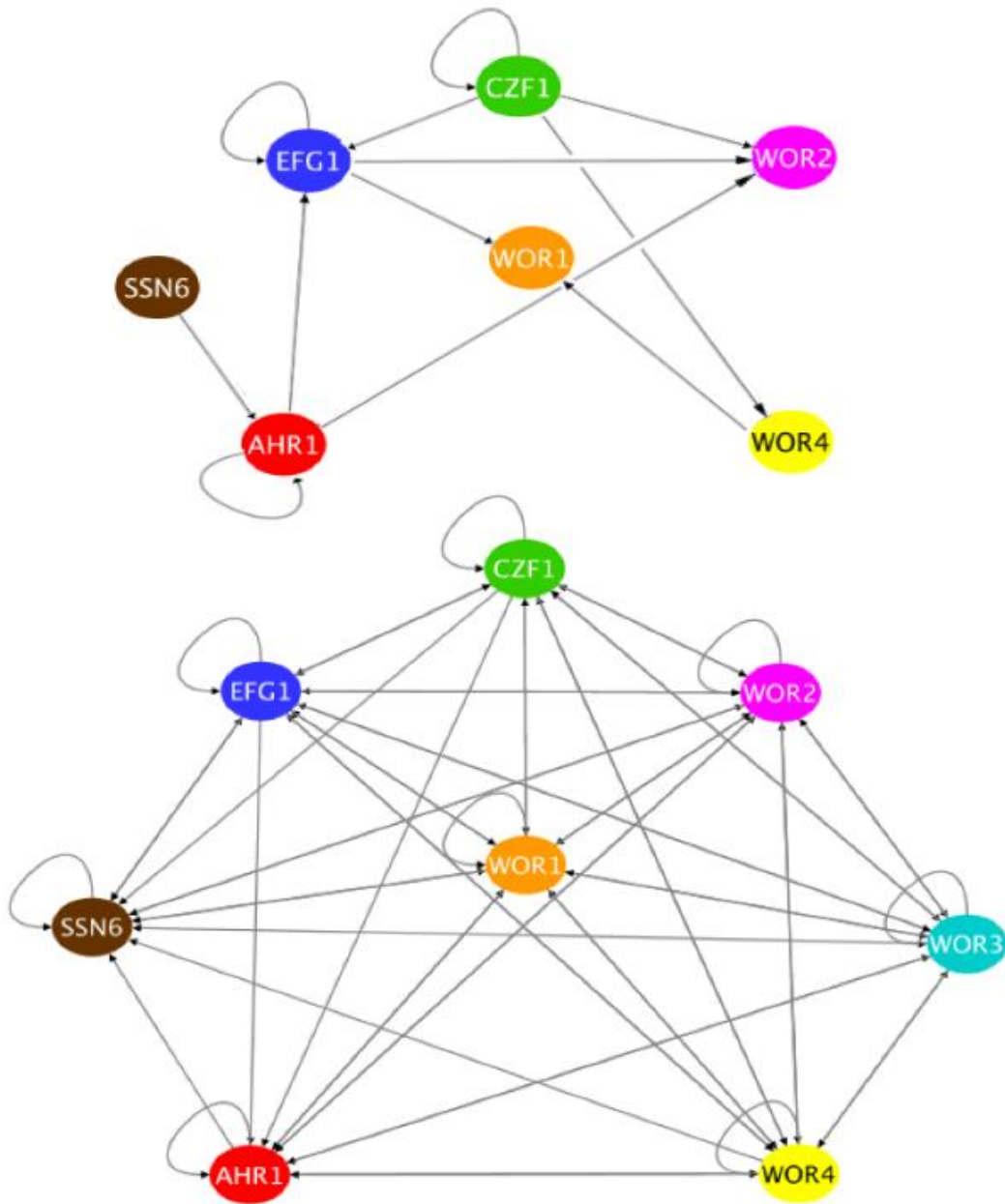


Figure 3-1: Core white and opaque transcriptional circuits. Representation of the core transcriptional circuits controlling the white (top) and the opaque (bottom) state¹. Nodes represent a given transcription factor and edges have directionality to represent a binding event of a given TF in the 5' intergenic region of another TF (i.e. Ssn6 binds in the 5' intergenic region of *AHR1* in the white state).

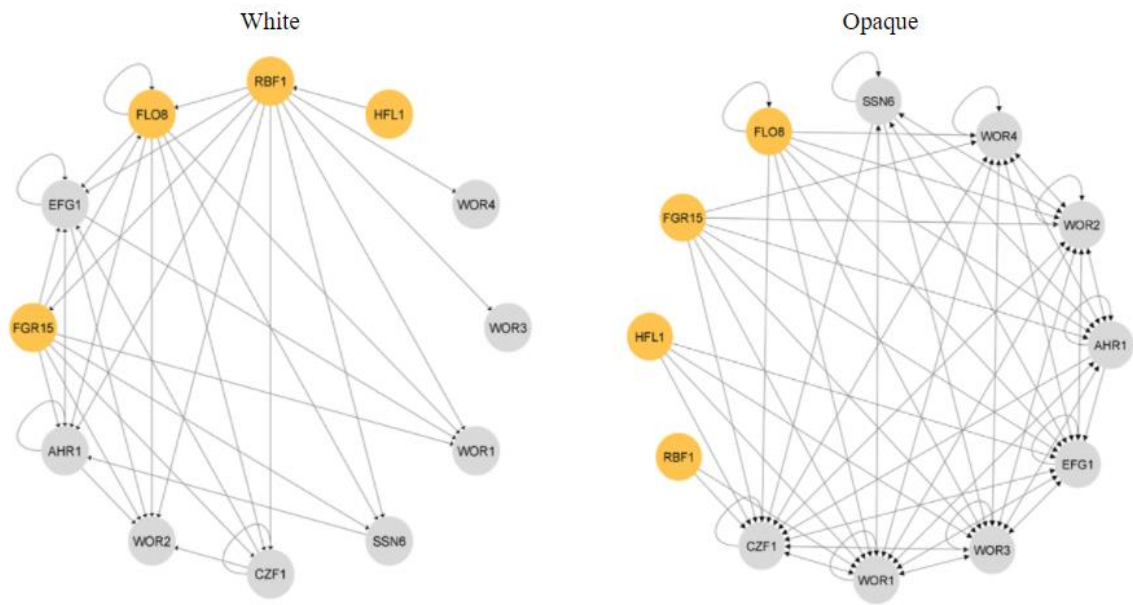


Figure 3-2: New white and opaque transcriptional circuits. All known genome wide binding data combine to give rise to newly developed white and opaque transcription circuits. Yellow nodes represent the newly characterized critical transcription factors through CUT&RUN and the gray nodes represent the previously characterized transcription factors through ChIP.

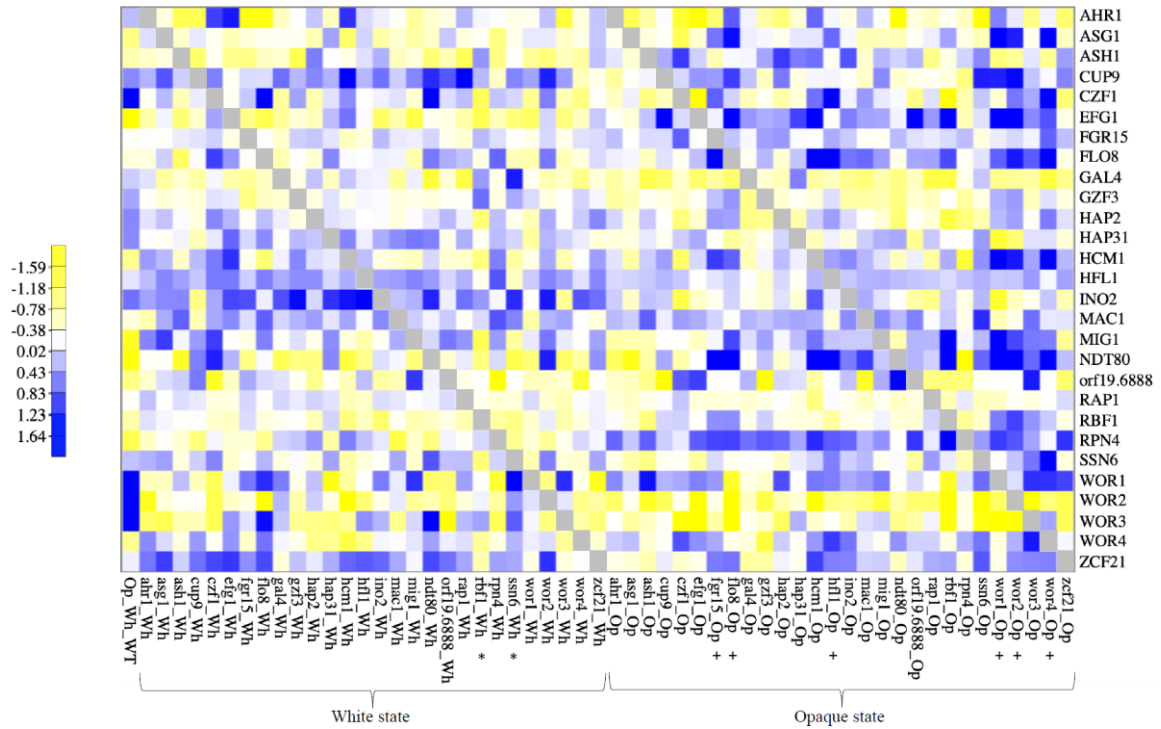


Figure 3-3: RNA-sequencing data Heat map. Heat map indicating fold changes in gene expression for 28 switch critical and switch modulating TF coding genes upon deletion of each individual TF coding gene. Mutant vs. wild-type fold change in expression is indicated based on RNA-seq analysis of the 28 TF mutants in both white (left section) and opaque (right section) cell types. TF coding genes are indicated on the y-axis label and TF gene deletion genotypes and cell type are indicated on the x-axis. Fold changes in gene expression between wild-type opaque and white cells are indicated for reference (first column on the left). Yellow indicates genes that are down regulated in the mutant relative to wild type, while blue indicates genes that are upregulated in the mutant relative to wild type. Genes that show the same level of expression in wild-type vs deletion strains are indicated in white. Grey squares indicate that it is not feasible to accurately determine the impact of deleting a particular TF coding gene upon expression of the same gene. All data is in log₂ format and the corresponding fold changes for different color intensities is indicated in the color key at the lower left of the figure. An * on the x-axis represents strains that have a secondary deletion of *WOR1*, a + on the x-axis indicates strains that have *WOR1* ectopically expressed, and an O on the y-axis represent genes that are often correlated with the opaque phenotype.

TABLES

Table 3-1: CUT&RUN data: (Top) Each TF that was examined (**Left**) Each 5' intergenic region of the genes within the white-opaque switch circuit. Black filled cells reflect binding of each of the examined TFs.

	Flo8		Fgr15		Rbf1		Hfl1	
	White	Opaque	White	Opaque	White	Opaque	White	Opaque
<i>WOR1</i>								
<i>CZF1</i>								
<i>EFG1</i>								
<i>WOR2</i>								
<i>WOR3</i>								
<i>WOR4</i>								
<i>SSN6</i>								
<i>AHR1</i>								
<i>FLO8</i>								
<i>FGR15</i>								
<i>RBF1</i>								
<i>HFL1</i>								

Table 3-2: TFs shared among the white-opaque, biofilm, and commensal-pathogenic networks: List of all known TFs to affect the white - opaque switch. An “X” in the column titled White - Opaque refers to how the TF affects switching by 3-fold or more, a single asterisk indicates the TF affects switching by 5-fold or more, and ** signifies the TF affect switching by 10-fold or more. An “X” has also been used to indicate TFs that are known to influence Biofilm development and the Commensal – Pathogenic circuits in their respective columns.

Orf19#	TF Name	White-Opaque	Biofilm	Commensal-Pathogenic
Orf19.7381	Ahr1	X*	X	
Orf19.3127	Czf1	X**	X	
Orf19.610	Efg1	X**	X	
Orf19.6798	Ssn6	X**		
Orf19.4884	Wor1	X**		
Orf19.5992	Wor2	X**		
Orf19.467	Wor3	X		
Orf19.6713	Wor4	X**		
Orf19.7436	Aaf1			
Orf19.2272	Aft2			
Orf19.4766	Arg81		X	
Orf19.166	Asg1	X**		
Orf19.5343	Ash1	X**		
Orf19.6874	Bas1		X	
Orf19.723	Bcr1		X	
Orf19.4056	Brg1		X	
Orf19.1623	Cap1	X		
Orf19.4670	Cas5		X	
Orf19.4433	Cph1			
Orf19.1187	Cph2			
Orf19.7359	Crz1	X*		

Orf19.3794	Csr1		X	
Orf19.7374	Cta4	X*		
Orf19.4288	Cta7			
Orf19.5001	Cup2			
Orf19.6514	Cup9	X**		
Orf19.3252	Dal81	X*	X	
Orf19.2088	Dpb4	X		
Orf19.2623	Ecm22			
Orf19.5498	Efh1			
Orf19.6817	Fcr1			
Orf19.2054	Fgr15	X**		
Orf19.1093	Flo8	X**	X	
Orf19.5338	Gal4	X**	X	
Orf19.3182	Gis2	X*		
Orf19.4000	Grf10	X*	X	
Orf19.2842	Gzf3	X**	X	
Orf19.1228	Hap2	X**		
Orf19.4647	Hap3			
Orf19.517	Hap31	X**		
Orf19.740	Hap41	X*		
Orf19.1481	Hap42			
Orf19.1973	Hap5	X*		
Orf19.4853	Hcm1	X**		
Orf19.3063	Hfl1	X**	X	
Orf19.7539	Ino2	X**		
Orf19.837.1	Ino4	X		
Orf19.7401	lsw2	X		
Orf19.3736	Kar4			
Orf19.4776	Lys143	X*		

Orf19.5380	Lys144			
Orf19.7068	Mac1	X**		
Orf19.4318	Mig1	X**	X	
Orf19.5326	Mig2		X	
Orf19.4752	Msn4	X		
Orf19.2119	Ndt80	X**	X	
Orf19.5910	Nto1			
Orf19.1543	Opi1	X		
Orf19.4231	Pth2	X		
Orf19.1773	Rap1	X**		
Orf19.5558	Rbf1	X**	X	
Orf19.6102	Rca1	X*		
Orf19.7521	Rep1			
Orf19.2823	Rfg1		X	
Orf19.3865	Rfx1			
Orf19.4590	Rfx2		X	
Orf19.1604	Rha1		X	
Orf19.4438	Rme1			
Orf19.513	Ron1			
Orf19.1069	Rpn4	X*		
Orf19.4722	Rtg1			X
Orf19.2315	Rtg3			X
Orf19.1926	Sef2	X		
Orf19.454	Sfl1			
Orf19.971	Skn7			
Orf19.1032	Sko1			
Orf19.4961	Stp2	X*	X	
Orf19.909	Stp4	X		
Orf19.4545	Swi4	X		

Orf19.4941	Tye7		X	X
Orf19.7317	Uga33		X	
Orf19.1822	Ume6		X	
Orf19.2745	Ume7			
Orf19.391	Upc2	X	X	
Orf19.1035	War1	X		
Orf19.5210	Xbp1	X*		
Orf19.2808	Zcf16			
Orf19.3305	Zcf17			
Orf19.431	Zcf2			
Orf19.4145	Zcf20			
Orf19.4166	Zcf21	X**		X
Orf19.4251	Zcf22			
Orf19.4524	Zcf24	X		
Orf19.4568	Zcf25	X*		
Orf19.4649	Zcf27			
Orf19.5251	Zcf30			
Orf19.5924	Zcf31	X	X	
Orf19.6182	Zcf34	X	X	
Orf19.1685	Zcf7	X		
Orf19.1718	Zcf8		X	
Orf19.6781	Zfu2		X	
Orf19.6888	Zfu3	X**		
Orf19.5026	Zms1			
Orf19.1150				
Orf19.1274				
Orf19.1577				
Orf19.1757				
Orf19.217				

Orf19.2476				
Orf19.2612				
Orf19.2961				
Orf19.3928				
Orf19.7098				